



Homogeneous quadrator control: theory and experiment

Siyuan Wang

► To cite this version:

Siyuan Wang. Homogeneous quadrator control: theory and experiment. Automatic. Centrale Lille Institut, 2020. English. NNT : 2020CLIL0026 . tel-03247401

HAL Id: tel-03247401

<https://theses.hal.science/tel-03247401>

Submitted on 3 Jun 2021

HAL is a multi-disciplinary open access archive for the deposit and dissemination of scientific research documents, whether they are published or not. The documents may come from teaching and research institutions in France or abroad, or from public or private research centers.

L'archive ouverte pluridisciplinaire **HAL**, est destinée au dépôt et à la diffusion de documents scientifiques de niveau recherche, publiés ou non, émanant des établissements d'enseignement et de recherche français ou étrangers, des laboratoires publics ou privés.

N° d'ordre : XXX

CENTRALE LILLE

THESE

Présentée en vue
d'obtenir le grade de

DOCTEUR

En

**Spécialité : Automatique, Génie Informatique,
Traitement du Signal et des Images**

Par

Siyuan WANG

DOCTORAT DELIVRE PAR CENTRALE LILLE

Titre de la thèse :

**Contrôle homogène de quadrotor :
Théorie et Expérience**

Soutenue le 15 Décembre 2020 devant le jury d'examen :

Président :	Vincent COCQUEMPOT	Professeur, Université de Lille
Rapporteur :	Isabelle QUEINNEC	Directrice de Recherche CNRS, LAAS-CNRS
Rapporteur :	Franck PLESTAN	Professeur, Centrale Nantes
Examineur :	Bernard BROGLIATO	Directeur de Recherche, INRIA Grenoble
Directeur de thèse :	Gang ZHENG	Chargé de Recherche INRIA, HDR, INRIA Lille
Co-Directeur de thèse :	Andrey POLYAKOV	Chargé de Recherche INRIA, HDR, INRIA Lille

Thèse préparée dans l'Inria Lille - Nord Europe et le Centre de Recherche en Informatique,
Signal et Automatique de Lille, CRISTAL, CNRS UMR 9189

Ecole Doctorale SPI 072

Order Number: XX

CENTRALE LILLE

THESIS

Presented in order to obtain the grade of

DOCTOR

In

Specialty: Control, Computer Science,

Signal and Image Processing

By

Siyuan WANG

DOCTORATE DELIVERED BY CENTRALE LILLE

Title of the thesis:

**Homogeneous quadrotor control:
Theory and Experiment**

Defended on December 15, 2020 before the committee:

President:	Vincent COCQUEMPOT	Professor, University of Lille
Referee:	Isabelle QUEINNEC	CNRS Senior Researcher, LAAS-CNRS
Referee:	Franck PLESTAN	Professor, Centrale Nantes
Examiner:	Bernard BROGLIATO	INRIA Senior Researcher, INRIA Grenoble
Supervisor:	Gang ZHENG	INRIA Researcher, HDR, INRIA Lille
Co- Supervisor:	Andrey POLYAKOV	INRIA Researcher, HDR, INRIA Lille

Thesis prepared in Inria Lille - Nord Europe and the Centre de Recherche en Informatique,
Signal et Automatique de Lille, CRIStAL, CNRS UMR 9189

Doctoral School SPI 072

Cette thèse a été préparée dans les laboratoires suivants:

INRIA Lille - Nord Europe

Parc scientifique de la Haute-Borne
40, avenue Halley - Bât A - Park Plaza
59650 Villeneuve d'Ascq - France

☎ (33)(0)3 59 57 78 00

Web Site <https://www.inria.fr/centre/lille>



Centrale Lille

Cité Scientifique - CS 20048
59651 Villeneuve d'Ascq - France

☎ 33 (0)3 20 33 54 87

Web Site <https://centralelille.fr/>



CRISTAL UMR 9189 CNRS

University Lille 1
Bâtiment M3 extension
Avenue Carl Gauss
59655 Villeneuve d'Ascq - France

☎ (33)(0)3 28 77 85 41

Web Site <https://www.cristal.univ-lille.fr/>



Acknowledge

Firstly, I would like to express my sincere gratitude to my advisors Gang Zheng and Andrey Polyakov for the continuous support of my Ph.D study and related research, for their patience, motivation, and immense knowledge. Their guidance helped me in all the time of research and writing of this thesis. I could not have imagined having a better advisor and mentor for my Ph.D study. It is you who change the way my life unfolds.

Secondly, I would also like to thank Denis Efimov and Rosane Ushirobira, who organize the research team and make the laboratory as warm as home.

Besides, I would like to thank the external members of the jury DR. Isabelle Queinnec, Prof. Franck Plestan, Prof. Vincent Cocquempot, DR. Bernard Brogliato for accepting to review my thesis manuscript.

Finally I wish to acknowledge the help provided by my family, my friends and my colleagues!

Abstract

In the past several decades, quadrotor control problems attract more attentions of the researcher comparing with other flying vehicles. However, most of the commercial products still use linear PID controller, which provides sufficiently good performance. Developing a controller, that would convince the industry to use it instead of linear PID, is still a challenge. The aim of this thesis is to show that homogeneous controller is a possible alternative to linear one. For this purpose, a new method of upgrading linear algorithm to homogeneous one is proposed. It uses the gains of linear controller/observer provided by the manufacturer for tuning of homogeneous algorithm. The experimental results support the theoretical developments and confirm a significant improvement of quadrotor's control quality: better precision, more robustness and faster response.

Table of Contents

Acknowledge	vii
Abstract	ix
Table of Contents	xi
List of Figures	xiii
List of Tables	xv
Notations	xvii
1 Introduction	1
1.1 Quadrotor as unmanned aerial vehicle	1
1.2 Quadrotor system	4
1.3 State of the art in quadrotor control	14
1.4 Experiment setup: QDrone of Quanser	20
1.5 Contribution and outline of thesis	26
2 Mathematical backgrounds	29
2.1 Homogeneity	29
2.2 Implicit Lyapunov function method	44
2.3 Linear Matrix Inequalities	53
3 Generalized homogenization of linear controller	61
3.1 Motivating Example	61
3.2 Homogenization of linear controllers	64
3.3 An “upgrade” of a linear controller for Quanser QDrone TM	78
3.4 Conclusion	82
4 Generalized homogenization of Linear Observer	87
4.1 Homogeneous State-Estimation of Linear MIMO Systems	87
4.2 From a linear observer to a homogeneous one	90
4.3 An “upgrade” of a linear filter for QDrone of Quanser TM	92

4.4 Conclusion	100
5 Homogeneous stabilization under constraints	101
5.1 Problem statement	102
5.2 Controller Design with Time and state Constraint	102
5.3 Simulation results	110
5.4 Conclusion	113
Conclusion and perspective	115
Bibliography	119
Résumé substantiel	129

List of Figures

1.1	Earth (E), local (L) and body (B) axis [2]	5
1.2	Quadrotor orientation using Euler angles [2]	6
1.3	PID controller on quadrotor	15
1.4	LQG controller on quadrotor	16
1.5	SMC applied to quadrotor	18
1.6	adaptive controller applied to quadrotor	18
1.7	FLC controller applied to quadrotor [120]	19
1.8	OptiTrack Flex 13	20
1.9	6 cameras configuration (top view)	21
1.10	OptiHubs	21
1.11	6 cameras with one OptiHub	22
1.12	Markers used for location	22
1.13	QDrone's Inter Aero compute board	23
1.14	Cobra 2100kv motor(left) and 6045 poly-carbonate propellers(right)	23
1.15	Router rear view	25
1.16	Server model	25
1.17	Command model	25
2.1	Invariant shape after dilation	29
2.2	uniform dilation \mathbf{d}_1 , weighted dilation \mathbf{d}_2 , generalized dilation \mathbf{d}_3 [85]	39
2.3	Lyapunov stability	45
2.4	Locally attractive	46
3.1	Comparison of "overshoots" for linear (left) and homogeneous (right) controllers	64
3.2	Quadrotor position tracking comparison in x, y, z and ψ	83
3.3	Input L_2 norm of linear PID signal and Homogeneous PID signal	84
3.4	The response of linear controller and homogeneous controller to the added load disturbance	85
4.1	Quanser's filter	93
4.2	Bode diagram of transfer functions H_{Q_1}, H_{Q_2} and H_{L_1}, H_{L_2}	97
4.3	Quadrotor position stabilization comparisons on x	98

4.4	Quadrotor position stabilization comparisons on y	99
4.5	Quadrotor position stabilization comparisons on z	99
4.6	Quadrotor position stabilization comparisons on ψ	100
5.1	Quadrotor position x, y, z by implicit PID controller	111
5.2	Quadrotor attitude ϕ, θ, ψ by implicit PID controller	111
5.3	Angle velocity $\dot{\psi}$ by implicit PID controller	111
5.4	Log of the norm of vector $v = [x, y, \phi, \theta, z, \psi]$ by implicit PID controller	112
5.5	Quadrotor position x, y, z by implicit PD controller	112
5.6	Quadrotor attitude ϕ, θ, ψ by implicit PD controller	112

List of Tables

1.1	Quadrotor platforms for research	5
1.2	Recommended camera number and work space	20
1.3	Motor and propeller	24
1.4	Parameter of propulsion system	24
1.5	Quadrotor mechanical parameters	24
3.1	Mean values of stabilization error	81
4.1	Mean value of stabilization error	98

Notations

- \mathbb{R} the set of real numbers;
- \mathbb{R}^n the n -dimensional Euclidean space;
- $C(X, Y)$ the space of continuous functions $X \rightarrow Y$, where X, Y are subsets of \mathbb{R}^n ;
- $C^p(X, Y)$ the space of functions continuously differentiable at least up to the order p ;
- $\lambda_{\min}(P)$ and $\lambda_{\max}(P)$ are the maximal and minimal eigenvalues of the symmetric matrix P ;
- If $A \in \mathbb{R}^{n \times n}$ then $\|A\| := \sup_{x \neq 0} \frac{\|Ax\|}{\|x\|}$, $\lfloor A \rfloor = \inf_{x \neq 0} \frac{\|Ax\|}{\|x\|}$, where $\|x\|$ is a vector norm in \mathbb{R}^n ;
- $\text{diag}\{\lambda_i\}_{i=1}^n$ the diagonal matrix with elements λ_i ;
- $P > 0 (< 0, \geq 0, \leq 0)$ for $P \in \mathbb{R}^{n \times n}$ means that P is symmetric and positive(negative) definite(semidefinite);
- $\mathbf{d}(s) : \mathbb{R}^n \rightarrow \mathbb{R}^n$ is a one-parameter group of dilations in \mathbb{R}^n where $s \in \mathbb{R}$;
- $\mathbb{F}_{\mathbf{d}}(\mathbb{R}^n)$ the set of \mathbf{d} -homogeneous vector fields $\mathbb{R}^n \rightarrow \mathbb{R}^n$;
- $\mathbb{H}_{\mathbf{d}}(\mathbb{R}^n)$ the set of \mathbf{d} -homogeneous functions $\mathbb{R}^n \rightarrow \mathbb{R}$;
- $\deg_{\mathbb{F}_{\mathbf{d}}}(f)$ homogeneity degree of $f \in \mathbb{F}_{\mathbf{d}}(\mathbb{R}^n)$;
- $\deg_{\mathbb{H}_{\mathbf{d}}}(h)$ homogeneity degree of $h \in \mathbb{H}_{\mathbf{d}}(\mathbb{R}^n)$;
- $\text{sign}(x) = \begin{cases} 1 & x > 0 \\ 0 & x = 0 \\ -1 & x < 0 \end{cases}$;
- $\lfloor x_i \rfloor^{\alpha_i} = |x_i|^{\alpha_i} \text{sign}(x_i)$;
- By default $\|x\| = \sqrt{x^\top P x}$ is the weighted Euclidean norm with some $P > 0$;
- $\|x\|_{\mathbb{R}^n} = \sqrt{x^\top x}$;

- The canonical homogeneous norm is $\|x\|_{\mathbf{d}} = e^{s_x}$, where $s_x \in \mathbb{R} : \|\mathbf{d}(-s_x)x\| = 1$;
- ϕ, θ, ψ are Euler angles represent roll, pitch, and yaw of quadrotor;
- ${}^B R_L$ is rotation matrix from local frame to body frame;
- ω is angular velocity in body frame $\omega = (p, q, r)$;
- F_T denotes total thrust produced by propellers in body frame;
- I_{com} moment of inertia of quadrotor; I_{xx} roll inertia; I_{yy} pitch inertia; I_{zz} yaw inertia;
- L_{roll} roll motor distance;
- L_{pitch} pitch motor distance;
- c drag coefficient;
- k_c thrust coefficient;
- m mass of quadrotor;
- g gravitational acceleration;
- τ torque of producing roll, pitch, and yaw;
- f_i thrust produced by each propeller $i = 1, 2, 3, 4$;
- A continuous function $\sigma : [0, +\infty] \rightarrow [0, +\infty]$ belongs to the class \mathcal{K} if it is monotone increasing and $\sigma(0) = 0$;
- A function $\sigma \in \mathcal{K}$ belongs to the class \mathcal{K}_∞ if $\sigma(t) \rightarrow \infty$ as $t \rightarrow +\infty$;
- For $P \geq 0$ the square root of P is a matrix $M = P^{\frac{1}{2}}$ such that $M^2 = P$.

Introduction

This chapter presents the context and motivation of the research. Then it reviews the state of the art of quadrotor control, which includes linear, nonlinear and intelligent controllers. The experimental platform is considered as well. The contribution and the outline of the thesis are presented in the last section.

1.1 Quadrotor as unmanned aerial vehicle

In this section, we provide a general introduction to quadrotor control problem. Initially, we survey quadrotor's application domains and present advantages of the quadrotor system. Next, we discuss some challenges related with its control and navigation. Finally, we formulate a general problem to be tackled in this thesis.

1.1.1 Applications

Quadrotor is a rotary-wing UAV (Unmanned Aerial Vehicle) which has become very reliable and affordable in the last years. Besides quadrotor applications are rather popular and cover many important flight tasks.

- Quadrotor as transport vehicle: This kind of application uses mainly the quadrotor's ability to transport a payload. For example, Amazon proposed "Prime Air" service to deliver the package using quadrotor. Meanwhile the quadrotor could work for carrying medical equipment to save lives. Ambulance Drone was created by TU Delft and applied in the real life several years ago.
- Quadrotor with camera: Quadrotor working with camera is one of the applications

which attracts a lot of attention recently. The main contribution of camera is to record high quality video. The company “DJI Technology” (one of the main players of commercial quadrotor) provides many kinds of products for aerial photography and videography. Target surveillance, searching and detection are also important quadrotor applications [18], [73]. Several targets could be tracking at the same time [49]. This application has potential market in traffic monitoring, military tasks of some dangerous places [62], etc. Of course it can be extended to the outdoor application of mapping and exploring unknown environments [27].

- Quadrotor with robot arm: Quadrotor equipped with an arm provides the quadrotor a possibility of working in the air. For example, a two degrees of freedom robotic arm is equipped with quadrotor to pick and hold a payload. One of the application domains is in autonomous inspection and maintenance of power lines, which is a new project proposed by [Robotics & perception group of ETH](#) in this year. Besides quadrotor with multi-link arm can handle the assembly tasks in the air [40]. The application of multiple quadrotors’ cooperation with robotic arm could be found in [16], [28], [92].

Further research of quadrotor platform would allow to develop wider range applications.

1.1.2 Advantages

As shown in the previous section, the quadrotor has been applied in many domains. The following advantages of quadrotor could be the reason of this phenomenon.

- Small size, lightweight: The quadrotor could be made to be a relatively small size [29] which gives more safety [31] than other aerial vehicles.
- Simple configuration of the multirotor type: The motors with propeller are the only moving parts. This makes the platform more reliable and mechanically robust [89]. The propellers mostly have a fixed blade pitch, thus quadrotor thrust and attitude can be controlled by changing the motor speed. This is done by electronic speed controller (ESC).
- Vertical take-off and landing: This makes quadrotor to be possible staying airborne without moving, which is required in many tasks, such as videography, photography, inspection, surveillance, manipulation and so on. It needs minimal space for take-off and landing.

- Relatively high thrust-to-weight-ratio: Quadrotor is possible to carry rather large payload [39] and be able to perform agile maneuvers.
- Cheap prototype: This could be the main advantage for researchers to verify their ideas on quadrotor platform.

Quadrotor is a good option as a research platform, since it is simple, cheap, robust, reliable and agile. It needs small laboratory space for making experiments due to vertical take-off and landing.

1.1.3 Challenges

Development of a control system that properly governs quadrotor motion is important for all applications mentioned above. Several challenges related with the quadrotor control problem are listed below:

- Quadrotor is unstable, nonlinear, multi-variable, coupled, under-actuated system. Indeed a stable hovering flight cannot be achieved by applying constant inputs to four motors. The mechanical model has 6 degrees of freedom (DOF), while four thrusts produced by propellers are the only inputs of system. The simplest dynamical model of quadrotor is highly nonlinear and has coupled variables. Since the number of inputs is smaller than the DOF, quadrotor is an underactuated system [11]. It is not able to independently produce any force orientation. This leads to many control problems, for example, take-off from an inclined surface [106].
- Quadrotors hardware limitations: saturation of motors [103], limited battery and computational capabilities. The quadrotor may reach the physical limit of actuators while performing some flight tasks. This may leads to the inability [25]. Battery is the main challenge of any electrical vehicle. Quadrotor generally cannot carry too heavy battery due to the small size, which is the reason why quadrotor cannot stay too long in the air with one recharge. The improvement of battery technologies plays an important role in the quadrotor applications. Quadrotor also requires a small and powerful processor for on-board performing various tasks such as realization advanced control strategies motivated by nonlinear system theory, image processing or learning control.

1.1.4 Problem studied in this thesis

A lot of control strategies have been developed for quadrotor platform such as PID (Proportional-Integral-Derivative), sliding mode, back-stepping and other algorithms (see Section 1.3 for more details). Most of commercial products use the classical (linear) PID controller, which provides sufficiently good quality and admits rather simple well-developed design methodology. The linear PID control theory is very well developed, so the further improvements of control quality using the same linear strategy seems impossible. Nonlinearity of the quadrotor system motivates the researchers for development of nonlinear control algorithms. However, it is hard to convince the industry to invest a lot of time/money for such developments while the linear PID works good enough. That is why this thesis proposes an alternative solution. We take already designed and well-tuned linear PID controller and transform it into nonlinear one providing better performance.

Therefore the main goals of this thesis are

- to develop a methodology for upgrading linear PID controllers/observers to nonlinear ones with a guaranteed improvement of the control/estimation quality.
- to validate this methodology on a quadrotor platform existing on the market.

Moreover it is worthy noting that in the view of challenges mentioned above, the upgraded quadrotor controllers/observers must be simple for implementation without any hardware upgrade.

1.2 Quadrotor system

This section presents more details of the quadrotor system. We follow the researches made by many well-known international labs. Table 1.1 lists the most famous ones.

1.2.1 Model of dynamics

Since most of quadrotor control algorithms are model based, it is indispensable to deduce a precise dynamical model for quadrotor. The most popular methods of quadrotor modeling are based on Newton-Euler equation and Euler-Lagrange equation which will be recalled hereafter. The dynamic model presented below assumes that the Coriolis Force and hub force are relatively smaller terms.


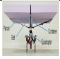
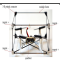

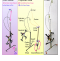



Picture	Organization	Recent Research
	ETH Autonomous Systems Lab	search and rescue; precision farming; swarm quadrotor; aerial service
	EPFL Laboratory of intelligent system	aerial delivery; version based swarm; embodied flight; accurate control
	University of Pennsylvania GRASP Laboratory	docking module
	University of South California ACT lab	crazy swarm; mixed reality
	University of South California BDML lab	quadrotor perching
	UTC Heudiasyc lab	formation control transportation
	university of Zurich Robotics and Perception Group	drone racing; exploration; agile drone flight; multi-robot system
	Qanser	commercial product

Table 1.1 – Quadrotor platforms for research

1.2.1.1 Coordinate frames

The various coordinate systems (Fig. 1.1) that are commonly used in the flight model need to be presented before introducing different modeling approaches.

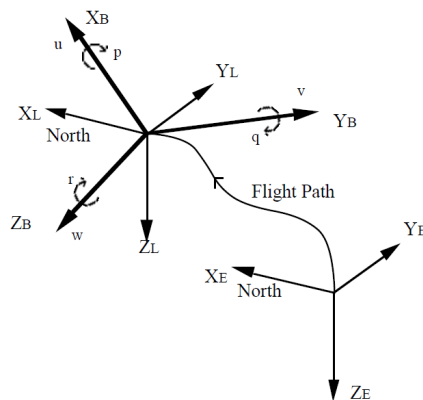


Figure 1.1 – Earth (E), local (L) and body (B) axis [2]

- Body axis system. The body axis has its origin at the quadrotor center of mass (CoM) and is fixed to the quadrotor while moving along with it. It forms a right-handed rule Fig. 1.1. The terms p, q, r are three body axis rotational velocities.

- Local axis system. The local axis system also has its origin point at the CoM of quadrotor, but has a fixed orientation 1.1.
- Earth axis system. It is an inertial frame that has its origin fixed at some point on earth's surface. Inertial frame is also depicted in Fig. 1.1.

Let the generalized coordinates of quadrotor be presented as

$$\mathbf{q} = (x, y, z, \phi, \theta, \psi) \in \mathbb{R}^6 \quad (1.1)$$

where $\xi = (x, y, z) \in \mathbb{R}^3$ denotes the position vector of mass center of quadrotor respecting to the Earth frame E , and $\eta = (\phi, \theta, \psi) \in \mathbb{R}^3$ represents the Euler angle of quadrotor. The quadrotor orientation is described by an ordered set of three Euler angles that relate the orientation of the body axis relative to the local axis system. In Fig. 1.2, X_1, Y_1 and Z_1 are Earth frame which corresponds to local frame in Fig. 1.1. The Euler angle order here is ψ, θ, ϕ around Z_1, Y_2 and X_3 axes respectively. Other sequence of 3 rotations can be chosen, however once the sequence is fixed, it must be retained.

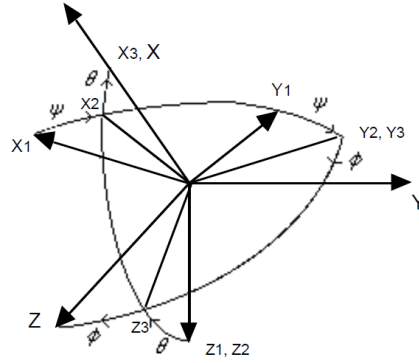


Figure 1.2 – Quadrotor orientation using Euler angles [2]

After doing the first rotation ψ ,

$$\begin{bmatrix} X_2 \\ Y_2 \\ Z_2 \end{bmatrix} = \begin{bmatrix} \cos \psi & \sin \psi & 0 \\ -\sin \psi & \cos \psi & 0 \\ 0 & 0 & 1 \end{bmatrix} \begin{bmatrix} X_1 \\ Y_1 \\ Z_1 \end{bmatrix} = {}^2R_1 \begin{bmatrix} X_1 \\ Y_1 \\ Z_1 \end{bmatrix} \quad (1.2)$$

Next doing the second rotation θ ,

$$\begin{bmatrix} X_3 \\ Y_3 \\ Z_3 \end{bmatrix} = \begin{bmatrix} \cos \theta & 0 & -\sin \theta \\ 0 & 1 & 0 \\ \sin \theta & 0 & \cos \theta \end{bmatrix} \begin{bmatrix} X_2 \\ Y_2 \\ Z_2 \end{bmatrix} = {}^3R_2 \begin{bmatrix} X_2 \\ Y_2 \\ Z_2 \end{bmatrix} \quad (1.3)$$

Finally doing the last rotation ϕ , the body frame is

$$\begin{bmatrix} X_B \\ Y_B \\ Z_B \end{bmatrix} = \begin{bmatrix} X \\ Y \\ Z \end{bmatrix} = \begin{bmatrix} 1 & 0 & 0 \\ 0 & \cos \phi & \sin \phi \\ 0 & -\sin \phi & \cos \phi \end{bmatrix} \begin{bmatrix} X_3 \\ Y_3 \\ Z_3 \end{bmatrix} = {}^BR_3 \begin{bmatrix} X_3 \\ Y_3 \\ Z_3 \end{bmatrix} \quad (1.4)$$

Therefore the relation between local frame X_1, Y_1, Z_1 and body frame X_B, Y_B, Z_B is given by combining (1.2)- (1.4):

$$\begin{bmatrix} X_B \\ Y_B \\ Z_B \end{bmatrix} = {}^BR_L \begin{bmatrix} X_L \\ Y_L \\ Z_L \end{bmatrix} \quad (1.5)$$

where BR_L is the transformation matrix from local frame to body frame.

$${}^BR_L = \begin{bmatrix} \cos \theta \cos \psi & \cos \theta \sin \psi & -\sin \theta \\ -\cos \phi \sin \psi + \sin \phi \sin \theta \cos \psi & \cos \phi \cos \psi + \sin \phi \sin \theta \sin \psi & \sin \phi \cos \theta \\ \sin \phi \sin \psi + \cos \phi \sin \theta \cos \psi & -\sin \phi \cos \psi + \cos \phi \sin \theta \sin \psi & \cos \phi \cos \theta \end{bmatrix} \quad (1.6)$$

Since the transformation matrix is orthogonal, the inverse matrix can be calculated by

$${}^BR_L {}^LR_B = \mathbf{I} \quad (1.7)$$

and

$${}^LR_B = \begin{bmatrix} \cos \psi \cos \theta & \cos \psi \sin \theta \sin \phi - \sin \psi \cos \phi & \cos \psi \sin \theta \cos \phi + \sin \psi \sin \phi \\ \sin \psi \cos \theta & \sin \psi \sin \theta \sin \phi + \cos \psi \cos \phi & \sin \psi \sin \theta \cos \phi - \sin \psi \sin \phi \\ -\sin \theta & \cos \theta \sin \phi & \cos \theta \cos \phi \end{bmatrix} \quad (1.8)$$

In the real experiment, the Earth frame is initially set to be the same orientation and position to local frame system.

1.2.1.2 Derivative of Euler angle and body axis rotational velocities

The body axis angle velocities are presented by a projection of the angle velocity on the body axis. Angle velocity can be presented by the sum of three following terms

1. $\dot{\psi}$ is measured in the local frame (X_1, Y_1, Z_1)
2. $\dot{\theta}$ is measured in the intermediate frame (X_2, Y_2, Z_2)
3. $\dot{\phi}$ is measured in the intermediate frame (X_3, Y_3, Z_3)

Thus the body axis rotational velocities is

$$\begin{aligned} \omega = \begin{bmatrix} p \\ q \\ r \end{bmatrix} &= {}^B R_3 \begin{bmatrix} \dot{\phi} \\ 0 \\ 0 \end{bmatrix} + {}^B R_2 \begin{bmatrix} 0 \\ \dot{\theta} \\ 0 \end{bmatrix} + {}^B R_1 \begin{bmatrix} 0 \\ 0 \\ \dot{\psi} \end{bmatrix} \\ &= \begin{bmatrix} 1 & 0 & -\sin \theta \\ 0 & \cos \phi & \sin \phi \cos \theta \\ 0 & -\sin \phi & \cos \phi \cos \theta \end{bmatrix} \begin{bmatrix} \dot{\phi} \\ \dot{\theta} \\ \dot{\psi} \end{bmatrix} = {}^B W_1 \dot{\eta} \end{aligned} \quad (1.9)$$

where ${}^B W_1$ is the transformation matrix between derivative of Euler angle and body axis rotational velocities. The following approaches will use the frames defined in the previous part.

1.2.1.3 Euler-lagrange approach

The Euler-Lagrange equation with external generalized forces is

$$\frac{d}{dt} \left(\frac{\partial L}{\partial \dot{\mathbf{q}}} \right) - \frac{\partial L}{\partial \mathbf{q}} = \begin{bmatrix} \mathbf{F} \\ \boldsymbol{\tau} \end{bmatrix} \quad (1.10)$$

where the Lagrangian is defined as

$$L(\mathbf{q}, \dot{\mathbf{q}}) = T_{trans} + T_{rot} - P \quad (1.11)$$

where $T_{trans} = \frac{1}{2} m \dot{\boldsymbol{\xi}}^T \dot{\boldsymbol{\xi}}$ is the transnational kinetic energy, $T_{rot} = \frac{1}{2} \boldsymbol{\omega}^T I_{com} \boldsymbol{\omega}$ is the rotational kinetic energy, $P = mgz$ is the potential energy of quadrotor, m is the quadrotor mass, $\boldsymbol{\omega} = (p, q, r)$ is the vector of body axis rotational velocities, I_{com} is the inertia matrix and g is the gravity acceleration. Remark that when ϕ , and θ are smaller, the matrix ${}^B W_1$ of (1.9) is approximated to an identity matrix, then there will be $\boldsymbol{\omega} \approx \dot{\boldsymbol{\eta}}$. In most

of the research articles, this approximation is adopted to simplify the dynamic model [116]. F and τ are the external force and moment in the Earth frame.

From (1.9), we have

$$\omega = \begin{bmatrix} 1 & 0 & -\sin \theta \\ 0 & \cos \phi & \sin \phi \cos \theta \\ 0 & -\sin \phi & \cos \phi \cos \theta \end{bmatrix} \dot{\eta} = {}^B W_1 \dot{\eta} \quad (1.12)$$

Define

$$J(\phi, \theta) = {}^B W_1^T I_{com} {}^B W_1 \quad (1.13)$$

where

$$I_{com} = \begin{bmatrix} I_{xx} & 0 & 0 \\ 0 & I_{yy} & 0 \\ 0 & 0 & I_{zz} \end{bmatrix} \quad (1.14)$$

Therefore

$$T_{rot} = \frac{1}{2} \dot{\eta}^T J \dot{\eta} \quad (1.15)$$

Finally the Lagrangian is

$$L(q, \dot{q}) = \frac{1}{2} m \dot{\xi}^T \dot{\xi} + \frac{1}{2} \dot{\eta}^T J \dot{\eta} - mgz \quad (1.16)$$

Since the Lagrangian term L has no coupled term between $\dot{\xi}$ and $\dot{\eta}$, the Euler-Lagrange equation can be separated into dynamics equation of ξ and η .

- ξ dynamics equation:

$$\frac{d}{dt} \left(\frac{\partial L}{\partial \dot{\xi}} \right) - \frac{\partial L}{\partial \xi} = F \quad \Rightarrow \quad m \ddot{\xi} + \begin{bmatrix} 0 \\ 0 \\ mg \end{bmatrix} = F \quad (1.17)$$

where

$$F = {}^E R_B F_B = {}^E R_B \begin{bmatrix} 0 \\ 0 \\ F_T \end{bmatrix} \quad (1.18)$$

and $F_T = \sum_{i=1}^4 f_i$ is the main thrust where f_i with $i = 1, 2, 3, 4$ is the thrust produced by propellers. If the Earth frame coincides with the local frame before the quadrotor moving, then ${}^E R_B = {}^L R_B$ referring to (1.8).

- η dynamic equation is

$$\frac{d}{dt}\left(\frac{\partial L}{\partial \dot{\eta}}\right) - \frac{\partial L}{\partial \eta} = \tau \quad (1.19)$$

thus one obtains

$$J\ddot{\eta} + \dot{J}\dot{\eta} - \frac{1}{2}\frac{\partial}{\partial \eta}(\dot{\eta}^T J \dot{\eta}) = \tau \quad (1.20)$$

where

$$\tau = \begin{bmatrix} \tau_\phi \\ \tau_\theta \\ \tau_\psi \end{bmatrix} = \begin{bmatrix} l_{roll}k_c(\omega_1^2 - \omega_3^2) \\ l_{pitch}k_c(\omega_2^2 - \omega_4^2) \\ l_{yaw}c(-\omega_1^2 + \omega_2^2 - \omega_3^2 + \omega_4^2) \end{bmatrix} \quad (1.21)$$

$l_{roll}(l_{pitch})$ is the roll (pitch) motor to CoM distance, c is drag coefficient and k_c is thrust coefficient.

Define Coriolis-centripetal vector as

$$\begin{aligned} \bar{V}(\eta, \dot{\eta}) &= \dot{J}\dot{\eta} - \frac{1}{2}\frac{\partial}{\partial \eta}(\dot{\eta}^T J \dot{\eta}) \\ &= \left(\dot{J} - \frac{1}{2}\frac{\partial}{\partial \eta}(\dot{\eta}^T J)\right)\dot{\eta} \\ &= C(\eta, \dot{\eta})\dot{\eta} \end{aligned} \quad (1.22)$$

where $C(\eta, \dot{\eta})$ is the Coriolis term. Finally η dynamic equation is

$$J\ddot{\eta} = \tau - C(\eta, \dot{\eta})\dot{\eta} \quad (1.23)$$

Then the dynamic equations of quadrotor based on Euler-Lagrange approach are

$$m\ddot{\xi} + \begin{bmatrix} 0 \\ 0 \\ mg \end{bmatrix} = {}^E R_B \begin{bmatrix} 0 \\ 0 \\ F_T \end{bmatrix} \quad (1.24)$$

$$\dot{\eta} = \bar{\tau} \quad (1.25)$$

where $\bar{\tau} = J^{-1}(\tau - C(\eta, \dot{\eta})\dot{\eta}) = [\bar{\tau}_\phi, \bar{\tau}_\theta, \bar{\tau}_\psi]^T$.

Finally the dynamic equations of quadrotor system are

$$\ddot{x} = \frac{F_T}{m}(\cos \phi \sin \theta \cos \psi + \sin \phi \sin \psi) \quad (1.26)$$

$$\ddot{y} = \frac{F_T}{m}(\cos \phi \sin \theta \sin \psi - \sin \phi \cos \psi) \quad (1.27)$$

$$\ddot{z} = \frac{F_T}{m} \cos \phi \cos \theta - g \quad (1.28)$$

$$\ddot{\phi} = \bar{\tau}_\phi \quad (1.29)$$

$$\ddot{\theta} = \bar{\tau}_\theta \quad (1.30)$$

$$\ddot{\psi} = \bar{\tau}_\psi \quad (1.31)$$

Notice that in most cases of experiment, ϕ and θ are supposed to be small such that $\cos \theta \approx 1, \cos \phi \approx 1$ and $\sin \theta \approx \theta, \sin \phi \approx \phi$.

1.2.1.4 Linear parameter varying (LPV) model of quadrotor

The quadrotor model built in the previous part is a nonlinear one, which sometimes is not convenient for controller design. A LPV quadrotor model will be utilized hereafter. From (1.26)-(1.31), suppose that

$$\sigma = (x, y, \dot{x}, \dot{y}, \phi, \theta, z, \psi, \dot{\phi}, \dot{\theta}, \dot{z}, \dot{\psi})^\top$$

$$\bar{u} = \left(\frac{F_T \cos \phi \cos \theta}{m} - g, \bar{\tau}_\phi, \bar{\tau}_\theta, \bar{\tau}_\psi \right)^\top$$

then the system model can be represented in the following form

$$\dot{\sigma} = \bar{A}\sigma + B\bar{u},$$

and

$$\bar{A} = \bar{A}(\phi, \theta, \psi, F_T) = \begin{pmatrix} 0 & I & 0 & 0 & 0 & 0 \\ 0 & 0 & RE & 0 & 0 & 0 \\ 0 & 0 & 0 & 0 & I & 0 \\ 0 & 0 & 0 & 0 & 0 & I \\ 0 & 0 & 0 & 0 & 0 & 0 \\ 0 & 0 & 0 & 0 & 0 & 0 \end{pmatrix}, \quad B = \begin{pmatrix} 0 & 0 \\ 0 & 0 \\ 0 & 0 \\ 0 & 0 \\ \begin{pmatrix} \frac{1}{I_{xx}} & 0 \\ 0 & \frac{1}{I_{yy}} \end{pmatrix} & 0 \\ 0 & \begin{pmatrix} \frac{1}{m} & 0 \\ 0 & \frac{1}{I_{zz}} \end{pmatrix} \end{pmatrix}, \quad I = \begin{pmatrix} 1 & 0 \\ 0 & 1 \end{pmatrix} \quad (1.32)$$

$$E = E(\theta, \phi, F_T) := \begin{pmatrix} \frac{\sin \phi F_T}{\phi m} & 0 \\ 0 & \frac{\sin \theta \cos \phi F_T}{\theta m} \end{pmatrix}, \quad R = R(\psi) := \begin{pmatrix} \sin \psi & \cos \psi \\ -\cos \psi & \sin \psi \end{pmatrix} \quad (1.33)$$

Let us introduce the new variable $\zeta = T\sigma$ where T is the orthogonal matrix depending on ψ as follows

$$T = T(\psi) := \begin{pmatrix} R^{-1} & 0 & 0 & 0 & 0 & 0 \\ 0 & R^{-1} & 0 & 0 & 0 & 0 \\ 0 & 0 & I & 0 & 0 & 0 \\ 0 & 0 & 0 & I & 0 & 0 \\ 0 & 0 & 0 & 0 & I & 0 \\ 0 & 0 & 0 & 0 & 0 & I \end{pmatrix} \quad (1.34)$$

Thus the quadrotor model can be rewritten in the form

$$\dot{\zeta} = (A + D)\zeta + B\bar{u}, \quad \zeta(0) = \zeta_0 := T(\psi(0))\sigma_0 \quad (1.35)$$

where

$$A = \begin{pmatrix} 0 & I & 0 & 0 & 0 & 0 \\ 0 & 0 & E & 0 & 0 & 0 \\ 0 & 0 & 0 & 0 & I & 0 \\ 0 & 0 & 0 & 0 & 0 & I \\ 0 & 0 & 0 & 0 & 0 & 0 \\ 0 & 0 & 0 & 0 & 0 & 0 \end{pmatrix}, \quad D = D(\dot{\psi}) := \dot{T}T^{-1} \quad (1.36)$$

In the rest of this thesis, the controller design will be mainly based on this reformulated model (1.35).

1.2.2 Sensors used for quadrotor

In order to stabilize the quadrotor system, knowing some of the state information is necessary. Therefore selecting a reasonable sensor is very important for designing autonomous quadrotor. Consequently, a fast, reliable and high precise sensing system is important in the system controller design. Many kinds of sensors have been applied on quadrotor, some of them measure the value concerned the system itself, for example internal temperature of electronic chip. Other sensors like IMU and camera can extract information about the quadrotor and its environment, which is then used to get the motion and location information of quadrotor. In this thesis, we mainly talk about the latter type of sensors.

The main sensors used to measure the state of quadrotor are following:

- **Accelerometer:** Accelerometer measures the linear acceleration in body frame. It is relatively accurate in long time measurement since there is no drift and the center of Earth gravity does not move. However it is a noisy measurement which makes it unreliable in short time. A well tuning filter is necessary before using it in controller algorithm.
- **Gyroscope:** Gyroscope measures the angular velocity in degree/sec. It usually works with accelerometer to become a 6 DOF sensor fusion.
- **Magnetometer:** Magnetometer measures magnetic field strength in uT or Gauss (1 Gauss = 100 uT). It can be regarded as complementary information of accelerometer to provide a higher precision of yaw (heading direction). However it is usually affected by metal, and needs to be well calibrated according to different locations.
- **IMU (Inertial measurement unit):** 9 DOF IMU is a chip including 3-axes gyroscope, 3-axes magnetometer and 3- axes accelerometer.

Notice that all the measurements of above sensor are taken in **body frame**. The main sensors used to detect the environment are following:

- **Ultrasonic sensor:** Ultrasonic sensor is an instrument of measuring the distance to an object by using ultrasonic sound waves. The working principle is that it can generate high frequency sound waves which is then reflected from the boundaries of object to produce distinct echo patterns. The time between sending waves and receiving waves is the key information to determine the distance to an object.
- **Laser range finder(LRF):** LRF is another device to measure the distance to an object by laser beam. In general, most of the LRFs are based on the time of flight principle which is sending a laser pulse in a narrow beam towards the object and then measuring the time taken between sending and receiving. LRF is widely applied for 3D object recognition and modeling while providing a high precision scanning ability.
- **Infrared sensor:** Infrared sensor has two types: active and passive. Active infrared sensor both emits and detects the infrared radiation. Passive infrared sensor only measures the infrared light radiation from objects. Active infrared sensor estimates the distance by measuring the time taken between sending and receiving. However infrared sensor works only for shorter distance than ultrasonic sensors.

- **Image sensor:** Image sensor is a sensor that detects and transmits the information of making an image. The working principle is converting the attenuation of light (electromagnetic) waves into signals while the light (electromagnetic) passes through or reflects off the objects. The image sensor includes such as digital cameras, medical imaging equipment, night vision device and so on. These equipments can provide amount of information around robot's environment. However image processing requires powerful computation chips, it is generally finished on the ground station.
- **Pressure sensor:** Pressure sensor is a device for pressure estimation of gases or liquids. In aircraft, weather balloon and rocket, the pressure sensor could generate an altitude output in function of the measured pressure, which gives the altitude information based on the pressure. Similarly, pressure sensor used in submarine will provide the depth information based on the pressure estimation of liquids.
- **Global positioning system(GPS):** GPS is a space-based global navigation satellite system that can provide absolute location of object on the Earth. Most of the outdoor aircrafts are working based on the GPS. Combining with the information from IMU, a better estimation can be given after a data fusion. However GPS can't work independently for the indoor cases, where the GPS signal is weak and distance measurement is not accurate. In this case, other sensors such as IMU, LRF, ultrasonic sensor and image sensor could be a better choice for giving a relative or absolute location.

On Quanser's QDrone platform which is used during the work of this thesis, many sensors such as IMU, gyroscope, magnetometer and depth camera are equipped. To stabilize the quadrotor, and track some references, the controller and observer design of our work will be mainly based on the output data of IMU and the positioning system (section 1.4.1).

1.3 State of the art in quadrotor control

Quadrotor has been studied for a few decade, this section will give a short introduction of three types of popular controllers: linear controllers, nonlinear controllers and intelligent controllers.

1.3.1 Linear controllers

Linear controllers are the most popular algorithms. They are easy to tune and require less computation power than other algorithms.

1.3.1.1 Proportional Integral Derivative (PID)

PID controller is the most widely applied controller in the industry. Classical PID controller has several advantages such as easy to design and optimize the parameter, and has a good robustness. One important advantage of PID is that it can be applied in the case of without the knowledge of dynamic model of quadrotor. However, applying PID controller on the quadrotor may limit its performance, since quadrotor model is an under-actuated system with nonlinear terms.

Many researchers have already applied PID controller to quadrotor [10], [31]. Generally the quadrotor control structure includes inner loop and outer loop which stabilize attitude and position respectively [53], [97]. Of course, the control method of inner loop and outer loop may be different, for example, inner loop uses PID controller and outer loop is based on dynamic surface controller [48].

Fig 1.3 shows the general PID controller for the quadrotor.

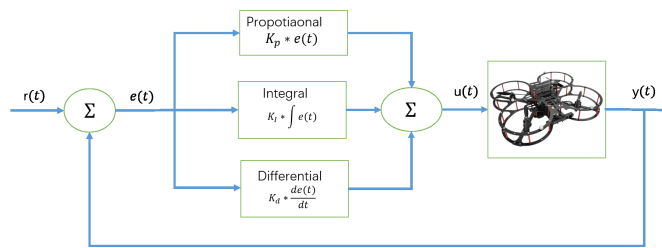


Figure 1.3 – PID controller on quadrotor

1.3.1.2 Linear Quadratic Regulator

The system operating by LQR optimal controller is based on finding a reasonable parameter gain while minimizing a suitable cost function [68]. Initially LQR was implemented for quadrotor OS4 [10] where LQR controller is compared with PID controller. LQR controller provides average results due to the model imperfections. It also works under wind and other perturbations [21]. Combining with LQR and Kalman filter, LQR is transformed into the Linear Quadratic Gaussian (LQG) algorithm while preserving the optimality of control. The idea behind is to have both optimal

controller and estimator simultaneously. The LQG with integral term was tested in [63] for stabilization of quadrotor attitude which has a good result in hovering case.

Fig 1.4 shows the general LQG controller for the quadrotor

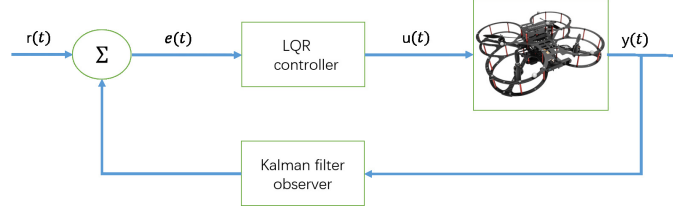


Figure 1.4 – LQG controller on quadrotor

1.3.1.3 Gain-scheduling

Gain-scheduling is one of the most commonly used controller design approaches for nonlinear systems (e.g. linear parameter varying and time varying system) requiring large operating region. It has a wide application in industrial [36]. Some examples of classical gain-scheduling (linearization based) can be found in [66], [94]. The main **advantage** of this kind of gain-scheduling is that it inherits the benefits of linear controller. However the main **drawback** is that each linear controller is only valid at the equilibrium point.

1.3.1.4 H_∞ control

Robust control methodology provides many techniques to control dynamical systems with unmodeled dynamics or bounded uncertainties. H_∞ is one of the important robust controllers to implement the system stabilization with guaranteed performance. Linear H_∞ controllers have been applied on the linearized model of quadrotor, for example in [64] a mixed linear H_∞ controller with robust feedback linearization is applied to a quadrotor model. The results show that the system becomes more robust under uncertainties and measurement noise when the weight functions are chosen properly.

1.3.2 Nonlinear algorithms

Many nonlinear control techniques such as feedback linearization, backstepping, sliding mode control (SMC), model predictive control (MPC) and adaptive control have been applied on quadrotors to overcome the shortcomings of linear control techniques.

1.3.2.1 Feedback Linearization

Feedback linearization is a nonlinear control design methodology allowing to design a nonlinear feedback and a change of coordinates which transform the original nonlinear control system in a linear one [37]. Some limitations of feedback linearization is that it requires more exact model to avoid the loss of precision due to linearization process [120]. This kind of method is frequently applied in robot control, but it still needs a control design after simplification [71], [47].

1.3.2.2 Backstepping Control

Backstepping controller is a well-known technique for underactuated system control. The basic idea behind is to break down the controller design problem of full system to a sequence of sub-systems and then stabilize each subsystem progressively [43], [99]. The advantage of this method is that the algorithm converges fast and guarantees boundedness of tracking error globally. The main limitation is the problem of explosion of terms. On quadrotor system, backstepping method can not only be used for orientation control [11], but also for position control [59], [33] under disturbance. The results show that backstepping method may provide a better performance than PID controller.

1.3.2.3 Sliding Mode Control (SMC)

Sliding mode control is a nonlinear control algorithm that works by applying a bounded discontinuous controller to the system [108], [45], [75], then forces the state variables converge to the prescribed surface and finally slides on it. It is also a method to reduce the dynamical dimension of system. The main advantage of SMC is that it does not need to simplify the dynamic model by linearization theory, while guaranteeing a good tracking result. Theoretically it is insensitive with respect to the model errors and other disturbances. However, the limitation of SMC is the discontinuity of controller that leads to the chattering problem. The magnitude of chattering is proportional to the gain applied. The chattering effect of SMC can be avoided in the control input by using the continuous approximation of the sign function [116]. Super twisting algorithm (STA) is another option to improve the robustness of system and to reduce chattering magnitude at same time [100], [57].

Fig 1.5 shows a SMC for the quadrotor.

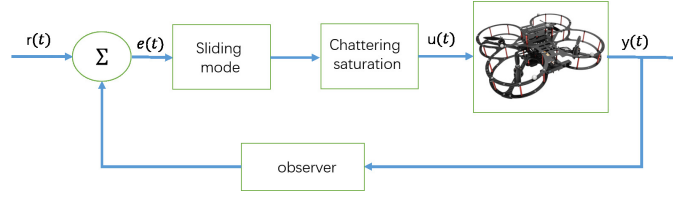


Figure 1.5 – SMC applied to quadrotor

1.3.2.4 Adaptive Control Algorithms

Adaptive control is the control of plants with unknown parameters, for example a time-varying system [22]. When the plant parameters change in time or unknown, the adaptive control needs to be considered to achieve or maintain the desired performance. In the presence of uncertainties, using prior and on-line information [14], [56], the controller will adapt itself. Comparing with robust control, adaptive control may provide a better performance for a large domain of uncertainty. Besides using a robust controller design method in adaptive control system may drastically improve the system performance as well [46]. For example, the adaptive control is able to stabilize the system with changes of gravity center of quadrotor while linear controller or feedback linearization controller may not work in this case [71].

Fig 1.6 shows an adaptive controller for the quadrotor.

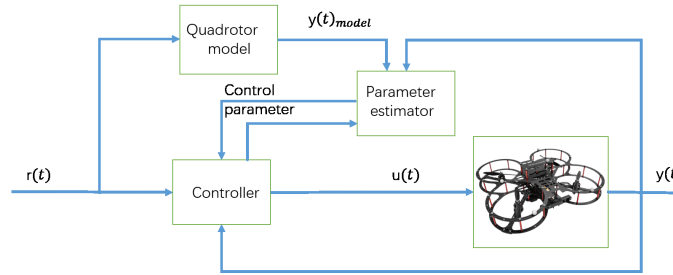


Figure 1.6 – adaptive controller applied to quadrotor

1.3.2.5 Model Predictive Control (MPC)

MPC is another nonlinear technique that has been applied on quadrotor. MPC uses dynamic model of system to estimate future system states while minimizing the error by solving optimal control problems. One important advantage of MPC is that the system subject to constraints can be stabilized through classical methods. For example, when the user gives a desired optimized reference to be tracked, the system will operate at the

optimized performance while satisfying the constraints. The key limit of MPC is that the optimization is on-line and requires relatively high computation power than other controllers. In the literature [93] combined MPC with nonlinear H_∞ controller for path tracking of quadrotor. A MPC for position and attitude control of quadrotor subject to wind disturbances was presented in [3].

1.3.3 Intelligent control

Intelligent control algorithms apply method of artificial intelligent approaches to control the system. The fussy logic and the neural networks are the most widely used methods, see [98].

Artificial neural networks are inspired by the central nervous system and brain. A robust neural network control is applied to the quadrotor in [67]. This adaptive neural network control is able to stabilize the quadrotor against modeling error and wind disturbance. It demonstrates a clear improvement of achieving a desired attitude. The neural network can also directly map the system state to the actuator command by reinforcement learning and implement the trajectory tracking [35].

Fig 1.7 shows the general block diagram of an fuzzy logic controller (FLC) for the quadrotor

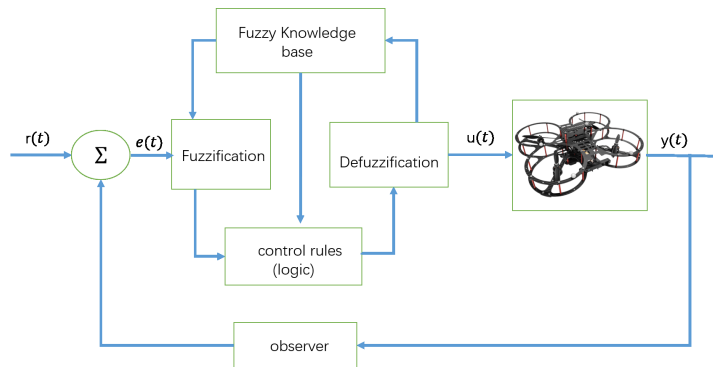


Figure 1.7 – FLC controller applied to quadrotor [120]

As evident from the literature, no single algorithm presents the best required features. The best performance usually requires a combination of robustness, adaptability, optimality, simplicity, tracking ability, fast response and disturbance rejection. PID controller is a good enough solution, since the industry appreciates it a lot. In this thesis we propose a methodology of for upgrading linear PID algorithms to homogeneous ones, which improves the control quality of linear PID but preserves all its advantages.

Vehicle	3	6	10
cameras	6	8	12
Minimum room size(m) (L×W×H)	4.5 × 4.5 × 2.5	6.0 × 6.0 × 2.5	7.0 × 7.0 × 2.5
WorkSpace(m) (L×W×H)	3.5 × 3.5 × 2	5.0 × 5.0 × 2.0	6.0 × 6.0 × 2.0

Table 1.2 – Recommended camera number and work space

1.4 Experiment setup: QDrone of Quanser

After reviewing the existing controller of quadrotor, the quadrotor platform (QDrone) used in this thesis is presented hereafter. QDrone platform globally involves a positioning system, one or several quadrotors, a ground control station PC and a Joystick. The control program is written in Matlab/Simulink, then compiled into C++ and finally uploaded to quadrotor.

1.4.1 Positioning system

The standard configuration of QDrone positioning system includes high speed cameras OptiTrack Flex 13 Fig. 1.8.



Figure 1.8 – OptiTrack Flex 13

The number of cameras, minimum size of room, and the corresponding approximate size of volume captured by camera depend on the number of quadrotors. Their relations are listed in Table 1.2.

In our lab, one quadrotor is enough for current experiments, which requires 6 cameras. A recommended configuration of camera mounted position is presented in Fig. 1.9.

Once the cameras are well mounted at the recommended location, the cameras need connect to the USB ports of OptiHubs, and then connect the OptiHub to the ground

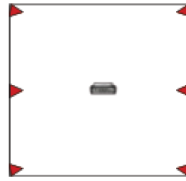


Figure 1.9 – 6 cameras configuration (top view)

control station PC by using USB port next to the power connector (see Fig. 1.10). Notice

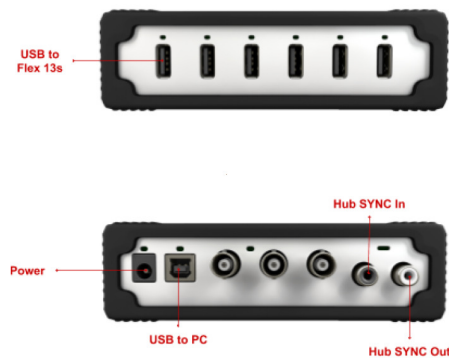


Figure 1.10 – OptiHubs

that one OptiHub can be only used to feed up to 6 cameras. The ports Hub SYNC In and Hub SYNC Out are designed for using more than one OptiHubs at same time. The global picture of location system can be seen in Fig. 1.11.

After well mounting the cameras, the next step is to do the calibration of cameras, which is very important to have a precision location of quadrotor. Here we use several markers to locate quadrotor (Fig. 1.12). More details about calibrating cameras can be found in [Quanser's documents](#).

1.4.2 Quadrotor hardware

Quadrotor system includes a powerful microcomputer called Intel Aero compute and a propulsion system. This microcomputer will focus on the calculation, send the command to propulsion system and then make the quadrotor stable.

1.4.2.1 Intel Aero Compute

The Intel Aero Compute (Fig. 1.13) has the following components

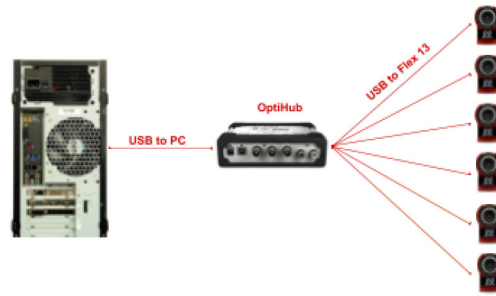


Figure 1.11 – 6 cameras with one OptiHub



Figure 1.12 – Markers used for location

- **One Processor:** Intel Atom x7-Z8750 quad-core 64-bit 2.56 GHz
- **Memory:** 4-GB LPDDR3-1600 RAM
- **Storage:** 32-GB eMMC
- **Sensors:** BM160 IMU (6-DOF triaxial accelerometer and gyroscope); BMM150 Magnetometer (3-axis geo-magnetic sensor); MS5611 Barometer (24 bit pressure and temperature sensor).
- **Wifi:** IEEE 802.11 b.g.n.ac-Intel Dual Band Wireless-AC 8620 2 × 2 MIMO.
- **Leds:** 1 tricolor and 1 orange user-programmable Led indicator

1.4.2.2 Propulsion system

The Intel Aero Compute is powerful and will send the command to propulsion system, which includes three main components: ESC (electronic speed control), motor and propeller, see Fig. 1.14 and Table 1.3.

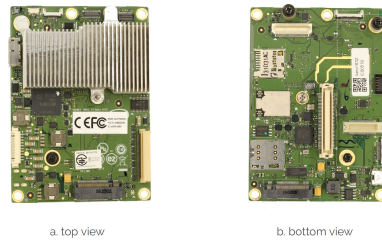


Figure 1.13 – QDrone's Inter Aero compute board



Figure 1.14 – Cobra 2100kv motor(left) and 6045 poly-carbonate propellers(right)

The command sent to ESC is throttle command (%), which is represented by u_p . Then the output signal of ESC will drive the motor with propellers to produce T_p thrust (N). The relation of u_p , T_p , and ω_p (angular velocity of propeller) can be presented by

$$T_p = c_t \left(\frac{\omega_p}{1000} \right)^2 \quad (1.37)$$

$$\omega_p = C_m u_p + \omega_b \quad (1.38)$$

where the parameters c_t , C_m and ω_b need to be determined by experiments. Table 1.4 gives the experimental results provided by QDrone producer. Besides the mechanical parameters provided in Table 1.5 will be used in research. The mapping between control input and thrust of each propeller is already designed by Quanser's engineer.

1.4.3 Matlab based design

The User Interface of QDrone platform is using Matlab/Simulink. Matlab is installed in the ground control station PC, the communication between quadrotor and Matlab is through the Router in Fig. 1.15.

QDrone as a Matlab based platform includes two main Simulink models. One is working as a server (see Fig. 1.16), that builds a bridge between cameras and quadrotor controller, and relays the position information to the second Simulink model (called commander model), see Fig. 1.17. Thus the main feedback controller can be imple-

Item	Description
Motor	
Kv	2100 RPM/V
Sator diameter/thickness	22.00mm/6.00mm
Stator slots/ magnet poles	12/14
Maximum continuous current	25 Amps
Time constant	40ms
Propellers	
Diameter	6.00 Inches
Pitch	4.5 Inches
Material	Polycarbonate

Table 1.3 – Motor and propeller

Parameter	Value	Units
C_m	15873	RPM/%
ω_b	1711	RPM
c_t	0.01935	N/(RPM) ²

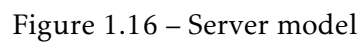
Table 1.4 – Parameter of propulsion system

Parameter	Description	Value	Units
g	Gravity	9.8	m/s^2
m	Total Mass	1.07	kg
L_{roll}	Roll motor distance	0.2136	m
L_{pitch}	Pitch motor distance	0.1758	m
I_{xx}	Roll Inertia	6.85×10^{-3}	kgm^2
I_{yy}	Pitch Inertia	6.62×10^{-3}	kgm^2
I_{zz}	Yaw Inertia	1.29×10^{-2}	kgm^2
k_c	Thrust Coefficient	1.93×10^{-8}	$\frac{N}{RPM^2}$
c	Drag Coefficient	0.26×10^{-9}	$\frac{Nm}{RPM^2}$

Table 1.5 – Quadrotor mechanical parameters



In this command Simulink model provided by Quanser, it contains the original feedback controller, and all its parameters have been well tuned by manufacturer.



1.5 Contribution and outline of thesis

1.5.1 Contribution

The main contributions of this thesis are following

- *A methodology for upgrading a linear controller to homogeneous one.* The homogeneous system has been studied a lot in previous works [119], [41], [6], [78]. However, the issues of practical implementation of homogeneous algorithms as well as their usefulness for control engineering practice have never been studied before. In our work, we proposed an easy way to apply this nonlinear homogeneous controller for the real nonlinear plant, i.e. Quanser's QDrone platform. We propose to use the gains of an already tuned linear PID controller provided by the manufacturer and design the nonlinear controller using a state dependent homogeneous scaling of these gains. Next, we develop a specific procedure of practical implementation of the homogeneous controller, which guarantees an improvement of the control quality.

The proposed methodology has been successfully validated on QDrone platform. The experiments showed the significant improvement of control precision, time response and robustness of the upgraded system.

- *A methodology for upgrading a linear observer to homogeneous one.* The idea of the homogeneous observer design is similar to the homogeneous controller design. We firstly design a Luenberger observer and then use the same gain of Luenberger to construct the homogeneous observer. The experiment with QDrone shows that the homogeneous observer also improves a lot the control precision.
- *A homogeneous controller design for quadrotor under time and state constraints.* Due to different working conditions and requirements, quadrotor may be asked to have a faster reaction and state constraints. We use full state feedback controller rather than the classical inner and outer loop structure. The simulation results prove that the system is finite time stabilized by the proposed homogeneous controller while satisfying all required constraints. This part of the research is purely theoretical.

1.5.2 Outline of thesis

This thesis is organized as follows

- Chapter 1 presents the context and the motivation of the research. Then it reviews the state of the art of quadrotor control, and modeling. A description of the experimental platform is provided as well.
- Chapter 2 surveys some mathematical tools required for analysis and design of homogeneous control systems. In particular, the elements of generalized homogeneity and implicit Lyapunov function theory are discussed.
- Chapter 3 contains the main result of the thesis. It presents some algorithms for homogeneous controllers design and proposes a methodology for methodology upgrading of linear PID controller to homogeneous ones. Both theoretical and experimental results are provided in this chapter. The experiment is based on the quadrotor platform.
- Chapter 4 applies the ideas from the previous chapter to the problem of homogeneous observer design and upgrades linear (Lunberger) observer. The theoretical results of this chapter are also experimentally validated on Quanser's QDrone platform.
- Chapter 5 deals with the theoretical analysis of quadrotor stabilization under time and state constraints. A full state homogeneous feedback controller design in this chapter makes the quadrotor to be stabilized in finite time under state constraints.
- Conclusion Finally we present the general conclusion and discuss some further research perspectives.

Mathematical backgrounds

In this chapter, the mathematical tools used in this thesis will be presented. The concepts of standard and generalized homogeneity are introduced. In particular, linear geometric homogeneity is considered. As a main tool for stability analysis of system, the Lyapunov function method is briefly discussed in the second section. Finally, elements of the theory of linear matrix inequalities (LMIs) are presented in the last section.

2.1 Homogeneity

Symmetry is a kind of invariance when some characteristics of an object do not change after a certain transformation. A simple example of a symmetry can be found in the geometry. For example in Fig. 2.1, the size of triangle is scaled, but the shape is invariant with respect to the scaling (dilation), which means the triangle is symmetric with respect to the dilation. The homogeneity is a symmetry with respect to the dilation.

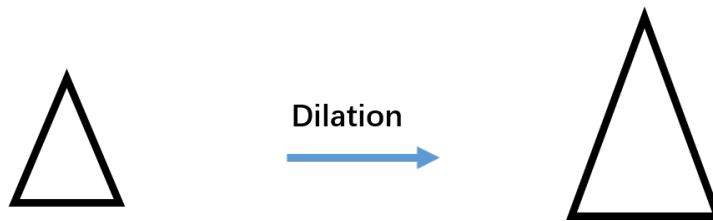


Figure 2.1 – Invariant shape after dilation

All linear and a lot of essentially nonlinear models of mathematical physics are homogeneous (symmetric) in a generalized sense, [70], [82]. Homogeneous models are utilized as local approximations of control systems [119], [4], if, for example, lin-

earization is too conservative, non-informative or simply impossible. Many methods of both linear and non-linear control theory can be applied for analysis and design of homogeneous control systems [79], [32], [101].

Homogeneous control laws appear as solutions of some classical control problems such as a minimum-time feedback control for the chain of integrators, see [19]. Most of the high-order sliding mode control and estimation algorithms are homogeneous in a generalized sense [50]. Homogeneity allows time constraints in control systems to be fulfilled easily by means of a proper tuning of the so-called homogeneity degree, [74]. Similarly to the linear case, stability of a homogeneous system implies its robustness (input-to-state stability) with respect to some classes of parametric uncertainties and exogenous perturbations, see [4], [6].

Many different homogeneous controllers are designed for linear plants (basically, for a chain of integrators), see e.g. [4], [20], [7], [50]. Usually, the existence of homogeneous controller of a certain form has been proven, however a proper tuning of control parameters also needs to be studied [110]. In addition, it is not clear if, in practice, a homogeneous controller could have a better performance than a well-tuned linear regulator. The following section provides a comparison of controller design based on homogeneity and linearity [78].

2.1.1 Homogeneity vs linearity in control system design

Quality of any control system is estimated by many *quantitative* indices (see e.g. [9], [102], [107]), which reflect control precision, energetic effectiveness, robustness of the closed-loop system with respect to disturbances, etc. From mathematical point of view, the design of a "good" control law is a multi-objective optimization problem. The mentioned criteria frequently contradict to each other, e.g. a time optimal feedback control could not be energetically optimal but it may be efficient for disturbance rejection [19]. In practice, an adjustment of a guaranteed (small enough) convergence time can be considered instead of minimum time control problem, and an exact convergence of systems states to a set-point is relaxed to a convergence into a sufficiently small neighborhood of this set-point.

A well-tuned linear controller, such as PID (Proportional-Integral-Differential) algorithm, guarantees a good enough control quality in many practical cases [9]. However, the further improvement of control performance using the same linear strategy looks impossible. Being a certain relaxation of linearity, the homogeneity could provide additional tools for improving control quality. In this context, it is worth knowing if

there exist some theoretical features of homogeneous systems, which may be useful (in practice) for a design of an advanced control system.

Finite-time and fixed-time stabilization

Finite-time and fixed-time stability are a rather interesting theoretical feature of homogeneous systems [7], [79], [55]. For example, if an asymptotically stable system is homogeneous of positive degree at infinity and homogeneous of negative degree at the origin, then its trajectory reaches the origin (a set point) in a fixed time independently of the initial condition [4]. This idea can be illustrated on the simplest scalar example

$$\dot{x}(t) = u(t), \quad t > 0, \quad x(0) = x_0,$$

where $x(t) \in \mathbb{R}$ is the state variable and $u(t) \in \mathbb{R}$ is the control signal. The control aim is to stabilize this system at the origin such that the condition $|u(x)| \leq 1$ must be fulfilled for $|x| \leq 1$.

- The classical approach gives the standard *linear* proportional feedback algorithm

$$u_{lin}(x) = -x,$$

which guarantees asymptotic (in fact, *exponential*) convergence to the origin of any trajectory of the closed-loop system:

$$|x(t)| = e^{-t}|x_0|.$$

- The globally homogeneous feedback of the form [7]

$$u_{ft}(x) = -\sqrt{|x|}\text{sign}(x).$$

stabilizes the system at the origin in a *finite-time*:

$$x(t) = 0, \quad \text{for } t \geq \mathfrak{T}(x_0).$$

The corresponding convergence time \mathfrak{T} depends on the initial condition $x(0) = x_0$, in particular, $\mathfrak{T}(x_0) = 2\sqrt{|x_0|}$ for the considered control law.

- The *fixed-time* stabilizing controller is locally homogeneous and has the form [77]:

$$u_{fxt}(x) = -\frac{1}{2}(|x|^{1/2} + |x|^{3/2})\text{sign}(x).$$

It guarantees a global uniform boundedness of the settling time, namely,

$$x(t) = 0, \quad t \geq 2\pi$$

for the considered control law.

Robustness issue

In general, homogeneity ensures robustness with respect to a larger class of uncertainties comparing to linear one. To show this, let us consider the simplest stabilization problem

$$\dot{x} = \lambda x + u$$

where $x \in \mathbb{R}$ is the system state, $\lambda > 0$ is an unknown constant parameter and $u \in \mathbb{R}$ is a state feedback to be designed. Since λ is unknown then any static linear feedback $u = -kx$ cannot guarantee a priori a boundedness of system trajectories. However, the homogeneous feedback

$$u = -kx^2 \text{sign}(x), \quad k > 0$$

always ensures practical stabilization of the system independently of the parameter λ . Indeed, estimating the derivative of the energy $V = x^2$ of the system along the trajectories we derive

$$\frac{d}{dt}x^2 \leq 2\lambda x^2 - 2k|x|^3 < 0 \quad \text{for} \quad |x| > \lambda/k.$$

This means boundedness of system trajectories and convergence to a zone:

$$\limsup_{t \rightarrow +\infty} |x(t)| \leq \frac{\lambda}{k}$$

Therefore, the homogeneous control system is robust with respect to larger class of uncertainties than the linear control system.

Elimination of an unbounded "peaking" effect

Finite-time and fixed-time stability is an interesting theoretical feature of homogeneous systems. However, a controllable linear system can be stabilized in a small neighbor-

hood of a set-point even by means of a static linear feedback. A time of convergence of trajectories from the unit ball into this neighborhood can be prescribed in advance by means of an appropriate tuning of the feedback gain. Such a stabilization is sufficient for many practical problems. The reasonable question in this case: *is there any advantage of a homogeneous controller comparing with a linear feedback?* The answer is yes, a homogeneous controller reduces much of the peaking effect (overshoot). The details can be found in chapter 3.

2.1.2 Dilations in \mathbb{R}^n

In this part, we first introduce the standard dilation, weighted dilation and then present the linear geometric dilation.

2.1.2.1 Standard homogeneity

In eighteen century, Leonhard Euler firstly introduced the homogeneity with respect to uniform dilation, which is called standard homogeneity given by the following definition.

Definition 2.1.1. Let n and m be two positive integers. A mapping $f : \mathbb{R}^n \mapsto \mathbb{R}^m$ is said to be standard homogeneous with degree $\mu \in \mathbb{R}$ with respect to the uniform dilation $x \rightarrow \lambda x$ iff

$$f(\lambda x) = \lambda^\mu f(x), \quad \forall \lambda > 0 \quad (2.1)$$

Definition 2.1.2. (Euler's theorem on standard homogeneity) Let $f : \mathbb{R}^n \mapsto \mathbb{R}^m$ be a differentiable mapping. Then f is standard homogeneous of degree μ iff $\forall i \in \{1, 2, \dots, m\}$

$$\sum_{j=1}^n x_j \frac{\partial f_i}{\partial x_j}(x) = \mu f_i(x), \quad \forall x \in \mathbb{R}^n \quad (2.2)$$

that the regularity of the homogeneous mapping f is related to its degree:

- if $0 \leq \mu < 1$ then either the Lipschitz conditions are not satisfied for function f at 0 or f is constant;
- if $\mu < 0$ then f is either discontinuous at the origin or zero vector field.

Let us present some examples:

- The continuous function

$$f : x = (x_1, x_2) \mapsto \begin{cases} \frac{x_1^{\frac{5}{2}} + x_2^{\frac{5}{2}}}{x_1^2 + x_2^2} & \text{if } x \neq 0 \\ 0 & \text{if } x = 0 \end{cases} \quad (2.3)$$

is homogeneous of degree $\frac{1}{2}$ and continues:

$$f(\lambda x) = \frac{(\lambda x_1)^{\frac{5}{2}} + (\lambda x_2)^{\frac{5}{2}}}{(\lambda x_1)^2 + (\lambda x_2)^2} = \lambda^{\frac{1}{2}} f(x)$$

- The function

$$f : x = (x_1, x_2) \mapsto \begin{cases} \frac{\lfloor x_1 \rfloor^{1/2} + \lfloor x_2 \rfloor^{1/2}}{x_1 + x_2} & \text{if } x_1 + x_2 \neq 0 \\ 0 & \text{else} \end{cases} \quad (2.4)$$

is standard homogeneous of degree $-\frac{1}{2}$.

- The polynomial function

$$f : x = (x_1, x_2) \rightarrow x_1^2 + x_1 x_2 + x_2^2$$

is homogeneous of degree 2.

$$f(\lambda x) = \lambda^2 x_1^2 + \lambda^2 x_1 x_2 + \lambda^2 x_2^2 = \lambda^2 f(x)$$

$$\frac{\partial f(x)}{\partial x_1} x_1 + \frac{\partial f(x)}{\partial x_2} x_2 = (2x_1 + x_2)x_1 + (2x_2 + x_1)x_2 = 2(x_1^2 + x_1 x_2 + x_2^2) = 2f(x)$$

- The functions

$$x \rightarrow f(x) = 1$$

$$x \rightarrow f(x) = \text{sign}(x_1^2 - x_2^2)$$

$$x \rightarrow f(x) = \frac{x_1 + x_2}{x_1 - x_2}$$

are homogeneous of degree 0.

- A combination of homogeneous functions is homogeneous as well. For example,

the function f given by

$$f(x) = \text{sign}\left(\frac{x_1 + x_2}{x_1 - x_2}\right)(x_1^2 + x_1x_2 + x_2^2)^{\frac{1}{4}}$$

is homogeneous of degree 0.5.

Theorem 2.1.1. *Let $f : \mathbb{R}^n \rightarrow \mathbb{R}^n$ be continuous standard homogeneous vector field of a degree $\mu \in \mathbb{R}$ such that the Cauchy problem*

$$\dot{x} = f(x), \quad x(0) = x_0 \in \mathbb{R}^n \quad (2.5)$$

admits a solution $x(t, x_0)$ defined for all $t > 0$. Then

$$x(\lambda^{1-\mu}t, \lambda x_0) = \lambda x(t, x_0), \quad \lambda > 0 \quad (2.6)$$

where $x(\cdot, \lambda x_0)$ is a solution to the same problem with the scaled initial condition $x(0) = \lambda x_0$

The main feature of homogeneous systems is global expansion of any local result. For example, local regularity of f (in a neighborhood of the origin) implies its global regularity, local stability of homogeneous system guarantees global stability, etc.

2.1.2.2 Weighted homogeneity

The standard homogeneity presented above is introduced by means of the uniform dilation $x \mapsto \lambda x, \lambda > 0$. Changing the dilation rule, a generalized homogeneity can be defined. The *Weighted dilation* (introduced by [119]) is defined as follows

$$(x_1, x_2, \dots, x_n) \mapsto (\lambda^{r_1}x_1, \lambda^{r_2}x_2, \dots, \lambda^{r_n}x_n) \quad (2.7)$$

where $\lambda > 0$ is the scaling factor and $r = [r_1, r_2, r_3, \dots, r_n]$ with $r_i > 0$ is the vector of weights, which specify dilation rate along different coordinates. If $r_1 = r_2 = r_3 = \dots = r_n = 1$ then weighted dilation becomes the uniform dilation. The transformation of coordinates for weighted dilation denoted as

$$x \mapsto \Lambda(r)x \quad (2.8)$$

is a linear mapping $\mathbb{R}^n \mapsto \mathbb{R}^n$ where

$$\Lambda(r) = \begin{bmatrix} \lambda^{r_1} & 0 & 0 & \cdots & 0 \\ 0 & \lambda^{r_2} & 0 & \cdots & 0 \\ 0 & 0 & \lambda^{r_3} & \cdots & 0 \\ \cdots & \cdots & \cdots & \cdots & \cdots \\ 0 & 0 & 0 & \cdots & \lambda^{r_n} \end{bmatrix} \quad (2.9)$$

Definition 2.1.3. ([119]) Let \mathbf{r} be a vector of weights, a function $f : \mathbb{R}^n \mapsto \mathbb{R}$ is said to be \mathbf{r} -homogeneous of degree μ iff

$$f(\Lambda(r)x) = \lambda^\mu f(x), \quad \forall x \in \mathbb{R}^n, \quad \forall \lambda > 0 \quad (2.10)$$

Example 2.1.1. A polynomial function

$$(x_1, x_2) \mapsto x_1^4 + x_1^2 x_2^4 + x_2^8 \quad (2.11)$$

is \mathbf{r} -homogeneous of degree 8 with respect to weighted dilation

$$(x_1, x_2) \mapsto (\lambda^2 x_1, \lambda x_2)$$

but it is not homogeneous with respect to the uniform dilation $(x_1, x_2) \mapsto (\lambda x_1, \lambda x_2)$

Definition 2.1.4. ([119]) Let \mathbf{r} be a vector of weights, a vector field $f : \mathbb{R}^n \rightarrow \mathbb{R}^n$ is said to be \mathbf{r} -homogeneous with degree μ iff

$$f(\Lambda(r)x) = \lambda^\mu \Lambda(r)f(x), \quad \forall x \in \mathbb{R}^n, \quad \forall \lambda > 0 \quad (2.12)$$

Here we see a difference about the degrees of two definitions: a vector field is standard homogeneous of degrees μ (in Definition 2.1.1) iff it is \mathbf{r} -homogeneous of degree $\mu - 1$ (in Definition 2.1.4). For example, every linear vector field is \mathbf{r} -homogeneous of degree 0.

Definition 2.1.5. ([30]) The system (2.5) is \mathbf{r} -homogeneous iff f is so.

Remark 2.1.1. A vector field f is \mathbf{r} -homogeneous of degree μ iff each coordinate function f_i is \mathbf{r} -homogeneous of degree $\mu + r_i$.

Example 2.1.2. • The function $\phi : x \rightarrow x_1^2 + x_2^4$ is $[2, 1]$ -homogeneous of degree 4.

- let $\alpha_1, \alpha_2, \dots, \alpha_n$ be strictly positive. The n -integrator system:

$$\begin{aligned} \dot{x}_1 &= x_2 \\ &\vdots \\ \dot{x}_{n-1} &= x_n \\ \dot{x}_n &= \sum_{i=1}^n k_i |x_i|^{\alpha_i} \end{aligned} \quad (2.13)$$

is \mathbf{r} -homogeneous of degree μ with $\mathbf{r} = [r_1, r_2, \dots, r_n]$, $r_i > 0$ iff the following relations hold

$$\begin{aligned} r_i &= r_n + (i - n)\mu, \quad \forall i \in \{1, 2, \dots, n\} \\ r_i \alpha_i &= r_n + \mu, \quad \forall i \in \{1, 2, \dots, n\} \end{aligned}$$

If we chose $r_n = 1$, it implies $\mu > -1$, then we have

$$\begin{cases} r_i = 1 + (i - n)\mu, & \forall i \in \{1, 2, \dots, n\} \\ \alpha_i = \frac{1+\mu}{1+(i-n)\mu}, & \forall i \in \{1, 2, \dots, n\} \end{cases} \quad (2.14)$$

If $\mu = -1$, then the vector field defining the system is discontinuous on each coordinate.

If $\mu = 0$, then it is a chain of integrators of n^{th} -order with linear feedback.

2.1.2.3 Linear geometric homogeneity

As explained in the standard and weighted homogeneity, once the dilation of system is established, many properties of nonlinear system can be studied easily. In order to extend the homogeneous property to more general systems, a more general form of dilation is introduced as follows

$$x \rightarrow \mathbf{d}(s)x, \quad s \in \mathbb{R}, \quad x \in \mathbb{R}^n \quad (2.15)$$

To become a dilation, the family of transformations $\mathbf{d}(s) : \mathbb{R}^n \rightarrow \mathbb{R}^n$ must satisfy certain restrictions [34], [41].

Definition 2.1.6. A mapping $\mathbf{d} : \mathbb{R} \mapsto \mathbb{R}^{n \times n}$ is called linear **dilation** in \mathbb{R}^n if it satisfies

- **Group property:** $\mathbf{d}(0) = I_n$ and $\mathbf{d}(t + s) = \mathbf{d}(t)\mathbf{d}(s) = \mathbf{d}(s)\mathbf{d}(t)$, $\forall t, s \in \mathbb{R}$;
- **Continuity property:** $s \mapsto \mathbf{d}(s)$ is continuous map, i.e.

$$\forall t, \epsilon > 0, \exists \sigma > 0 : |s - t| < \sigma \Rightarrow \|\mathbf{d}(s) - \mathbf{d}(t)\| \leq \epsilon$$

- **Limit property:** $\lim_{s \rightarrow -\infty} \|\mathbf{d}(s)x\| = 0$ and $\lim_{s \rightarrow +\infty} \|\mathbf{d}(s)x\| = +\infty$ uniformly on the unit sphere $S := \{x \in \mathbb{R}^n : \|x\| = 1\}$

In this thesis, we mainly deal with the following special form of dilation which is a matrix exponential linear dilation [72]

$$\mathbf{d}(x) = e^{sG_{\mathbf{d}}} = \sum_{i=0}^{+\infty} \frac{s^i G_{\mathbf{d}}^i}{i!}, \quad s \in \mathbb{R} \quad (2.16)$$

where $G_{\mathbf{d}}$ is an anti-Hurwitz matrix, that is called the generator of dilation \mathbf{d} . The matrix $G_{\mathbf{d}} \in \mathbb{R}^{n \times n}$ is defined as

$$G_{\mathbf{d}} = \lim_{s \rightarrow 0} \frac{\mathbf{d}(s) - I}{s} \quad (2.17)$$

and satisfies the following property

$$\frac{d}{ds} \mathbf{d}(s) = G_{\mathbf{d}} \mathbf{d}(s) = \mathbf{d}(s) G_{\mathbf{d}}, \quad s \in \mathbb{R} \quad (2.18)$$

Linear dilation in \mathbb{R}^n includes both uniform dilation

$$\mathbf{d}_1(s) = e^s I_n, \quad s \in \mathbb{R} \quad (2.19)$$

and weighted dilation

$$\mathbf{d}_2(s) = \begin{bmatrix} e^{r_1 s} & 0 & \dots & 0 \\ 0 & e^{r_2 s} & \dots & 0 \\ \dots & \dots & \dots & \dots \\ 0 & 0 & \dots & e^{r_n s} \end{bmatrix} \quad s \in \mathbb{R}, \quad r_i > 0, \quad i = 1, 2, \dots, n \quad (2.20)$$

corresponding to $G_{\mathbf{d}_1} = I_n$ and $G_{\mathbf{d}_2} = \text{diag}\{r_i\}$, respectively. This means that uniform dilation and weighted dilation are just particular cases of linear dilation. Weighted dilation is the generalized dilation as well. Everything what is not standard is generalized (it was called like this starting from [119]). In two dimensions case, the relation between uniform, weighted and linear dilation can be illustrated in Fig. 2.2, which depicts homogeneous curve $\{\mathbf{d}(s)x : s \in \mathbb{R}\}$ of three dilation groups

$$\mathbf{d}_1(s) = e^s I, \quad \mathbf{d}_2(s) = \begin{bmatrix} e^{2s} & 0 \\ 0 & e^s \end{bmatrix}, \quad \mathbf{d}_3(s) = e^{sG_{\mathbf{d}}} \quad (2.21)$$

For any position x , the homogeneous curve $\{\mathbf{d}(s)x : s \in \mathbb{R}\}$ is different for different

dilation. All the dilations satisfy the properties in Definition 2.1.6. For example, When $\mathbf{d}(s) = \mathbf{d}_1(s)$, for any value s , $\mathbf{d}_1(s)$ will scale x uniformly in all the directions, which makes the homogeneous curve $\{\mathbf{d}_1(s)x : s \in \mathbb{R}\}$ be a straight line. When s converges to $-\infty$ and $+\infty$, $\mathbf{d}_1(s)x$ converges to the origin and $+\infty$ respectively. Another important

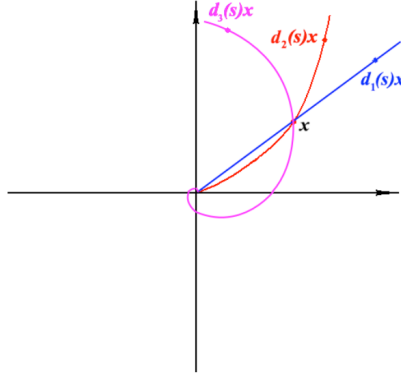


Figure 2.2 – uniform dilation \mathbf{d}_1 , weighted dilation \mathbf{d}_2 , generalized dilation \mathbf{d}_3 [85]

property of linear dilation in \mathbb{R}^n is its monotonicity, which plays an important role for analyzing homogeneous dynamical systems.

Definition 2.1.7. ([84]) The dilation \mathbf{d} is said to be **monotone** if $\|\mathbf{d}(s)x\| < 1$ as $s < 0, x \in \mathbb{R}$.

It is clear to see that the monotonicity of dilation depends on the norm $\|\cdot\|$. For instance the dilation

$$\mathbf{d}(s) = e^s \begin{bmatrix} \cos(s) & \sin(s) \\ -\sin(s) & \cos(s) \end{bmatrix} \quad \text{with} \quad G_{\mathbf{d}} = \begin{bmatrix} 1 & 1 \\ -1 & 1 \end{bmatrix} \quad (2.22)$$

is monotone on \mathbb{R}^2 , if we chose the norm $\|x\| = \sqrt{x^T P x}$ with $P = \begin{pmatrix} 1 & 1/\sqrt{2} \\ 1/\sqrt{2} & 1 \end{pmatrix} > 0$. However it is non-monotone if $P = \begin{pmatrix} 1 & 3/4 \\ 3/4 & 1 \end{pmatrix} > 0$. Monotonicity of dilation means that the linear map $\mathbf{d}(s) : \mathbb{R}^n \rightarrow \mathbb{R}^n$ is strong contraction if $s < 0$. Hence $\mathbf{d}(s)^{-1} = \mathbf{d}(-s)$ are strong expansions for $s > 0$. Other important properties of monotone dilation are listed as follows

Theorem 2.1.2. ([85]) The next four conditions are equivalent

- 1) the dilation \mathbf{d} is monotone;
- 2) $\lfloor \mathbf{d}(s)x \rfloor > 1, \quad \forall s > 0$

- 3) the continuous function $\|\mathbf{d}(\cdot)x\| : \mathbb{R} \rightarrow \mathbb{R}_+$ is strictly increasing for any fixed $x \in S$;
- 4) for any $x \in \mathbb{R}^n \setminus \{0\}$ there exists a unique pair $(s_0, x_0) \in \mathbb{R} \times S$ such that $x = \mathbf{d}(s_0)x_0$.

Definition 2.1.8. ([85]) The dilation \mathbf{d} is said to be strictly monotone on \mathbb{R}^n if $\exists \beta > 0$ such that $\|\mathbf{d}(s)\| \leq e^{\beta s}$ for $s \leq 0$.

The following theorem prove that any dilation \mathbf{d} is strictly monotone on \mathbb{R}^n if it is equipped with the weighted Euclidean norm $\|x\| = \sqrt{x^\top P x}$ provided that $P > 0$ and P satisfies (2.24).

Theorem 2.1.3. ([85]) Let \mathbf{d} be a dilation in \mathbb{R}^n then

- 1) all eigenvalues λ_i of the matrix $G_{\mathbf{d}}$ are placed in the right complex half-plane, i.e.

$$\Re(\lambda_i) > 0, \quad i = 1, 2, \dots, n; \quad (2.23)$$

- 2) there exists a matrix $P \in \mathbb{R}^{n \times n}$ such that

$$P G_{\mathbf{d}} + G_{\mathbf{d}}^\top P > 0, \quad P = P^\top > 0 \quad (2.24)$$

- 3) the dilation \mathbf{d} is strictly monotone with respect to the weighted Euclidean norm $\|\cdot\| = \sqrt{\langle \cdot, \cdot \rangle}$ induced by the inner product $\langle x, z \rangle = x^\top P z$ with P satisfying (2.24):

$$e^{\alpha s} \leq \lfloor \mathbf{d}(s) \rfloor \leq \|\mathbf{d}(s)\| \leq e^{\beta s} \quad \text{if } s \leq 0 \quad (2.25)$$

$$e^{\beta s} \leq \lfloor \mathbf{d}(s) \rfloor \leq \|\mathbf{d}(s)\| \leq e^{\alpha s} \quad \text{if } s \geq 0 \quad (2.26)$$

where

$$\alpha = \frac{1}{2} \lambda_{\max}(P^{\frac{1}{2}} G_{\mathbf{d}} P^{-\frac{1}{2}} + P^{-\frac{1}{2}} G_{\mathbf{d}}^\top P^{\frac{1}{2}})$$

$$\beta = \frac{1}{2} \lambda_{\max}(P^{\frac{1}{2}} G_{\mathbf{d}} P^{-\frac{1}{2}} + P^{-\frac{1}{2}} G_{\mathbf{d}}^\top P^{\frac{1}{2}})$$

2.1.3 Canonical homogeneous norm

In this part, we introduce the canonical homogeneous norm in \mathbb{R}^n , which is used for the analysis and design of homogeneous control system.

Definition 2.1.9. A continuous function $p : \mathbb{R}^n \rightarrow [0, +\infty)$ is said to be \mathbf{d} -homogeneous norm in \mathbb{R}^n if

- $p(u) \rightarrow 0$ as $u \rightarrow \mathbf{0}$;
- $p(\pm \mathbf{d}(s)u) = e^s p(u) > 0$ for $u \in \mathbb{R}^n \setminus \{\mathbf{0}\}$, $s \in \mathbb{R}$;

where \mathbf{d} is a dilation.

The functional p may not satisfy triangle inequality $p(u+v) \leq p(u)+p(v)$, so, formally, it is not even a semi-norm. However, many authors (see e.g. [4], [24], [5]) call functions satisfying the above definition by "homogeneous norm". We follow this tradition. For example, if the dilation is given by $\mathbf{d}(s) = \text{diag}\{e^{r_1 s}, e^{r_2 s}, \dots, e^{r_n s}\}$, a homogeneous norm $p : \mathbb{R}^n \rightarrow [0, +\infty)$ can be defined as follows [4]

$$p(u) = \sum_{i=1}^n |u_i|^{\frac{1}{r_i}}, \quad u = (u_1, u_2, \dots, u_n)^\top \in \mathbb{R}^n.$$

For strictly monotone dilations the so-called canonical homogeneous norm [80] can be introduced by means of a homogeneous projection to the unit sphere, which is unique in the case of monotone dilation due to Theorem 2.1.2.

Definition 2.1.10. ([80]) The function $\|\cdot\|_{\mathbf{d}} : \mathbb{R}^n \setminus \{\mathbf{0}\} \rightarrow (0, +\infty)$ defined as

$$\|x\|_{\mathbf{d}} = e^{s_x}, \text{ where } s_x \in \mathbb{R} : \|\mathbf{d}(-s_x)x\| = 1, \quad (2.27)$$

is called the canonical homogeneous norm, where \mathbf{d} is a strictly monotone dilation.

Obviously, $\|\mathbf{d}(s)x\|_{\mathbf{d}} = e^s \|x\|_{\mathbf{d}}$ and $\|x\|_{\mathbf{d}} = \|-x\|_{\mathbf{d}}$ for any $x \in \mathbb{R}^n$ and any $s \in \mathbb{R}$. The homogeneous norm defined by (2.27) was called canonical since it is induced by a canonical norm $\|\cdot\|$ in \mathbb{R}^n and

$$\|x\|_{\mathbf{d}} = 1 \quad \Leftrightarrow \quad \|x\| = 1$$

The monotonicity of the dilation group guarantees that the function $\|\cdot\|_{\mathbf{d}}$ is single-valued and continuous at the origin.

Theorem 2.1.4. ([80]) If \mathbf{d} is a strictly monotone linear dilation on \mathbb{R}^n then

- the function $\|\cdot\|_{\mathbf{d}} : \mathbb{R}^n \setminus \{\mathbf{0}\} \rightarrow \mathbb{R}_+$ given by (2.27) is single-valued and positive;
- $\|x\|_{\mathbf{d}} \rightarrow 0$ as $x \rightarrow \mathbf{0}$;
- if the norm in \mathbb{R}^n is defined as $\|x\| = \sqrt{x^\top P x}$ with $P \in \mathbb{R}^{n \times n}$ satisfying (2.24) then

$$\frac{\partial \|x\|_{\mathbf{d}}}{\partial x} = \|x\|_{\mathbf{d}} \frac{x^\top \mathbf{d}^\top (-\ln \|x\|_{\mathbf{d}}) P \mathbf{d} (-\ln \|x\|_{\mathbf{d}})}{x^\top \mathbf{d}^\top (-\ln \|x\|_{\mathbf{d}}) P G_{\mathbf{d}} \mathbf{d} (-\ln \|x\|_{\mathbf{d}}) x} \quad (2.28)$$

for any $x \neq \mathbf{0}$.

It is well known (see e.g. [5]) that the norm $\|x\| = \sqrt{x^\top P x}$ is a Lyapunov function for any stable linear system $\dot{x} = Ax, A \in \mathbb{R}^{n \times n}$. In this thesis, the canonical homogeneous norm ($\|x\|_{\mathbf{d}}$) will be considered as a Lyapunov function candidate for a class of homogeneous systems. It is easy to see that this Lyapunov function candidate is defined implicitly in (2.27). How to use this Lyapunov function candidate to design the homogeneous controller is presented in Chapter 3.

2.1.4 Generalized homogeneous functions and vectors fields

Vector fields which are homogeneous with respect to a dilation \mathbf{d} , have many useful properties for control design and state estimation of both linear and nonlinear systems. They are also important while analyzing the convergence rate.

Definition 2.1.11. ([85]) A function $h : \mathbb{R}^n \rightarrow \mathbb{R}$ is said to be \mathbf{d} -homogeneous of degree $\mu \in \mathbb{R}$ if

$$h(\mathbf{d}(s)x) = e^{\mu s} h(x), \quad \forall x \in \mathbb{R}^n \setminus \{0\}, \quad \forall s \in \mathbb{R} \quad (2.29)$$

Definition 2.1.12. ([85]) A vector field $f : \mathbb{R}^n \rightarrow \mathbb{R}^n$ is said to be \mathbf{d} -homogeneous of degree $\mu \in \mathbb{R}$ if

$$f(\mathbf{d}(s)x) = e^{\mu s} \mathbf{d}(s) f(x), \quad \forall x \in \mathbb{R}^n \setminus \{0\}, \quad \forall s \in \mathbb{R} \quad (2.30)$$

Example 2.1.3. The vector field may have different degrees of homogeneity depending on the dilation group. For example the vector field

$$f : \mathbb{R}^n \rightarrow \mathbb{R}^n, \quad f(x) = Ax, \quad x \in \mathbb{R}^n \quad (2.31)$$

with $A = \begin{pmatrix} 0 & I_{n-1} \\ 0 & 0 \end{pmatrix}$ is \mathbf{d} -homogeneous of degree $\mu \in [-1, 1]$ with dilation

$$\mathbf{d}(s) = \text{diag}\{e^{(n+(i-1)\mu)s}\}_{i=1}^n.$$

Lemma 2.1.5. ([85]) If $G_{\mathbf{d}} \in \mathbb{R}^{n \times n}$ is a generator of dilation, i.e. $\mathbf{d}(s) = e^{G_{\mathbf{d}} s}, s \in \mathbb{R}$, then this vector field $x \rightarrow Ax$ is \mathbf{d} -homogeneous of degree $\mu \in \mathbb{R}$ if and only if

$$AG_{\mathbf{d}} = (\mu I_n + G_{\mathbf{d}})A \quad (2.32)$$

Homogeneity allows a local property (e.g. Lipschitz continuity or differentiability) to be extended globally. For example, in [85] it is shown that a \mathbf{d} -homogeneous vector field is locally Lipschitz continuous (resp. differentiable) on $\mathbb{R}^n \setminus \{\mathbf{0}\}$ if and only if it

is Lipschitz continuous (differentiable) on the unit sphere $x^\top P x = 1$, where P satisfies (2.24).

Homogeneity of a function (or a vector field) is inherited by mathematical object induced by this function such as derivatives or solutions of differential equations. For example, if the right hand side of the following differential equation

$$\dot{\xi} = f(\xi), \quad t > 0, f : \mathbb{R}^n \rightarrow \mathbb{R}^n \quad (2.33)$$

is \mathbf{d} -homogeneous of degree μ then

$$x_{\mathbf{d}(s)x_0}(t) = \mathbf{d}(s)x_{x_0}(e^{\mu s}t), t > 0$$

where $x_{x_0}(t), t > 0$ denotes a solution of (2.33) with the initial condition $x(0) = x_0$.

Theorem 2.1.6. ([85]) *Let $f \in C(\mathbb{R}^n \setminus \{0\}, \mathbb{R}^n)$ be \mathbf{d} -homogeneous of degree $\mu \in \mathbb{R}$. The next claims are equivalent.*

- 1) *The origin of the system (2.33) is asymptotically stable.*
- 2) *The origin of the system*

$$\dot{z} = \|z\|^{1+\mu} \left(\frac{(I_n - G_{\mathbf{d}})z^\top z^P}{z^\top P G_{\mathbf{d}} z} + I_n \right) f\left(\frac{z}{\|z\|}\right) \quad (2.34)$$

is asymptotically stable, where $\|z\| = \sqrt{z^\top P z}$ with P satisfying

$$P G_{\mathbf{d}} + G_{\mathbf{d}}^\top P > 0, \quad 0 < P = P^\top \in \mathbb{R}^{n \times n}. \quad (2.35)$$

- 3) *For any matrix $P \in \mathbb{R}^{n \times n}$ satisfying (2.35) there exists a \mathbf{d} -homogeneous vector field $\Psi : \mathbb{R}^n \rightarrow \mathbb{R}^n$ of degree $\mathbf{0}$ such that $\Psi \in C^\infty(\mathbb{R}^n \setminus \{0\}, \mathbb{R}^n)$ is diffeomorphism on $\mathbb{R}^n \setminus \{0\}$, homeomorphism on \mathbb{R}^n , $\Psi(0) = 0$ and*

$$\frac{\partial(\Psi^\top(\xi)P\Psi(\xi))}{\partial \xi} f(\xi) < 0 \quad \text{if} \quad \Psi^\top(\xi)P\Psi(\xi) = 1. \quad (2.36)$$

Moreover, $\|\Psi\|_{\mathbf{d}} \in \mathbb{H}_{\mathbf{d}}(\mathbb{R}^n) \cap C^\infty(\mathbb{R}^n \setminus \{0\})$ is Lyapunov function for the system (2.33), where $\|\cdot\|_{\mathbf{d}}$ is the canonical homogeneous norm induced by $\|\xi\| = \sqrt{\xi^\top P \xi}$.

The latter theorem particularly proves that any asymptotically stable \mathbf{d} -homogeneous system is topologically equivalent to the standard homogeneous system (2.34) (homeomorphic on \mathbb{R}^n and diffeomorphic on $\mathbb{R}^n \setminus \{0\}$). The latter means that all results existing for standard and weighted homogeneous systems hold for \mathbf{d} -homogeneous ones.

The next proposition characterizes the convergence rates of the homogeneous system. Originally it has been proven in [65] for the weighted dilation.

Proposition 2.1.1. ([65]) *Let \mathbf{d} be a linear dilation in \mathbb{R}^n and $f : \mathbb{R}^n \rightarrow \mathbb{R}^n$. If the system (2.33) is \mathbf{d} -homogeneous of degree $\mu \in \mathbb{R}$ and its origin is locally uniformly asymptotically stable then*

- *for $\mu < 0$ it is globally uniformly finite-time stable, i.e. there exists a function $\mathcal{T} : \mathbb{R}^n \rightarrow [0, +\infty)$, which is locally bounded and continuous at $\mathbf{0}$, such that*

$$x_{x_0}(t) = \mathbf{0}, \quad \forall t \geq \mathcal{T}(x_0);$$

- *for $\mu = 0$ it is globally uniformly asymptotically stable;*
- *for $\mu > 0$ it is globally uniformly nearly fixed-time stable,*

$$\forall r > 0, \quad \exists \mathcal{T} = \mathcal{T}(r) > 0 \quad : \quad \|x_{x_0}(t)\| < r, \quad \forall t \geq \mathcal{T}, \quad \forall x_0 \in \mathbb{R}^n.$$

The definitions of finite-time and fixed-time stability mentioned in the previous proposition are discussed below.

2.2 Implicit Lyapunov function method

In this section, we consider the following system

$$\dot{x}(t) = f(x(t), t), \quad t > t_0, \quad x(t_0) = x_0 \quad (2.37)$$

where $f : \mathbb{R}^n \rightarrow \mathbb{R}^n$ is a continuous vector field with an equilibrium at the origin $f(0) = 0$. Meanwhile, assume that system (2.37) has unique solution in forward time outside the origin. Denote $x(t, t_0, x_0)$ as a trajectory of (2.37).

2.2.1 Stability notions

Stability is one of the most important properties of system. In this part, we survey stability notions following the paper [87].

Definition 2.2.1. *The origin of system (2.37) is said to be **Lyapunov stable** if $\forall \epsilon > 0$ and $\forall t_0 \in \mathbb{R}$, there exists a $\delta = \delta(\epsilon, t_0) \in \mathbb{R}_+$ such that if $\|x(0)\| \leq \delta$ then $\|x(t, t_0, x_0)\| \leq \epsilon$ for all $t > 0$, or more compactly: $\forall \epsilon > 0, \exists \delta > 0$ such that $\|x(0)\| < \delta \Rightarrow \|x(t, t_0, x_0)\| < \epsilon, \forall t \geq 0$.*

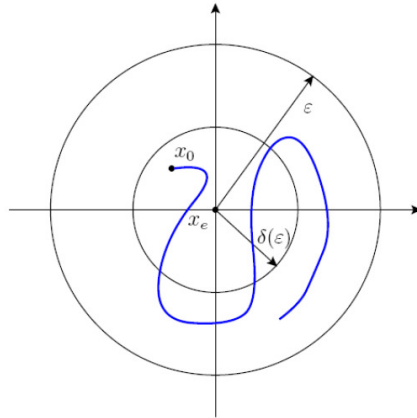


Figure 2.3 – Lyapunov stability

The above definition means, the origin is stable if small variation of initial condition close to zero implies small of variation of the system trajectory. If any condition of definition 2.2.1 is not satisfied, the origin is called unstable.

Remark 2.2.1. If the function δ of definition 2.2.1 does not depend on the initial time t_0 , then the origin is called **uniformly Lyapunov stable**. For example if $f(t, x)$ is a time-invariant system (independent of t) and origin is Lyapunov stable, then it is called **uniformly Lyapunov stable**.

Proposition 2.2.1. ([8]) If the origin of system (2.37) is Lyapunov stable, then $x(t) = 0$ is the unique solution of Cauchy of (2.37) with $x_0 = 0$ and $t_0 \in \mathbb{R}$.

Definition 2.2.2. The origin of system (2.37) is said to be **asymptotically attractive** (locally attractive), if $\forall t_0 \in \mathbb{R}_+$ there exists a set $\mathcal{U}(t_0) \subset \mathbb{R}^n : 0 \in \text{int}(\mathcal{U}(t_0))$ such that $\forall x_0 \in \mathcal{U}(t_0)$, $\lim_{t \rightarrow \infty} x(t, t_0, x_0) = 0$. The set $\mathcal{U}(t_0)$ is called attraction domain of system (2.37).

Notice that this attractivity does not guarantee the stability [109]. It only tells that any motion with initial state close to the equilibrium will finally converge to it.

Definition 2.2.3. An equilibrium point is **locally asymptotically stable** if it is both locally attractive and Lyapunov stable.

If the attraction domain is the whole state space, the system is called **Globally asymptotically stable**. In general the global asymptotic stability is harder to prove than the local one, but the two coincide in the case of homogeneous system.

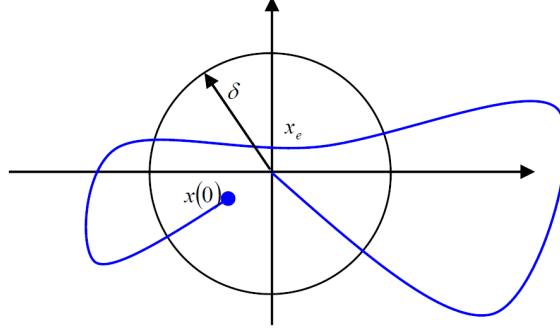


Figure 2.4 – Locally attractive

Definition 2.2.4. The origin of the system (2.37) is said to be **uniformly asymptotically attractive** if it is asymptotically attractive with a time-invariant attraction domain $\mathcal{U} \subset \mathbb{R}^n$ and for $\forall \delta \in \mathbb{R}_+, \forall \epsilon \in \mathbb{R}_+$, there exists $\mathcal{T} = \mathcal{T}(\delta, \epsilon) \in \mathbb{R}_+$ such that $x_0 \in B(\delta) \cap \mathcal{U}$ and $t_0 \in \mathbb{R}_+$ imply $x(t, t_0, x_0) \in B(\epsilon)$ for $t > t_0 + \mathcal{T}$.

The time-invariant attraction domain is the main difference between asymptotic attractivity and uniform asymptotic attractivity.

Definition 2.2.5. The origin of system (2.37) is said to be **uniformly asymptotically stable** if it is uniformly Lyapunov stable and uniformly asymptotic attractive.

If the attraction domain can be extended to \mathbb{R}^n i.e. $\mathcal{U} = \mathbb{R}^n$, then an uniformly asymptotically stable (attractive) origin of system (2.37) is called **globally uniformly asymptotically stable (resp. attractive)**. Notice that uniform asymptotic stability always implies asymptotic stability, and the converse proposition only holds for time-invariant systems.

In order to provide a better performance for control system, the rate of transition process need to be tuned somehow. Other concepts of stability such as exponential, finite-time and fixed-time stability can be used for this purpose.

Definition 2.2.6. The origin of system (2.37) is said to be **exponential stable** if $\exists \delta \in \mathbb{R}$, such that $\|x_0\| \leq \delta$ implies

$$\|x(t, x_0, t_0)\| \leq C \|x_0\| e^{-r(t-t_0)}, t > t_0 \quad (2.38)$$

for $C, r \in \mathbb{R}_+, t_0 \in \mathbb{R}_+$

The inequality (2.38) guarantees that the state trajectory will exponentially converge to the origin, which is the reason why it is called exponential stability. Obviously exponential stability implies Lyapunov stability and asymptotic stability.

Besides, another concept of stability is the so-called finite-time stability. Before introducing it, we will give the definition of settling time function.

Definition 2.2.7. The function $(x_0, t_0) \rightarrow \mathcal{T}(x_0, t_0)$ defined as $\mathcal{T}(x_0, t_0) = \inf\{\mathcal{T} \geq 0 : x(t, x_0, t_0) = 0, \forall t \geq \mathcal{T}\}$ is called the **settling-time function** of the system (2.37).

The settling time tells the moment when the trajectory of system reach origin.

Definition 2.2.8. The origin of the system (2.37) is said to be **finite-time attractive**, if $\mathcal{T}(x_0, t_0) < +\infty$ for any $x_0 \in \mathcal{U}(t_0)$ and any $t_0 \in \mathbb{R}$, where $\mathcal{U}(t_0)$ is, as before, an attraction domain.

The main difference between finite-time and asymptotic attractivity is the trajectory will reach origin in a finite time $\mathcal{T}(x_0, t_0)$ or $+\infty$.

Definition 2.2.9. ([96]) The system (2.37) is said to be **finite-time stable** if it is Lyapunov stable and finite-time attractive.

In other words, finite-time stability means the system will be stabilized at origin at settling time $\mathcal{T}(x_0, t_0)$.

If $\mathcal{U} = \mathbb{R}^n$, then the origin of (2.37) is called **globally finite-time stable**.

Proposition 2.2.2. ([8]) If the origin of system (2.37) is finite-time stable then it is asymptotically stable and $x(t, x_0, t_0) = 0$ for $t > t_0 + \mathcal{T}_0(t_0, x_0)$.

Definition 2.2.10. The origin of system (2.37) is said to be **uniformly finite-time attractive**, if it is finite-time attractive with a time-invariant attraction domain $\mathcal{U} \subseteq \mathbb{R}^n$.

Definition 2.2.11. ([70]) The origin of system (2.37) is said to be **uniformly finite-time stable**, if it is uniformly Lyapunov stable and uniformly finite-time attractive with a time-invariant attraction domain $\mathcal{U} \subseteq \mathbb{R}^n$. The origin of (2.37) is said to be **globally uniformly finite-time stable** if $\mathcal{U} = \mathbb{R}^n$.

Obviously, for time-invariant system, if it is finite-time stable then the settling time does not depend on initial time t_0 , i.e. $\mathcal{T} = \mathcal{T}(x_0)$. Notice that finite-time stability of time-invariant system does not imply the uniformly finite-time stable generally, which is different with Lyapunov and asymptotic stability. Besides uniform finite-time stability usually is the property of sliding mode system and more detail can be found in [51].

Definition 2.2.12. ([79]) The origin of system (2.37) is said to be **fixed-time attractive**, if it is uniformly finite-time attractive with an attractive domain \mathcal{U} and the settling time function $\mathfrak{T}(t_0, x_0)$ is bounded, i.e. there exists a $\mathfrak{T}_{max} \in \mathbb{R}_+$ such that $\mathfrak{T}(x_0, t_0) < \mathfrak{T}_{max}$ if $t_0 \in \mathbb{R}$ and $x_0 \in \mathcal{U}$.

Definition 2.2.13. [79] The origin of system 2.37 is said to be **fixed-time stable** if it is Lyapunov stable and fixed-time attractive.

The origin of (2.37) is said to be **globally fixed-time stable** if the attraction domain $\mathcal{U} = \mathbb{R}^n$. In the globally stable case, fixed-time stable has a faster convergence than finite-time.

Example 2.2.1. The system

$$\dot{x} = -x^{\frac{1}{2}} - x^{\frac{3}{2}}, x \in \mathbb{R}, t > t_0 \quad (2.39)$$

has following solutions for $t > t_0$

$$x(t, t_0, x_0) = \begin{cases} \text{sign}(x_0) \tan^2(\arctan(\|x_0\|^{\frac{1}{2}}) - \frac{t-t_0}{2}), & t \leq t_0 + 2\arctan(\|x_0\|^{\frac{1}{2}}) \\ 0, & t > t_0 + 2\arctan(\|x_0\|^{\frac{1}{2}}) \end{cases} \quad (2.40)$$

The solution $x(t, t_0, x_0)$ converges to origin in finite time and $x(t, t_0, x_0) = 0$ holds for all $t > t_0 + \pi$, which means the system is globally fixed-time stable with $\mathfrak{T}_{max} = \pi$.

2.2.2 Implicit Lyapunov function theorems

Implicit Lyapunov function combines two important notions from mathematical and stability analysis: Implicit Lyapunov function and Lyapunov function. A function V satisfying the following theorem (known as Lyapunov theorem) traditionally is called Lyapunov function.

Theorem 2.2.1. ([58]) Let $x = 0$ be an equilibrium point for (2.37), and $\mathcal{U} \subset \mathbb{R}^n$ be a domain containing $x = 0$. Let $V : \mathcal{U} \rightarrow \mathbb{R}$ be a continuously differentiable function such that

$$V(0) = 0, \quad V(x) > 0 \quad x \in \mathcal{U} \setminus \{0\} \quad (2.41)$$

$$\dot{V}(x) \leq 0 \quad x \in \mathcal{U} \quad (2.42)$$

Then, the equilibrium $x = 0$ is **stable**. Moreover, if

$$\dot{V}(x) < 0 \quad x \in \mathcal{U} \setminus \{0\} \quad (2.43)$$

the equilibrium $x = 0$ is **asymptotically stable**.

A classical form of Lyapunov function V is the quadratic form

$$V(x) = x^\top P x = \sum_{i=1}^n \sum_{j=1}^n p_{ij} x_i x_j \quad (2.44)$$

where P is a positive definite symmetric matrix.

Lemma 2.2.2. ([91]) *If a function $V : \mathbb{R}_+ \rightarrow \mathbb{R}_+$ satisfies the differential inequality*

$$\dot{V}(x(t)) \leq -\alpha V(x(t)) + \beta, \quad \alpha > 0, \beta > 0 \quad (2.45)$$

then

$$\overline{\lim}_{t \rightarrow \infty} V(x) \leq \frac{\beta}{\alpha} \quad (2.46)$$

Example 2.2.2. *Consider the pendulum dynamics with friction*

$$\ddot{\theta} + \frac{g}{l} \sin \theta + k\dot{\theta} = 0 \quad (2.47)$$

Suppose $x_1 = \theta, x_2 = \dot{\theta}, a = \frac{g}{l}$ then pendulum dynamics equation can be rewritten as

$$\begin{aligned} \dot{x}_1 &= x_2 \\ \dot{x}_2 &= -a \sin x_1 - kx_2 \end{aligned}$$

Let us study the stability of equilibrium point at $x_1 = x_2 = 0$. Propose a Lyapunov function candidate

$$V(x) = \frac{1}{2}x_2^2 + a(1 - \cos x_1), \quad x_1 \in [-2\pi, 2\pi] \quad (2.48)$$

Obviously we have $V(0) = 0$ and $V(x) > 0$. If $x_1 \neq 0$ and $x_2 \neq 0$, the derivative of $V(x)$ is

$$\dot{V}(x) = a\dot{x}_1 \sin x_1 + x_2 \dot{x}_2 = -kx_2 \quad (2.49)$$

Thus the condition of (2.41) and (2.43) are satisfied, which means the point $x_1 = x_2 = 0$ is asymptotically stable.

Example 2.2.3. *If a linear system $\dot{x} = Ax$ is asymptotically stable, then $V(x) = x^\top P x$ can be its Lyapunov function, where the positive definite matrix P is solved by the following Lyapunov equation*

$$A^\top P + PA = -Q \quad (2.50)$$

where Q is an arbitrary positive definite matrix.

If there exist a Lyapunov function $V(\mathbf{x})$ for system $\dot{\mathbf{x}} = \mathbf{f}(\mathbf{x})$, such that

$$S = \{\mathbf{x} | V(\mathbf{x}) < c\} \quad (2.51)$$

is bounded, then S is a positively invariant set i.e. **a region where every trajectory starts from there then never leaves it.**

Theorem 2.2.3. ([8]) Suppose there exists a continuous proper function $V(x) : \mathbb{R}^n \rightarrow \mathbb{R}$ such that the following conditions hold

- 1) V is positive definite.
- 2) There exist $c > 0$ and $\alpha \in (0, 1)$ and an open neighborhood $\mathcal{U} \subseteq d$ of the origin such that

$$\dot{V}(x) + c(V(x))^\alpha \leq 0, \quad x \in \mathcal{U} \setminus \{0\} \quad (2.52)$$

then the origin is **finite-time stable** equilibrium of system (2.37) and the settling-time function is

$$\mathfrak{T}(x) \leq \frac{1}{c(1-\alpha)} V(x)^{1-\alpha} \quad (2.53)$$

If additionally $\mathcal{U} = \mathbb{R}^n$ then the origin is a **globally finite-time stable** equilibrium of (2.37).

The following result provides a converse of Theorem 2.2.3

Theorem 2.2.4. ([8]) Suppose the origin is a finite-time stable equilibrium of (2.37), and the settling-time function $\mathfrak{T}(x) : \mathcal{U} \rightarrow \mathbb{R}$ is continuous at $\mathbf{0}$. Let $\alpha \in (0, 1)$, then there exists a continuous function $V : \mathcal{U} \rightarrow \mathbb{R}$ such that the following conditions are satisfied

- 1) V is positive definite
- 2) \dot{V} is real valued and continuous on \mathcal{U} and $c > 0$ such that

$$\dot{V}(x) + c(V(x))^\alpha \leq 0, \quad x \in \mathcal{U} \quad (2.54)$$

Theorem 2.2.5. ([87]) Let a continuous function $V : \mathbb{R}^n \rightarrow \mathbb{R}$ be proper on an open connected set $\mathcal{U} : 0 \in \text{int}(\mathcal{U})$. If for a real number $\mu \in (0, 1)$, $\nu \in \mathbb{R}_+$, $r_\mu \in \mathbb{R}_+$, $r_\nu \in \mathbb{R}_+$, the following inequality

$$\dot{V}(x) \leq \begin{cases} -r_\mu V^{1-\mu}(x) & \text{for } x \in \mathcal{U} : V(x) \leq 1 \\ -r_\nu V^{1+\nu}(x) & \text{for } x \in \mathcal{U} : V(x) \geq 1 \end{cases} \quad t > t_0, x \in \mathcal{U} \quad (2.55)$$

holds, then the origin of system (2.37) is fixed-time stable equilibrium point with the maximum settling time

$$\mathfrak{T}(x) \leq \mathfrak{T}_{\max} \leq \frac{1}{\mu r_\mu} + \frac{1}{\nu r_\nu} \quad (2.56)$$

If $\mathcal{U} = \mathbb{R}^n$ and function V is radially unbounded then the origin of (2.37) is said to be **globally fixed-time stable**.

The above theorems state the result involving the Lyapunov function in an explicit way, however, it is challengeable to find such an explicit function for some systems, which is the main reason to use implicit method. In mathematics, the implicit function is a relation of the form $G(x, y) = 0$, that defines the variable x, y implicitly rather than define explicitly $y = g(x)$. In order to find the function $x \rightarrow g(x)$ that defines the variable y , one needs to solve the equation $G(x, y) = 0$ with respect to y . The first question needs to be answered is under which condition there exists a unique solution of $G(x, y) = 0$. The following classical result can be found in [42].

Theorem 2.2.6. Implicit function theorem Assume that a function $G : \mathbb{R}^n \times \mathbb{R}^m \rightarrow \mathbb{R}^n$ is continuously differentiable at each point (x, y) of an open set $S \subset \mathbb{R}^n \times \mathbb{R}^m$. Let x_0, y_0 be a point in S such that

- $G(x_0, y_0) = 0$
- Jacobian matrix $\left[\frac{\partial G}{\partial y} \right](x_0, y_0)$ is nonsingular.

Then there exists a neighborhood set $\mathcal{U} \subset \mathbb{R}^n$ of x_0 and $Y \subset \mathbb{R}^m$ of y_0 such that for all $x \in \mathcal{U}$, the equation $G(x, y) = 0$ has a unique solution $y \in Y$. Moreover this solution can be given as $y = g(x)$, where g is continuously differentiable at $x = x_0$.

The next theorem combines Lyapunov and Implicit function theorem.

Theorem 2.2.7. ([1]) If there exists a continuous function

$$\begin{aligned} Q : \mathbb{R}_+ \times \mathbb{R}^n &\rightarrow \mathbb{R} \\ (V, x) &\rightarrow Q(V, x) \end{aligned}$$

satisfying the conditions

C1) Q is continuously differentiable outside the origin;

C2) for any $x \in \mathbb{R}^n \setminus \{0\}$ there exists $V \in \mathbb{R}_+$ such that $Q(V, x) = 0$;

C3) let $\Omega = \{(V, x) \in \mathbb{R}_+ \times \mathbb{R}^n : Q(V, x) = 0\}$ and

$$\lim_{x \rightarrow 0, (V, x) \in \Omega} V = 0^+, \quad \lim_{V \rightarrow 0^+, (V, x) \in \Omega} \|x\| = 0, \quad \lim_{\|x\| \rightarrow \infty, (V, x) \in \Omega} V = +\infty$$

C4) $\frac{\partial Q(V, x)}{\partial V} < 0$ for all $V \in \mathbb{R}_+$ and $x \in \mathbb{R}^n \setminus \{0\}$;

C5)

$$\frac{\partial Q(V, x)}{\partial x} y < 0$$

for all $(V, x) \in \Omega$,

then the origin of system is globally uniformly asymptotically stable.

If continuous function Q satisfies C1)-C5), then it is called **implicit Lyapunov function (ILF)**. C1) guarantees the smoothness of Lyapunov function. C2) and the first two limits of C3) imply the positive definite property of Lyapunov function. The third limit of C3) provides the radial unboundedness of Lyapunov function. C4) is required to have a unique Lyapunov function as a solution of equation $Q(V, x) = 0$. C5) is to guarantee that the derivative of Lyapunov function to be negative.

Theorem 2.2.8. ([86]) If there exists a continuous function $Q : \mathbb{R}_+ \times \mathbb{R} \rightarrow \mathbb{R}$ that satisfies the conditions C1) – C4) of theorem 2.2.7 and following condition

C6) there exist $c > 0$ and $0 < \mu \leq 1$ such that

$$\frac{\partial Q(V, x)}{\partial x} y \leq c V^{1-\mu} \frac{\partial Q(V, x)}{\partial V}$$

for $(V, x) \in \Omega$, then the origin of the system is **globally uniformly finite-time stable** and $\mathfrak{T}(x_0) \leq \frac{V_0^\mu}{c\mu}$, where $Q(V_0, x_0) = 0$

Theorem 2.2.9. ([86]) If there exists two function Q_1 and Q_2 that satisfy the conditions C1) – C4) of theorem 2.2.7 and the following conditions

C7) $Q_1(1, x) = Q_2(1, x)$ for all $x \in \mathbb{R}^n \setminus \{0\}$

C8) there exists $c_1 > 0$ and $0 < \mu < 1$ such that the inequality

$$\frac{\partial Q_1(x, V)}{\partial x} y \leq c_1 V^{1-\mu} \frac{\partial Q_1(x, V)}{\partial V} \tag{2.57}$$

holds for all $V \in (0, 1]$ and $x \in \mathbb{R}^n \setminus \{0\}$ satisfying $Q_1(x, V) = 0$

C9) there exists $c_2 > 0$ and $0 < \nu < 1$ such that the inequality

$$\frac{\partial Q_2(x, V)}{\partial x} y \leq c_2 V^{1+\nu} \frac{\partial Q_2(x, V)}{\partial V} \quad (2.58)$$

holds for all $V \geq 1$ and $x \in \mathbb{R}^n \setminus \{0\}$ satisfying $Q_2(x, V) = 0$

then the system (2.37) is **globally fixed-time stable** with settling-time estimate $\mathcal{T}(x_0) \leq \frac{1}{c_1 \mu} + \frac{1}{c_2 \nu}$.

In chapters 3-5, we use the canonical homogeneous norm (see Definition 1.1.10) as an implicit Lyapunov function candidate for a homogeneous system. In many cases, such a selection allows us to reduce the tuning of parameters of homogeneous controller/observer by solving system of Linear Matrix Inequalities considered in the next section

2.3 Linear Matrix Inequalities

2.3.1 Definitions and illustrative examples

Definition 2.3.1. ([13]) A linear matrix inequality is an inequality

$$F(x) > 0 \quad (2.59)$$

where F is an affine mapping of a finite-dimensional vector space \mathbb{X} to a set of Hermitian \mathbb{H} or a set of symmetric matrix \mathbb{S} .

A matrix B is called Hermitian matrix if and only if

$$B = B^* = \overline{B}^\top$$

If B is a real matrix, then a Hermitian matrix is called **symmetric matrix**. The following property of Hermitian matrix is very useful while dealing with control problem.

If a square matrix P is Hermitian if and only if it satisfies

$$\langle \omega, Pv \rangle = \langle P\omega, v \rangle \quad (2.60)$$

for any pair of vector v, ω and $\langle \cdot, \cdot \rangle$ is inner product.

In the control theory, linear matrix inequality(LMI) is general an expression in the form of

$$F(x) = F_0 + x_1 F_1 + x_2 F_2 + \dots + x_m F_m > 0 \quad (2.61)$$

where

- $x = (x_1, x_2, \dots, x_m)$ is a unknown vector of n real numbers, called decision variables.
- $F_0, F_1, \dots, F_m \in \mathbb{R}^{n \times n}$ are real symmetric matrix,i.e.

$$F_i = F_i^\top, \quad i = 0, 1, \dots, m$$

- the inequality > 0 in (2.61) means that $F(x)$ is positive definitive, which is

$$\omega^\top F(x) \omega > 0$$

for any ω non-zero real vector. Since $F(x)$ is real symmetric matrix, the eigenvalues of $F(x)$ are also real and positive definite, i.e., $\lambda(F(x)) > 0$. In other words, the minimal eigenvalue of $F(x)$ is positive

$$\lambda_{\min}(F(x)) > 0$$

It is clear that (2.59) is a strict LMI, but we may also encounter the nonstrict LMI

$$F(x) \geq 0 \quad (2.62)$$

Strict LMI (2.59) and nonstrict LMI (2.62) are highly related, since for any nonstrict LMI $F(x)$, there is

$$\tilde{F}(x) = F(x) + Q \geq Q > 0 \quad (2.63)$$

for each positive definite matrix Q . In the following discussion, we will consider only the strict LMI in the form of (2.59).

Definition 2.3.2. ([90]) *A system of LMIs is a finite set of LMIs*

$$F_1(x) < 0, F_1(x) < 0, \dots, F_m(x) < 0 \quad (2.64)$$

LMIs system in (2.64) can be expressed as a single LMI in the form of following

diagonal matrix:

$$F(x) := \begin{bmatrix} F_1(x) & 0 & \cdots & 0 \\ 0 & F_2(x) & \cdots & 0 \\ \vdots & \vdots & \ddots & \vdots \\ 0 & 0 & \cdots & F_m(x) \end{bmatrix} < 0 \quad (2.65)$$

Obviously $F(x)$ is symmetric matrix for all x and the eigenvalue set of $F(x)$ is the union of eigenvalues sets of $F_1(x), F_2(x), \dots, F_m(x)$. Then we can conclude that multiple LMI constraints could always transform into a single LMI constraint.

When considering the constraints, LMIs can be written in the following form

$$\begin{cases} F(x) < 0 \\ Ax = b \end{cases} \quad (2.66)$$

where $F : \mathbb{R}^n \rightarrow \mathbb{S}$, A and b are matrices with appropriate dimension. By solving the equality $Ax = b$, (2.66) is equivalent to the following LMI

$$\hat{F}(x) < 0, \quad x \in M \quad (2.67)$$

where the set $M = \{x, x \in \mathbb{R}^n | b - Ax = 0\}$.

Example 2.3.1. Consider a linear autonomous system

$$\dot{x} = Ax \quad (2.68)$$

where $A \in \mathbb{R}^{n \times n}$. In order to study the stability of system, here we use Lyapunov method. Suppose there is a Lyapunov function candidate

$$V(x) = x^\top P x \quad (2.69)$$

where matrix $P > 0$ and is to be found by LMI.

If the derivative of $V(x)$ satisfies

$$\dot{V}(x) = x^\top P A x + x^\top A^\top P x \leq 0 \quad (2.70)$$

$$\Leftrightarrow PA + A^\top P \leq 0 \quad (2.71)$$

then the system (2.68) is stable at the origin. Therefore, we need to seek the feasible matrix P

satisfying the following two LMIs

$$\begin{cases} -P < 0 \\ PA + A^\top P \leq 0 \end{cases} \quad (2.72)$$

2.3.2 S-procedure and Schur complement

In order to transform a stability analysis or control design problem to LMI, certain procedures are frequently used. In this section, we recall some of them such as S-Lemma, Schur complement and Λ -inequality. The celebrated linear algebraic result named **S-Procedure** (or S-Lemma) is known also as Finsler's lemma [117]. The following theorem is about the S-procedure for two quadratic forms.

Theorem 2.3.1. *Let matrices $F_0 = F_0^\top, F_1 = F_1^\top \in \mathbb{R}^{n \times n}$, the following two claims are equivalent*

- $\exists \lambda \in \mathbb{R}$ such that the condition

$$F_0 + \lambda F_1 > 0 \quad (2.73)$$

-

$$z^\top F_1 z = 0 \Rightarrow z^\top F_0 z > 0 \quad z \in \mathbb{R}^n \setminus \{0\} \quad (2.74)$$

The next theorem is about S-procedure for several quadratic forms.

Theorem 2.3.2. *Let $F_0 = F_0^\top, F_1 = F_1^\top, \dots, F_m = F_m^\top \in \mathbb{R}^{n \times n}$, if there exists $\tau_1, \tau_2, \dots, \tau_m \geq 0$ such that*

$$F_0 \geq \tau_1 F_1 + \tau_2 F_2 + \dots + \tau_m F_m \quad (2.75)$$

then we have

$$x^\top F_1 x \geq 0, \dots, x^\top F_m x \geq 0 \Rightarrow x^\top F_0 x \geq 0 \quad (2.76)$$

Notice that the theorem above is only a sufficient condition, which is called lossy S-procedure.

Theorem 2.3.3. [Schur Complement] *Let $F : \mathbb{R}^n \rightarrow \mathbb{S}$ be the following affine mapping*

$$F = \begin{bmatrix} A & B \\ C & D \end{bmatrix} \quad (2.77)$$

where A, D are square matrices. The following three statements are equivalent.

$$(1) \quad F < 0 \quad (2.78)$$

$$(2) \quad \begin{cases} A < 0 \\ D - CA^{-1}B < 0 \end{cases} \quad (2.79)$$

$$(3) \quad \begin{cases} D < 0 \\ A - BD^{-1}C < 0 \end{cases} \quad (2.80)$$

The next auxiliary result is usually called Λ -matrix inequality.

Lemma 2.3.4. [Λ -matrix inequality] For any matrices $X, Y \in \mathbb{R}^{n \times m}$ and any symmetric positive definite matrix $\Lambda \in \mathbb{R}^{n \times n}$, the following inequality holds

$$X^\top Y + Y^\top X \leq X^\top \Lambda X + Y^\top \Lambda^{-1} Y \quad (2.81)$$

Moreover, the next one also holds

$$(X + Y)^\top (X + Y) \leq X^\top (I + \Lambda) X + Y^\top (I + \Lambda^{-1}) Y \quad (2.82)$$

Notice that if X, Y are two scalars, it becomes a quadratic inequality.

The proofs of above results can be found in [91].

2.3.3 Examples of LMIs

By using the techniques presented above, the following examples are to show how to formulate some inequalities in the form of LMIs.

Example 2.3.2. The matrix norm constraint such as

$$\|X\| < 1 \quad \Rightarrow \quad I_{n \times n} - X^\top X > 0, \quad X \in \mathbb{R}^{n \times n} \quad (2.83)$$

can be represented as

$$\begin{bmatrix} I_{n \times n} & X \\ X^\top & I_{n \times n} \end{bmatrix} > 0 \quad (2.84)$$

Example 2.3.3. The weighted norm constraint

$$c^\top P^{-1} c < 1 \quad (2.85)$$

where $c \in \mathbb{R}^n, 0 < P \in \mathbb{R}^{n \times n}$ depending affinely on x , can be rewritten in the following form

$$\begin{bmatrix} P & c \\ c^\top & 1 \end{bmatrix} < 0 \quad (2.86)$$

Example 2.3.4. *Lyapunov inequality*

$$PA + A^\top P < 0, \quad P > 0 \quad (2.87)$$

where $A \in \mathbb{R}^{n \times n}$ is stable constant matrix and $P \in \mathbb{R}^{n \times n}$ is symmetric matrix, can be rewritten as following form of LMI

$$\begin{bmatrix} -PA - A^\top P & 0 \\ 0 & P \end{bmatrix} > 0 \quad (2.88)$$

Example 2.3.5. *Trace norm constraint*

$$\text{Tr}(Z(x)P^{-1}Z(x)) < 1 \quad (2.89)$$

where $Z(x) \in \mathbb{R}^{n \times m}, 0 < P(x) \in \mathbb{R}^{n \times n}$ depend affinely on x , can be handled by introducing a new variable $Q = Q^\top \in \mathbb{R}^{m \times m}$ and LMIs system following

$$\text{Tr}(Q) < 1, \quad \begin{bmatrix} Q & Z^\top \\ Z(x) & P(x) \end{bmatrix} > 0 \quad (2.90)$$

Example 2.3.6. *Algebraic Riccati-Lurie's matrix inequality*

$$A^\top X + XA + XBR^{-1}B^\top X + Q < 0 \quad (2.91)$$

is a quadratic matrix inequality of $X = X^\top$, where $A > 0, B > 0, Q = Q^\top > 0, R = R^\top > 0$ are given matrices. It can be represented as LMI via Schur complement

$$\begin{bmatrix} -XA - A^\top X - Q & XB \\ B^\top X & R \end{bmatrix} > 0 \quad (2.92)$$

In the following two examples we will use LMI to study two basic problems of linear system: stability with bounded disturbance and observer design.

Example 2.3.7. *Let us use Lyapunov function $V(x) = x^\top Px$ to prove the stability of system*

$$\dot{x} = Ax + d(x), \quad \|d(x)\|_{\mathbb{R}^n} \leq \lambda \|x\|_{\mathbb{R}^n}, \quad \lambda \in \mathbb{R}_+ \quad (2.93)$$

where $A \in \mathbb{R}^{n \times n}$ is a constant matrix. The conditions we need are $P > 0$ and $\dot{V}(x) \leq -\alpha V(x)$ for all $x \in \mathbb{R}^n$ and $\alpha > 0$. Therefore we have

$$\dot{V}(x) + \alpha V(x) = 2x^\top P(Ax + d(x)) + \alpha x^\top Px \quad (2.94)$$

$$= x^\top (A^\top P + PA + \alpha P)x + 2x^\top P d(x) \quad (2.95)$$

$$= \begin{bmatrix} x \\ d(x) \end{bmatrix}^\top \begin{bmatrix} A^\top P + PA + \alpha P & P \\ P^\top & 0 \end{bmatrix} \begin{bmatrix} x \\ d(x) \end{bmatrix} \quad (2.96)$$

where $d(x)$ satisfies

$$d(x)^\top d(x) \leq \lambda x^\top x \Leftrightarrow \begin{bmatrix} x \\ d(x) \end{bmatrix}^\top \begin{bmatrix} \lambda^2 I & 0 \\ 0 & -I \end{bmatrix} \begin{bmatrix} x \\ d(x) \end{bmatrix} \geq 0 \quad (2.97)$$

Therefore we need the following two inequalities to be fulfilled.

$$-\begin{bmatrix} x \\ d(x) \end{bmatrix}^\top \begin{bmatrix} A^\top P + PA + \alpha P & P \\ P^\top & 0 \end{bmatrix} \begin{bmatrix} x \\ d(x) \end{bmatrix} \geq 0, \quad \text{and} \quad P > 0 \quad (2.98)$$

whenever

$$\begin{bmatrix} x \\ d(x) \end{bmatrix}^\top \begin{bmatrix} \lambda^2 I & 0 \\ 0 & -I \end{bmatrix} \begin{bmatrix} x \\ d(x) \end{bmatrix} \geq 0 \quad (2.99)$$

According to the S-procedure theorem, it happens if and only if there exists a $\tau \in \mathbb{R}$ and $\alpha \geq 0$ such that

$$-\begin{bmatrix} A^\top P + PA + \alpha P & P \\ P^\top & 0 \end{bmatrix} \geq \tau \begin{bmatrix} \lambda^2 I & 0 \\ 0 & -I \end{bmatrix} \quad (2.100)$$

Therefore the necessary and sufficient conditions for the existence of quadratic Lyapunov function of considered system can be written by following LMIs

$$-\begin{bmatrix} A^\top P + PA + \alpha P + \tau \lambda^2 I & P \\ P^\top & -\tau I \end{bmatrix} \leq 0, \quad P > 0 \quad (2.101)$$

within variables $\tau \geq 0, P > 0$

Example 2.3.8. The Luenberger observer of the system

$$\dot{x} = Ax, \quad A \in \mathbb{R}^{n \times n} \quad (2.102)$$

$$y = Cx, \quad C \in \mathbb{R}^{1 \times n} \quad (2.103)$$

can be presented by

$$\dot{\hat{x}} = A\hat{x} + L(\hat{y} - y), \quad L \in \mathbb{R}^{n \times 1} \quad (2.104)$$

$$\hat{y} = C\hat{x} \quad (2.105)$$

Then we derive the error dynamic system

$$\dot{e} = Ae + LCe \quad (2.106)$$

where $e = \hat{x} - x$. After introducing the Lyapunov function $V(e) = e^\top Pe$, the conditions we need are

$$P > 0$$

$$\dot{V} < 0$$

which is equivalent to

$$P > 0$$

$$P(A + LC) + (A + LC)^\top P < 0$$

Denote $W = PL$ thus the final LMIs are

$$P > 0$$

$$PA + A^\top P + WC + C^\top W^\top < 0$$

Therefore the gain L can be found by solving the above LMIs, since many toolboxes have been developed for solving them. In this thesis, the solution of LMIs is mainly based on Matlab toolbox [Yalmip](#) and the solver “[SDPT3](#)”.

The above two examples use explicit Lyapunov function and LMIs to design linear controller or observer. In the following chapters, we use the canonical homogeneous norm as an implicit Lyapunov function and LMIs to design homogeneous controller and observer, and then we validate them on Quanser’s QDrone platform.

Generalized homogenization of linear controller

In this chapter, we start by offering a motivating example to show one more possible advantage of homogeneous controller comparing with linear controller. Next, the second section presents the main results about upgrading a linear controller to homogeneous one. The theoretical results are supported by quadrotor experiments in the last section.

3.1 Motivating Example

Inspired by [78], let us consider the control system

$$\dot{x} = Ax + Bu(x), \quad A = \begin{pmatrix} 0 & 1 & 0 & \dots & 0 \\ 0 & 0 & 1 & \dots & 0 \\ \dots & \dots & \dots & \dots & \dots \\ 0 & 0 & 0 & \dots & 1 \\ 0 & 0 & 0 & \dots & 0 \end{pmatrix}, \quad B = \begin{pmatrix} 0 \\ 0 \\ \vdots \\ 0 \\ 1 \end{pmatrix}$$

where $x = (x_1, x_2, \dots, x_n)^\top$ is the state vector and $u : \mathbb{R}^n \rightarrow \mathbb{R}$ is the feedback control. Initial conditions of the latter system are assumed to be bounded as follows

$$\|x(0)\| \leq 1.$$

The control aim is to stabilize x into a ball of a small radius $\varepsilon > 0$ in a prescribed time $\mathfrak{T} > 0$, i.e.

$$\|x(t)\| \leq \varepsilon, \quad \forall t \geq \mathfrak{T}.$$

Let us firstly consider the static linear feedback

$$u_\ell(x) = kx, \quad k = (k_1, k_2, \dots, k_n).$$

The eigenvalues $\{\lambda_1, \dots, \lambda_n\}$ of the closed-loop linear system

$$\dot{x} = (A + Bk)x$$

can be placed in any given set of the complex plane \mathbb{C} by choosing the vector k . Therefore, it is possible to obtain a closed-loop system with an arbitrary fast damping speed, i.e.

$$\forall \varepsilon > 0, \quad \exists k \in \mathbb{R}^{1 \times n} : \sup_{\|x(0)\|=1} \|x(t)\| < \varepsilon, \quad t > \mathfrak{T}.$$

Indeed, the trajectories of this system converge to the origin exponentially fast

$$\|x(t)\| \leq C e^{-\sigma t}, \quad t > 0$$

where the constant $C \geq 1$ depends on λ_i , $i = 1, 2, \dots, n$ and $\Re(\lambda_i) < -\sigma$. Hence, smaller $\varepsilon > 0$ larger $\sigma > 0$ has to be assigned to solve the control problem, i.e. $\sigma \rightarrow +\infty$ as $\varepsilon \rightarrow 0$ provided that \mathfrak{T} is fixed. Therefore, we conclude that the linear state feedback is, indeed, a possible solution of the considered stabilization problem for any fixed $\varepsilon > 0$.

However, the trajectories of the closed-loop linear system with fast decays have large deviations from the origin during the initial phase of the stabilization. This phenomenon is called the "peaking" effect and the large deviation is referred to as an "overshoot" (see e.g. [76] for more details). In particular, it is shown by [38] that there exists $\gamma > 0$ independent of λ_i such that

$$\sup_{0 \leq t \leq \sigma^{-1}} \sup_{\|x(0)\|=1} \|x(t)\| \geq \gamma \sigma^{n-1}.$$

For $n > 1$ the linear closed-loop system has infinite "overshoot" as $\varepsilon \rightarrow 0$:

$$\sup_{0 \leq t \leq \mathfrak{T}} \sup_{\|x(0)\|=1} \|x(t)\| \rightarrow +\infty \quad \text{as} \quad \varepsilon \rightarrow 0.$$

This means that for sufficiently small $\varepsilon > 0$ the "overshoot" may be so huge that physical (practical) restrictions of the system states would not allow it. The static linear control needs to be somehow modified to overcome this difficulty. The simplest way is to use the input saturation, which, in fact, anyway must be taken into account in practice.

However, in this case it is not clear if the saturated feedback would solve the considered stabilization problem with the prescribed time $\mathfrak{T} > 0$ even if saturation would not destroy stability of the system.

The infinite "peaking" effect could also be eliminated by means of a transformation of the linear controller to a homogeneous one. Indeed, let us consider the following feedback law

$$u_h(x) = \tilde{k} \mathbf{d}(-\ln \|x\|_{\mathbf{d}}) x,$$

where \mathbf{d} is the weighted dilation

$$\mathbf{d}(s) = \begin{pmatrix} e^{ns} & 0 & \dots & 0 \\ 0 & e^{(n-1)s} & \dots & 0 \\ \dots & \dots & \dots & \dots \\ 0 & 0 & \dots & e^s \end{pmatrix}, \quad s \in \mathbb{R}$$

and $\|\cdot\|_{\mathbf{d}} : \mathbb{R}^n \rightarrow (0, +\infty)$ is the so-called canonical homogeneous norm studied in chapter 2. Since $\|\mathbf{d}(s)x\|_{\mathbf{d}} = e^s \|x\|_{\mathbf{d}}$ then the vector field f given by

$$f(x) := Ax + bu_h(x)$$

is weighted homogeneous of degree -1 , i.e. $f(\mathbf{d}(s)x) = e^{-s} \mathbf{d}(s) f(x)$.

Below we show that the vector $\tilde{k} = (\tilde{k}_1, \tilde{k}_2, \dots, \tilde{k}_n)^\top$ can be selected to guarantee

$$\sup_{\|x(0)\|=1} \|x(t)\| = 0, \quad t \geq \mathfrak{T}$$

for any fixed $\mathfrak{T} > 0$. In addition, the feedback law u_h is globally bounded:

$$\sup_{x \in \mathbb{R}^n} |u(x)| \leq M < +\infty,$$

where M depends on \mathfrak{T} as follows: smaller \mathfrak{T} implies larger M . The homogeneous control stabilizes the considered system globally and in a finite time. It solves the stabilization problem considered above independently of $\varepsilon > 0$. Due to global boundedness of the controller it does not have the unbounded "peaking" effect discovered for the linear system as $\varepsilon \rightarrow 0$.

The simulation results for the linear controller $u(x) = kx, k = (-100 - 20)$ and the homogeneous controller $u_h(x) = \tilde{k} \begin{pmatrix} \|x\|_{\mathbf{d}}^{-2} & 0 \\ 0 & \|x\|_{\mathbf{d}}^{-1} \end{pmatrix} x, \tilde{k} = (-4.1721 - 2.8718)$ are depicted in Fig. 3.1. Initial conditions $x(0)$ for the numerical simulations are taken from the unit sphere. Different colors represent the trajectories with different initial positions. In both cases, trajectories of the closed-loop system converge to the origin. The homogeneous

controller provides the (theoretically) exact stabilization of any solution of the closed-loop system with $\|x(0)\| \leq 1$ in the time $\mathcal{T} = 1$, i.e. $x(t) = 0$ for all $t \geq 1$ and for all $\|x(0)\| \leq 1$. The linear controller gain is selected to guarantee $\|x(t)\| \leq \varepsilon = 0.005$ for $t \geq 1$. Even in this case the "overshoot" of the homogeneous controller is twice smaller. The "overshoot" of the linear controller increases drastically for smaller ε . It is proven in [38] that when ε converges to zero, the overshoot of linear controller converges to be infinite.

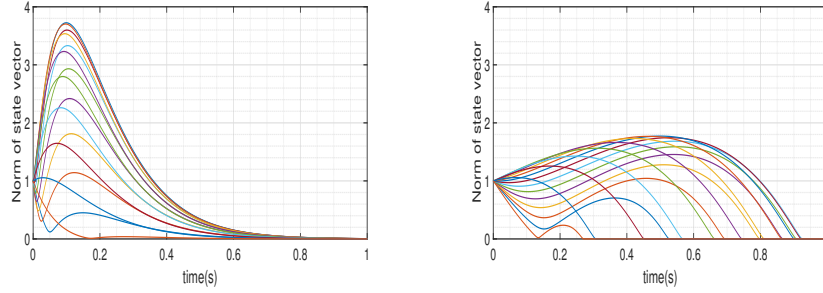


Figure 3.1 – Comparison of "overshoots" for linear (left) and homogeneous (right) controllers

For x belonging to the unit sphere $\|x\|_d = 1$, we have $u_h(x) = \tilde{k}x$. This means that the homogeneous controller u_h is designed by means of a certain homogeneous scaling of a linear stabilizing controller $u(x) = \tilde{k}x$. The aim of this chapter is show that an existing linear controller can be "upgraded" to a non-linear one (using the generalized homogeneity) in such a way that the new controller would provide a better control quality (at least, it will never be worst then the linear controller). The main price of this improvement is an additional computational power for the nonlinear control implementation. We develop the design scheme for a linear plant model and confirm our theoretical constructions by real experiments with the quadrotor Q-Drone of QuanserTM. To implement the suggested scheme to linear PID controllers we extend the results of [60] to the case of linear geometric dilations and MIMO systems. The results of this chapter are published in [111], [112].

3.2 Homogenization of linear controllers

The PID (Proportional-Integral-Derivative) controller is the most common linear feedback law for real physical control systems. The previous sections shows that homogeneous systems may have a better robustness properties and faster convergence rate. In

this section the question to be studied is : *Is it possible to upgrade an existing linear (in particular PID) controller in order to make a closed-loop locally or globally \mathbf{d} -homogeneous and improve convergence properties of the system?* A scheme of the upgrade must prevent a possible degradation of the control quality and only allow its improvement.

3.2.1 Homogeneous Stabilization of Linear MIMO Systems

Let us consider the linear control system

$$\dot{x} = Ax + Bu(x), \quad t > 0, \quad (3.1)$$

where $x(t) \in \mathbb{R}^n$ is the system state, $u : \mathbb{R}^n \rightarrow \mathbb{R}^m$ is the feedback control, $A \in \mathbb{R}^{n \times n}$ and $B \in \mathbb{R}^{n \times m}$ are system matrices.

Definition 3.2.1. *A system*

$$\dot{x} = f(x, u), t > 0, \quad f : \mathbb{R}^n \times \mathbb{R}^m \rightarrow \mathbb{R}^n$$

is said to be \mathbf{d} -homogeneously stabilizable with degree $\mu \in \mathbb{R}$ if there exists a (locally or a globally bounded) feedback law $u : \mathbb{R}^n \rightarrow \mathbb{R}^m$ such that the closed-loop system is globally asymptotically stable and \mathbf{d} -homogeneous of degree μ , where \mathbf{d} is a dilation in \mathbb{R}^n .

In [118], it shows that the system (3.1) can be homogeneously stabilized with a degree $\mu \neq 0$ if and only if the pair $\{A, B\}$ is controllable (or, equivalently, $\text{rank}(B, AB, \dots, A^{n-1}B) = n$). The following theorem is the corollary of a more general theorem proved [80] for evolution system in Hilbert spaces (see also [118] for more details about the finite dimensional case).

Theorem 3.2.1. *If the pair $\{A, B\}$ is controllable and $\mu \in [-1, k^{-1}]$, where $k \leq n$ and*

$$\text{rank}(B, AB, \dots, A^{k-1}B) = n$$

then a homogeneously stabilizing control for (3.1) can always be selected in the form

$$u(x) = K_0 x + \|x\|_{\mathbf{d}}^{1+\mu} K \mathbf{d}(-\ln \|x\|_{\mathbf{d}}) x \quad (3.2)$$

with $K = YX^{-1}$, $K_0 \in \mathbb{R}^{n \times m}$ such that $A_0 = A + BK_0$ is nilpotent, dilation \mathbf{d} generated by $G_{\mathbf{d}} \in \mathbb{R}^{n \times n}$ satisfying

$$A_0 G_{\mathbf{d}} = (G_{\mathbf{d}} + \mu I) A_0, \quad G_{\mathbf{d}} B = B \quad (3.3)$$

and $X \in \mathbb{R}^{n \times n}$, $Y \in \mathbb{R}^{m \times n}$ solving the following algebraic system

$$\begin{cases} XA_0^\top + A_0X + Y^\top B^\top + BY + XG_d^\top + G_dX = 0, \\ XG_d^\top + G_dX > 0, \quad X > 0, \end{cases} \quad (3.4)$$

where the canonical homogeneous norm $\|\cdot\|_d$ is induced by the norm $\|x\| = \sqrt{x^\top X^{-1}x}$.

The canonical homogeneous norm is a Lyapunov function of the closed-loop system (3.1), (3.2) and

$$\frac{d}{dt}\|x(t)\|_d = -\|x(t)\|_d^{1+\mu} \quad \text{for } t > 0 : x(t) \neq 0.$$

Theorem 3.2.1 shows that the homogeneous controller (3.2) guarantees the system (3.1) being homogeneous and asymptotically stable. The equation (3.3) is to guarantee that the system (3.1) is homogeneous with matrix A_0 and B . If A_0 is nilpotent, then (3.3) has a solution K_0 with respect to G_d [118], such that G_d is anti-Hurwitz matrix. The feasibility of (3.4) is to guarantee that the system (3.1) is asymptotically stable which is proven in [83] and refined in [118]. The proof of the latter theorem follows from the following computations

$$\frac{d}{dt}\|x\|_d = \frac{\partial\|x\|_d}{\partial x} \dot{x} = \|x\|_d \frac{x^\top d^\top (-\ln\|x\|_d)X^{-1}d(-\ln\|x\|_d)(A_0x + \|x\|_d^{1+\mu}BYX^{-1}d(-\ln\|x\|_d)x)}{x^\top d^\top (-\ln\|x\|_d)X^{-1}G_d d(-\ln\|x\|_d)x} \quad (3.5)$$

where the formula (2.28) is utilized on the last step. Indeed, from (3.3) we derive d -homogeneity of A_0 (namely, $A_0 d(s) = e^{\mu s} d(s)A_0$ for any $s \in \mathbb{R}$) and B (namely, $d(s)B = e^s B$ for all $s \in \mathbb{R}$). Hence, using (3.3) we immediately derive

$$\frac{d}{dt}\|x\|_d = \|x\|_d^{1+\mu} \frac{x^\top d^\top (-\ln\|x\|_d)X^{-1}(A_0 + BYX^{-1})d(-\ln\|x\|_d)x}{x^\top d^\top (-\ln\|x\|_d)X^{-1}G_d d(-\ln\|x\|_d)x} = -\|x\|_d^{1+\mu}$$

for $x \neq 0$. Obviously the homogeneous degree μ is an important parameter to impact the convergence rate of system.

Remark 3.2.1. If $m = 1$, then there exists a unique K_0 such that $(A + BK_0)G_d = (G_d + \mu I)(A + BK_0)$ with $\mu \neq 0$ [118]. If $m = 1$ and the matrix A is nilpotent (like in the example about the "peaking effect" given in the introduction) then $K_0 = 0$. In this case, for $\mu = -1$ any solution $x(t, x_0)$ of the closed loop system (3.1), (3.2) with the initial condition $x(0) = x_0$ satisfies

$$x(t, x_0) = 0, \quad \forall t \geq \|x_0\|_d$$

and

$$\|u(x)\| = \|YX^{-1}d(-\ln\|x\|_d)x\| \leq \|YX^{-1}\| \cdot \|d(-\ln\|x\|_d)x\| = \|YX^{-1}\| < +\infty.$$

The latter means that the presented homogeneous controller solves the stabilization problem without an unbounded "peaking effect". To guarantee that the settling time of the closed-loop system is bounded by a number $\mathfrak{T} > 0$, for all $x_0^\top x_0 \leq 1$, we just need to add the following linear matrix inequality

$$\mathbf{d}^\top (\ln \mathfrak{T}) X \mathbf{d} (\ln \mathfrak{T}) \leq I_n \quad (3.6)$$

to the system (3.4). The extended system of LMIs remains feasible. Indeed, if the pair X_0, Y_0 is a solution of (3.4) then for any $q > 0$ the pair $X = qX_0, Y = qY_0$ is a solution as well. Hence, the matrix inequality (3.6) is fulfilled for a sufficiently small $q > 0$. If $\text{rank}(B) = m$ and $\{A, B\}$ is controllable, then there exists K_0 such that (3.3) holds [83].

Comparing with linear controller design, homogeneous controller only requires additionally a monotone dilation $\mathbf{d}(s)$ ($XG_{\mathbf{d}} + G_{\mathbf{d}}X > 0$).

The following corollary studies the case of the perturbed linear system. The perturbations can be modeled by a set-valued or a discontinuous function (e.g. dry friction) provided that Filippov solution exists [26].

Corollary 3.2.1.1. *Let conditions of Theorem 3.2.1 hold and $F : \mathbb{R} \times \mathbb{R}^n \rightrightarrows \mathbb{R}^n$ satisfy the following inequality*

$$\frac{\sup_{y \in F(t,x)} \|\mathbf{d}(-\ln \|x\|_{\mathbf{d}})y\|}{x^\top \mathbf{d}^\top (-\ln \|x\|_{\mathbf{d}}) P G_{\mathbf{d}} \mathbf{d}(-\ln \|x\|_{\mathbf{d}}) x} \leq \kappa \|x\|_{\mathbf{d}}^\mu, \quad \forall x \in \mathbb{R}^n \setminus \{0\}, \forall t \geq 0 \quad (3.7)$$

for some $\kappa > 0$, where the canonical homogeneous norm $\|\cdot\|_{\mathbf{d}}$ is induced by $\|x\| = \sqrt{x^\top P x}$, $P = X^{-1}$. If, additionally,

$$(A + BK)^\top P + P(A + BK) + (\rho + \kappa)(G_{\mathbf{d}}^\top P + P G_{\mathbf{d}}) \leq 0, \quad \rho > 0, \quad (3.8)$$

and F is compact-valued, convex-valued and upper-semi continuous, then the control (3.2) stabilizes the system

$$\dot{x} \in Ax + Bu(x) + F(t, x), \quad t > 0 \quad (3.9)$$

and

$$\frac{d}{dt} \|x(t)\|_{\mathbf{d}} \leq -\rho \|x(t)\|_{\mathbf{d}}^{1+\mu}.$$

Proof. The existence of solutions of closed-loop system follows from Filippov theory

[26]. Stability immediately follows the following computations

$$\begin{aligned}
\frac{d}{dt} \|x\|_{\mathbf{d}} &= \|x\|_{\mathbf{d}} \frac{x^\top \mathbf{d}^\top (-\ln \|x\|_{\mathbf{d}}) X^{-1} \mathbf{d} (-\ln \|x\|_{\mathbf{d}}) x}{x^\top \mathbf{d}^\top (-\ln \|x\|_{\mathbf{d}}) X^{-1} G_{\mathbf{d}} \mathbf{d} (-\ln \|x\|_{\mathbf{d}}) x} \\
&\leq \|x\|_{\mathbf{d}}^{1+\mu} \frac{x^\top \mathbf{d}^\top (-\ln \|x\|_{\mathbf{d}}) X^{-1} (A_0 + BYX^{-1}) \mathbf{d} (-\ln \|x\|_{\mathbf{d}}) x}{x^\top \mathbf{d}^\top (-\ln \|x\|_{\mathbf{d}}) X^{-1} G_{\mathbf{d}} \mathbf{d} (-\ln \|x\|_{\mathbf{d}}) x} + \|x\|_{\mathbf{d}} \sup_{y \in F(t,x)} \frac{x^\top \mathbf{d}^\top (-\ln \|x\|_{\mathbf{d}}) X^{-1} \mathbf{d} (-\ln \|x\|_{\mathbf{d}}) y}{x^\top \mathbf{d}^\top (-\ln \|x\|_{\mathbf{d}}) X^{-1} G_{\mathbf{d}} \mathbf{d} (-\ln \|x\|_{\mathbf{d}}) x} \\
&\leq -(\rho + \kappa) \|x\|_{\mathbf{d}}^{\mu+1} + \kappa \|x\|_{\mathbf{d}}^{1+\mu} \leq -\rho \|x\|_{\mathbf{d}}^{1+\mu}
\end{aligned}$$

■

Notice that the obtained differential inequality for the canonical homogeneous norm specifies the convergence rate of the closed-loop system.

In the practice, a more conservative explicit estimate can be obtained using the relation

$$\sigma_1(\|x\|_{\mathbf{d}}) \leq \|x\| \leq \sigma_2(\|x\|_{\mathbf{d}}) \quad (3.10)$$

where σ_1, σ_2 are class \mathcal{K}_∞ functions (details defined in Lemma 7.2 of [78] where α, β defined by Theorem 2.1.3 of this thesis). Since (3.10) shows the relation between $\|\cdot\|_{\mathbf{d}}$ and $\|\cdot\|$, the disturbance estimated by $\|\cdot\|_{\mathbf{d}}$ in (3.7), can be replaced by $\|\cdot\|$ in practice.

In the next part, an integral controller will be introduced to compensate the static error of system.

3.2.2 Homogeneous Proportional Integral Controller

The linear control theory uses an integral term to improve robustness properties of a proportional feedback law. This idea is also useful for nonlinear controllers [52]. A similar integrator can be added to implicit homogeneous feedback [60].

Theorem 3.2.2. *Let $K_0 \in \mathbb{R}^{m \times n}$ be such that $A + BK_0$ is nilpotent, $\text{rank}(B) = m$ and an anti-Hurwitz matrix $G_{\mathbf{d}} \in \mathbb{R}^{n \times n}$ satisfy (3.3) with $\mu \in [-0.5, 1/k]$, where the number k is given in Theorem 3.2.1.*

Let $X \in \mathbb{R}^{n \times n}$ and $Y \in \mathbb{R}^{m \times n}$ satisfy (3.4), then for any positive definite matrix $Q \in \mathbb{R}^{m \times m}$ and any constant vector $p \in \mathbb{R}^m$ the control law

$$u(x) = K_0 x + u_{\text{hom}}(x) + \int_0^t u_{\text{int}}(x(s)) ds, \quad (3.11)$$

$$u_{\text{hom}}(x) = \|x\|_{\mathbf{d}}^{1+\mu} Y X^{-1} \mathbf{d} (-\ln \|x\|_{\mathbf{d}}) x,$$

$$u_{int}(x) = -\|x\|_{\mathbf{d}}^{1+2\mu} \frac{QB^T P \mathbf{d}(-\ln \|x\|_{\mathbf{d}})x}{x^T \mathbf{d}^T (-\ln \|x\|_{\mathbf{d}}) P G_{\mathbf{d}} \mathbf{d}(-\ln \|x\|_{\mathbf{d}})x}$$

stabilizes the origin of the system

$$\dot{x} = Ax + B(u + p),$$

where p is a constant, in a finite time if $\mu < 0$, exponentially if $\mu = 0$, and practically in a fixed-time if $\mu > 0$.

Proof. Let us introduce the following virtual variable

$$x_{n+1} = p + \int_0^t u_{int}(x(s)) ds.$$

In this case the closed-loop system becomes

$$\dot{x} = Ax + B(K_0 x + u_{hom}(x) + x_{n+1}), \quad \dot{x}_{n+1} = u_{int}(x). \quad (3.12)$$

Since $\|\mathbf{d}(-\ln \|x\|_{\mathbf{d}})x\| = 1$ then u_{int} is globally bounded and discontinuous at $x = \mathbf{0}$ if $\mu = -0.5$. In all other cases, the considered system has the continuous right-hand side.

Let us show that the latter system is globally asymptotically stable. For this purpose let us consider the following Lyapunov function candidate

$$V = \frac{1}{2+2\mu} \|x\|_{\mathbf{d}}^{2+2\mu} + \frac{1}{2} x_{n+1}^T Q^{-1} x_{n+1}.$$

Calculating the time derivative of V along the trajectories of the closed-loop system we derive

$$\begin{aligned} \dot{V} &= \|x\|_{\mathbf{d}}^{1+2\mu} \frac{\partial \|x\|_{\mathbf{d}}}{\partial x} \dot{x} + x_{n+1}^T Q^{-1} \dot{x}_{n+1} \\ &= -\|x\|_{\mathbf{d}}^{2+3\mu} + \|x\|_{\mathbf{d}}^{1+2\mu} \frac{\partial \|x\|_{\mathbf{d}}}{\partial x} B x_{n+1} - \frac{\|x\|_{\mathbf{d}}^{1+2\mu} x_{n+1}^T B^T P \mathbf{d}(-\ln \|x\|_{\mathbf{d}})x}{x^T \mathbf{d}^T (-\ln \|x\|_{\mathbf{d}}) P G_{\mathbf{d}} \mathbf{d}(-\ln \|x\|_{\mathbf{d}})x} = -\|x\|_{\mathbf{d}}^{2+3\mu} \end{aligned}$$

where the formula (2.28) and the identity $e^{sG_{\mathbf{d}}} B = e^s B$ are utilized on the last step.

Since $x = 0, x_{n+1} = 0$ is the unique equilibrium of system (3.12) and the hyperplane $\{(x, x_{n+1}) \in \mathbb{R}^{n+m} : x = \mathbf{0}\}$ does not contain non-zero trajectories of this system, then its origin is globally asymptotically stable (see, e.g. LaSalle principle [44] and its version for discontinuous ODEs [69]).

Finally, since the system (3.12) is $\tilde{\mathbf{d}}$ -homogeneous of the degree μ with respect to the

dilation

$$\tilde{\mathbf{d}}(s) = \begin{pmatrix} e^{sG_d} & \mathbf{0} \\ \mathbf{0} & e^{s(1+\mu)}I_m \end{pmatrix}$$

then using Proposition 2.1.1 we complete the proof. ■

In the case of the weighted homogeneous SISO system (3.1) the presented theorem with the degree $\mu = -0.5$ recovers the result of [60].

Remark 3.2.2. *Since the functional*

$$x \rightarrow x^\top \mathbf{d}^\top (-\ln \|x\|_d) P G_d \mathbf{d} (-\ln \|x\|_d) x$$

is \mathbf{d} -homogeneous of the degree 0 and uniformly bounded from above and from below, then its replacement in u_{int} with a constant does not destroy the homogeneity properties of the system. Therefore, for practical reasons the simplified integral term

$$u_{int}(x) = -\|x\|_d^{1+2\mu} Q B^\top P \mathbf{d} (-\ln \|x\|_d) x$$

can be utilized provided that the stability of the closed-loop system is preserved. This replacement could add some additional restrictions to parameters Q , X and μ . Some sufficient conditions of the quadratic-like stability of nonlinear generalized homogeneous systems presented in [85] can be utilized for the corresponding analysis. The stability of the obtained nonlinear system can also be studied using, for example, robustness properties of the homogeneous proportional integral controller (see [60] for more details about its robustness in the case of the weighted homogeneity). The derivation of a LMI-based condition allowing the simplified form of the integral term is an interesting theoretical problem for the future research.

Notice that the parameter p is assumed to be constant in Theorem 3.2.2. In most of the practice, p is a time-varying disturbance, homogeneous controller could further minimize the effect of disturbance on the system than linear controller, since it has a higher gain than linear controller which provides a faster convergence, better precision and robustness.

Tuning parameter is always a difficult work that takes a lot of time. In the following section, the homogeneous controller is implemented via the parameters from the existing linear controller, which saves a lot of time for engineers.

3.2.3 Design of a homogeneous controller from an existing linear feedback

Consider again the linear system (3.1) and assume that some linear control law

$$u_{lin}(x) = K_{lin}x, \quad K_{lin} \in \mathbb{R}^{m \times n}, \quad x \in \mathbb{R}^n$$

is already designed.

Corollary 3.2.2.1. *Let the pair $\{A, B\}$ be controllable, $K_0 \in \mathbb{R}^{m \times n}$ be such that the matrix $A_0 = A + BK_0$ is nilpotent and $K_{lin} \in \mathbb{R}^{m \times n}$ be such that the matrix $A + BK_{lin}$ is Hurwitz.*

Let $G_d \in \mathbb{R}^{n \times n}$ be a generator of the dilation \mathbf{d} such that (3.3) holds for $\mu = -1$. If a matrix $P = P^\top \in \mathbb{R}^{n \times n}$ satisfies the system of linear matrix inequalities

$$\begin{aligned} (A + BK_{lin})^\top P + P(A + BK_{lin}) &< 0 \\ G_d^\top P + PG_d &> 0, \quad P > 0 \end{aligned} \tag{3.13}$$

then the control u given by (3.2) with $\mu = -1$ and $K = K_{lin} - K_0$ \mathbf{d} -homogeneously stabilizes the origin of the system (3.1) in a finite-time, where $\|\cdot\|_d$ is the canonical homogeneous norm induced by the norm $\|x\| = \sqrt{x^\top Px}$. Moreover, $u_{lin}(x) = u(x)$ for $x \in S = \{x \in \mathbb{R}^n : \|x\| = 1\}$.

The proof immediately follows from the identity

$$(A + BK_{lin})^\top P + P(A + BK_{lin}) = (A_0 + BK)^\top P + P(A_0 + BK)$$

and Theorem 3.2.1. Finally, for $\|x\| = 1$ we have $\|x\|_d = 1$, $\mathbf{d}(-\ln \|x\|_d) = \mathbf{d}(0) = I_n$, i.e. $u_{lin}(x) = u(x)$ if $\|x\| = 1$.

The corollary shows that if a linear controllable plant is exponentially stabilized by means of a linear feedback, then it can also be homogeneously stabilized by means of the control (3.2) using the gains of the original linear controller. These two controllers coincide on the unit sphere $x^\top Px = 1$. Notice that the corresponding sphere can be always adjusted (if needed) by means of a variation of P satisfying (3.13).

Obviously when $x \rightarrow 0$, then $\|x\|_d \rightarrow 0$ as well, in this case, the homogeneous controller (3.2) may have a infinite gain provided $\mu = -1$. The infinite gain will lead to a serious chattering problem of system, which is not wanted in practice. In order to guarantee the homogeneous controller performance is always better than linear controller, the following saturation function is introduced.

$\text{sat}_{a,b} : \mathbb{R}_+ \rightarrow \mathbb{R}_+$ is defined as

$$\text{sat}_{a,b}(\rho) = \begin{cases} b & \text{if } \rho \geq b, \\ \rho & \text{if } a < \rho < b, \\ a & \text{if } \rho < a, \end{cases} \quad \rho \in \mathbb{R}_+. \quad (3.14)$$

Let us consider the control law

$$u_{a,b}(x) = K_0 x + K \mathbf{d} (-\ln \text{sat}_{a,b}(\|x\|_{\mathbf{d}})) x, \quad (3.15)$$

where \mathbf{d} , $\|x\|_{\mathbf{d}}$, K_0 and $K = K_{lin} - K_0$ are defined in Corollary 3.2.2.1. After adding the saturation function, it provides an admissible interval of the gain to improve the system performance, for example the smaller a we give, the higher gain we obtain in the homogeneous controller. The parameter b is generally set to be 1 for finite-time controller. In the case of fixed time controller, we can select $b > 1$.

From (3.14) we conclude that

$$u_{1,1}(x) = K_{lin} x, \quad \forall x \in \mathbb{R}^n$$

and

$$u_{0,+\infty}(x) = K_0 x + K \mathbf{d} (-\ln \|x\|_{\mathbf{d}}) x, \quad \forall x \in \mathbb{R}^n.$$

In other words, the pair $a \in (0, 1]$ and $b \in [1, +\infty)$ parametrize a family of non-linear controllers which has the linear and homogeneously stabilizing feedbacks as the limit cases.

Notice that for $b = 1$ the controller (3.15) coincide with the linear controller outside the unit ball $x^\top P x > 1$ and the gains of the linear controller are scaled by means of dilation \mathbf{d} only close to the origin, i.e. for $x^\top P x < 1$.

The following scheme for an “upgrade” of linear control to non-linear (locally homogeneous) one can be suggested :

1. Find a matrix $K_0 \in \mathbb{R}^{m \times n}$ such that $A + BK_0$ is nilpotent and (3.3) is satisfied.
2. Find a symmetric matrix $P = P^\top$ satisfying the inequalities (3.13), which is required to define the canonical homogeneous norm $\|\cdot\|_{\mathbf{d}}$.
3. Select $a = b = 1$ (i.e. we start with a linear controller).
4. Increase $b > 1$ and decrease $a < 1$ while this improves the static state precision.

Theoretically, an improvement of control quality (faster transitions or better robustness) is proved by Corollary 3.2.1.1 even for the case $\alpha = 0$ and $\beta = +\infty$. However, the proofs of the corollaries are model-based, but any model of a system is just an approximation of the reality. In practice, a difference between a dynamic model and a real motion of the system may not allow to realize all theoretical properties of the closed-loop system or, even more, it may imply a serious degradation of some performance indices, which characterize the control quality. That is why, the tuning of parameters a and b suggested above is required to guarantee that the non-linear control always has the quality which is never worse than the original linear one. It would allow a control engineer to prevent any possible degradation of the control quality during the non-linear "upgrade" of a linear control system. Below the real experiment tested on quadrotor will be presented.

Notice that if the gains of the linear controller are already optimally adjusted, then improvements provided by homogeneous controller could not be huge and the parameters a and b could, possibly, be close 1 in this case. If small variations of the parameters a and b from 1 imply degradation of the control quality, then the proposed "upgrade" is impossible.

3.2.4 On digital realization of implicit homogeneous feedback

In order to implement an implicit homogeneous control (e.g. (3.15)) in practice, an algorithm for computation of the canonical homogeneous norm $\|x\|_{\mathbf{d}}$ is required. This norm can be computed explicitly for $n \leq 2$ or approximated by an explicit homogeneous norm for $n \geq 3$ (see [85]). However, even for the second order case, the representation of the canonical homogeneous norm is rather cumbersome, so a digital realization of the homogeneous control law requires much more computational power than the linear algorithm. Therefore, an algorithm of a digital realization of the implicit homogeneous control is required for its successful practical application. Some additional properties of the implicit homogeneous controller are established below for this purpose.

Theorem 3.2.3. *If all conditions of Corollary 3.2.1.1 hold for $G_{\mathbf{d}}$ (as in Theorem 3.2.1) then for any fixed $r > 0$ the closed \mathbf{d} -homogeneous ball $\bar{B}_{\mathbf{d}}(r)$ is a strictly positively invariant compact set¹ of the closed-loop system (3.9) with the linear control*

$$u_r(x) = r^{1+\mu} K \mathbf{d}(-\ln r)x. \quad (3.16)$$

¹A set Ω is said to be a strictly positively invariant for a dynamical system if $x(t_0) \in \Omega \Rightarrow x(t) \in \text{int}\Omega, t \geq t_0$, where x denotes a solution x of this system.

Proof. Let us denote

$$K_r = r^{1+\mu} K \mathbf{d}(-\ln r), \quad P_r = \mathbf{d}^\top(-\ln r) P \mathbf{d}(-\ln r), \quad \rho_r = r^\mu \rho, \quad \kappa_r = r^\mu \kappa.$$

In this case, multiplying (3.8) on $\mathbf{d}^\top(-\ln r)$ from the left and on $\mathbf{d}(-\ln r)$ from the right, we derive

$$\begin{aligned} & \mathbf{d}^\top(-\ln r)(A + BK)^\top \mathbf{d}^\top(\ln r)P_r + P_r \mathbf{d}(\ln r)(A + BK)\mathbf{d}(-\ln r) + \\ & (\rho + \kappa)(\mathbf{d}^\top(-\ln r)G_\mathbf{d}^\top \mathbf{d}^\top(\ln r)P_r + P_r \mathbf{d}(\ln r)G_\mathbf{d}\mathbf{d}(-\ln r)) \leq 0. \end{aligned}$$

Taking into account $G_\mathbf{d}\mathbf{d}(-\ln r) = \mathbf{d}(-\ln r)G_\mathbf{d}$, $A\mathbf{d}(-\ln r) = r^{-\mu}\mathbf{d}(-\ln r)A$ and $\mathbf{d}(\ln r)B = rB$, we derive

$$r^{-\mu}[(A + BK_r)^\top P_r + P_r(A + BK_r)] + (\rho + \kappa)(G_\mathbf{d}^\top P_r + P_r G_\mathbf{d}) \leq 0$$

or, equivalently,

$$(A + BK_r)^\top P_r + P_r(A + BK_r) + (\rho_r + \kappa_r)(G_\mathbf{d}^\top P_r + P_r G_\mathbf{d}) \leq 0.$$

Hence, the time derivative of the Lyapunov function candidate $V(x) = x^\top P_r x$, $x \in \mathbb{R}^n$ along a trajectory of the closed-loop linear system we have

$$\begin{aligned} \dot{V}(x(t)) &= x^\top(t)[P_r(A + BK_r) + (A + BK_r)^\top P_r + \rho_r(G_\mathbf{d}^\top P_r + P_r G_\mathbf{d})]x(t) + \\ & 2f^\top(t)P_r x(t) - \rho_r x^\top(t)(P_r G_\mathbf{d} + G_\mathbf{d}^\top P_r)x(t), \end{aligned}$$

where $f(t) \stackrel{a.e.}{\in} F(t, x(t))$. For $\|x(t)\|_\mathbf{d} = r$ from (3.7) we derive

$$2f^\top(t)P_r x(t) \leq 2\sqrt{f^\top(t)P_r f(t)} \leq \kappa_r x^\top(t)(P_r G_\mathbf{d} + G_\mathbf{d}^\top P_r)x(t).$$

Hence, we conclude that $\dot{V}(x) \leq -\rho_r x^\top(P_r G_\mathbf{d} + G_\mathbf{d}^\top P_r)x < 0$ if $\|x(t)\|_\mathbf{d} = r$ (or, equivalently, if $V(x) = 1$). The latter immediately implies that $B_\mathbf{d}(r)$ is strictly positively invariant set of the closed-loop linear system. ■

Now we assume that the value $\|x(t)\|_\mathbf{d}$ can be changed only in some sampled instances of time and let us show that the corresponding linear switched feedback robustly stabilizes the perturbed linear system.

Corollary 3.2.3.1. *If*

- 1) the conditions of Corollary 3.2.1.1 hold;

2) $\{t_i\}_{i=0}^{+\infty}$ is an arbitrary sequence of time instances such that

$$0 = t_0 < t_1 < t_2 < \dots \quad \text{and} \quad \lim_{i \rightarrow +\infty} t_i = +\infty;$$

3) the switched control u has the form

$$u(x(t)) = \|x(t_i)\|_{\mathbf{d}}^{1+\mu} K \mathbf{d} (-\ln \|x(t_i)\|_{\mathbf{d}}) x(t), \quad t \in [t_i, t_{i+1}) \quad (3.17)$$

then the closed-loop system (3.9) and (3.17) is globally asymptotically stable.

Proof. I. Let us show that the sequence $\{\|x(t_i)\|_{\mathbf{d}}\}_{i=1}^{+\infty}$ is monotone decreasing along any solution of the closed-loop system. Notice that the function $t \rightarrow \|x(t)\|_{\mathbf{d}}$ is continuous since the solution x of the closed-loop system is a continuous function of time.

Let us define the quadratic positive definite function $V_i : \mathbb{R}^n \rightarrow R_+$ given by $V_i(x) := x^\top P_i x$, where $P_i := \mathbf{d}^\top (-\ln \|x(t_i)\|_{\mathbf{d}}) P \mathbf{d} (-\ln \|x(t_i)\|_{\mathbf{d}}) > 0$.

On the time interval $[t_i, t_{i+1})$ we have $u(x) = K_i x$, where

$$K_i := \|x(t_i)\|_{\mathbf{d}}^{1+\mu} K \mathbf{d} (-\ln \|x(t_i)\|_{\mathbf{d}}).$$

Repeating the proof of Theorem 3.2.3 we derive

$$\dot{V}_i(x(t)) \leq -\rho \|x(t_i)\|_{\mathbf{d}}^\mu x(t)^\top (P_i G_{\mathbf{d}} + G_{\mathbf{d}}^\top P_i) x(t) < 0$$

for $t \in [t_i, t_{i+1})$, i.e. the function $t \rightarrow V_i(x(t))$ is strictly decreasing on $[t_i, t_{i+1})$.

On the one hand, for any fixed $x \neq 0$ the scalar-valued function $r \rightarrow q(r)$ defined as

$$q(r) = x^\top \mathbf{d}^\top (-\ln r) P \mathbf{d} (-\ln r) x, \quad r > 0$$

is also strictly decreasing due to $G_{\mathbf{d}}^\top P + P G_{\mathbf{d}} > 0$. On the other hand, from the definition of the canonical homogeneous norm $\|\cdot\|_{\mathbf{d}}$ we derive $V_i(x(t_i)) = 1$ and $\forall t \in (t_i, t_{i+1}]$ we have

$$\begin{aligned} V_i(x(t)) - 1 &= x^\top(t) \mathbf{d}^\top (-\ln \|x(t_i)\|_{\mathbf{d}}) P (-\ln \|x(t_i)\|_{\mathbf{d}}) x(t) - 1 < 0 = \\ &= x^\top(t) \mathbf{d}^\top (-\ln \|x(t)\|_{\mathbf{d}}) P (-\ln \|x(t)\|_{\mathbf{d}}) x(t) - 1. \end{aligned}$$

The latter implies $\|x(t)\|_{\mathbf{d}} < \|x(t_i)\|_{\mathbf{d}}$ for all $t \in (t_i, t_{i+1}]$, i.e. the sequence $\{\|x(t_i)\|_{\mathbf{d}}\}_{i=1}^{+\infty}$ is monotone decreasing and $x(t) \in B_{\mathbf{d}}(\|x(t_i)\|_{\mathbf{d}})$ for all $t \geq t_i$. Moreover, $V(x(t)) \leq V(x(0))$ for all $t \geq 0$, i.e. the origin of the closed-loop system is *Lyapunov stable*.

II. Since the canonical homogeneous norm $\|\cdot\|_{\mathbf{d}}$ is positive definite then the monotone decreasing sequence $\{\|x(t_i)\|_{\mathbf{d}}\}_{i=1}^{\infty}$ converges to some limit. Let us show now that this limit

is zero. Suppose the contrary, i.e. $\lim_{i \rightarrow \infty} \|x(t_i)\|_{\mathbf{d}} = V_* > 0$ or equivalently $\forall \varepsilon > 0 \quad \exists N = N(\varepsilon) : V_* \leq \|x(t_i)\|_{\mathbf{d}} < V_* + \varepsilon, \forall i \geq N$.

The control function $u(V, s)$ is continuous $\forall s \in \mathbb{R}^n \setminus \{0\}$ and $\forall V \in \mathbb{R}_+$. The latter means

$$\left\| \|x(t_i)\|_{\mathbf{d}}^{\mu+1} K \mathbf{d}(-\ln \|x(t_i)\|_{\mathbf{d}})x - V_*^{\mu+1} K \mathbf{d}(-\ln V_*)x \right\| \leq \sigma(\varepsilon) \|s\|, \quad \forall i \geq N,$$

where $\sigma(\cdot) \in \mathcal{K}$. The definition of $\|$ can be found in [86]. This means that for $t > t_N$ the closed-loop system can be presented in the form

$$\dot{x}(t) = (A + B(K_* + \Delta(t, \varepsilon)))x + f(t), \quad (3.18)$$

where $K_* = V_*^{1+\mu} K \mathbf{d}(-\ln V_*)$, $f(t) \in F(t, x(t))$ and $\Delta(t, \varepsilon) \in \mathbb{R}^{m \times n} : \|\Delta\| \leq \sigma(\varepsilon)$.

Let us consider the quadratic positive definite Lyapunov function candidate $V_*(x) = x^\top P_* x$, where $P_* = \mathbf{d}^\top(-\ln V_*) P \mathbf{d}(-\ln V_*)$. For $t > t_N$ we have

$$\begin{aligned} \dot{V}_*(x(t)) &\leq -(\rho + \kappa) V_*^\mu x(t)^\top (P_* G_{\mathbf{d}} + G_{\mathbf{d}}^\top P_*) x(t) + \\ &\quad x^\top(t) (P_* B \Delta + \Delta^\top B^\top P_*) x(t) + \sqrt{f^\top(t) P_* f(t)}. \end{aligned}$$

Hence, taking into account $\sigma \in \mathcal{K}$ for sufficiently small $\varepsilon > 0$ (i.e. for sufficiently large t_N) we have

$$x^\top(t) (P_* B \Delta + \Delta^\top B^\top P_*) x(t) \leq \frac{\rho}{3} V_*^\mu x(t)^\top (P_* G_{\mathbf{d}} + G_{\mathbf{d}}^\top P_*) x(t).$$

Since $\|x(t_i)\|_{\mathbf{d}} \rightarrow V_*$ as $i \rightarrow +\infty$ then for sufficiently small $\varepsilon > 0$ (i.e. sufficiently large t_N) the inequality (3.7) implies

$$\sqrt{f^\top(t) P_* f(t)} \leq \left(\frac{\rho}{3} + \kappa \right) V_*^\mu x(t)^\top (P_* G_{\mathbf{d}} + G_{\mathbf{d}}^\top P_*) x(t).$$

Therefore, we have

$$\dot{V}_*(x(t)) \leq -\frac{\rho}{3} V_*^\mu x(t)^\top (P_* G_{\mathbf{d}} + G_{\mathbf{d}}^\top P_*) x(t)$$

and the solution of the closed-loop system decays exponential implying the existence of an instant of time $t^* > t_N$ such that $\|x(t^*)\|_{\mathbf{d}} < V_*$. This contradicts our supposition and means $\lim_{i \rightarrow \infty} \|x(t_i)\|_{\mathbf{d}} = 0$. Hence, taking into account the Lyapunov stability proven above we conclude the global asymptotic stability of the closed-loop system with the switched homogeneous control (3.17). ■

The linear switched control (3.17) is obtained from the non-linear homogeneous one. It can be utilized, for example, in the case when the control system is already equipped with a linear controller allowing a dynamic change of feedback gains with

some sampling period.

According to the corollary, the proposed sampled-time realization of the implicit homogeneous controller guarantees asymptotic stabilization of the closed-loop system *independently of the dwell time* (a time between to sampling instants). Such property is rather unusual for sampled and switched control systems with additive disturbances [54]. However, without any assumption on the dwell-time we cannot estimated the convergence rate of this system. Obviously, if the dwell time tends to zero the convergence rate tends to the rate of the original continuous system.

Some advanced schemes for a discrete-time approximation of homogeneous control systems are developed in [81]. They preserve the convergence rate(e.g. finite/fixed time) of the origin continuous-time homogeneous system in its discrete-time counterpart. However, this algorithm still needs on-line computation of the canonical homogeneous norm (or its discrete-time analog). Fortunately, rather simple numerical procedures can be utilized for this purpose.

Let we have some sequence of time instants $0 = t_0 < t_1 < t_2 < \dots$ and $\lim t_i = +\infty$. Let a, b be the parameters of the sat function defined in the previous section.

Algorithm 1 Algorithm of solving Implicit Lyapunov function

```

if  $x^\top(t_i) \mathbf{d}^\top (-\ln \bar{V}) P \mathbf{d} (-\ln \bar{V}) x(t_i) > 1$  then
     $\underline{V} = \bar{V}; \bar{V} = \min(b, 2\bar{V});$ 
else if  $x^\top(t_i) \mathbf{d}^\top (-\ln \underline{V}) P \mathbf{d} (-\ln \underline{V}) x(t_i) < 1$  then
     $\bar{V} = \underline{V}; \underline{V} = \max(0.5\underline{V}, a);$ 
else
    for  $i = 1 : N_{\max}$  do
         $V = \frac{\underline{V} + \bar{V}}{2}$ 
        if  $x^\top(t_i) \mathbf{d}^\top (-\ln \underline{V}) P \mathbf{d} (-\ln \underline{V}) x(t_i) < 1$  then
             $\bar{V} = V;$ 
        else
             $\underline{V} = V;$ 
        end if
    end for
end if
 $\|x(t_i)\|_{\mathbf{d}} \approx \bar{V};$ 

```

Let $x(t_i) \in \mathbb{R}^n \setminus \{0\}$ be a given vector and $a = 0, b = +\infty$. If the **Step** of the presented algorithm is applied recurrently many times to the same $x(t_i)$ then Algorithm 1 realizes:

1) a localization of the unique positive root of the equation $\|\mathbf{d}(-\ln V)x(t_i)\| = 1$ with respect to $V > 0$, i.e. $V \in [\underline{V}, \bar{V}]$;

2) improvement of the obtained localization by means of the bisection method, i.e. $(\bar{V} - \underline{V}) \rightarrow 0$.

Such an application of Algorithm 1 allows us to calculate $V \approx \|x(t_i)\|_{\mathbf{d}}$ with rather high precision but it requests a high computational capability of a control device. If the computational power is very restricted, then the **Step** of Algorithm 1 may be realized *just once at each sampled instant of time*. Theorem 3.2.3 implies practical stability of the closed-loop system in this case. Indeed, Theorem 3.2.3 proves that the \mathbf{d} -homogeneous ball $\bar{B}_{\mathbf{d}}(\bar{V})$ is a strictly positively invariant set of the the closed-loop system with the control $u(x) = \bar{V}^\mu K \mathbf{d}(-\ln \bar{V})$. If the root of the equation $\|\mathbf{d}(-\ln V)x(t_i)\| = 0$ is localized (i.e. $x(t_i) \leq \bar{V}$), Algorithm 1 always selects the upper estimate of V to guarantee $x(t_i) \in \bar{B}_{\mathbf{d}}(\bar{V})$. This means that $\|x(t_i)\|_{\mathbf{d}}$ never leaves the ball $\bar{B}_{\mathbf{d}}(\bar{V})$ even when $x(t)$ varies in time.

The parameters a and b defines lower and upper admissible values for V . As explained in the previous section, this restriction is caused by practical issues. For instance, the parameter a can not be selected arbitrary small due to finite numerical precision of digital devices and measurement errors, which may imply $x(t_i) \notin \bar{B}_{\mathbf{d}}(\bar{V})$ due to the computational errors.

3.3 An “upgrade” of a linear controller for Quanser QDrone™

3.3.1 Linearized models

To design homogeneous controllers, let us consider the simplified model of the quadrotor system (1.35) assuming that ϕ and θ are small, and quadrotor has a slow motion, thus $D \approx 0, \cos \theta \approx 1, \cos \phi \approx 1, \sin \phi \approx \phi, \sin \theta \approx \theta$.

Denoting $\xi = (x, y, \dot{x}, \dot{y}, \theta, -\phi, \dot{\theta}, -\dot{\phi})^\top$ and

$$\begin{bmatrix} \tau_\phi \\ \tau_\theta \\ \tau_\psi \end{bmatrix} = \begin{bmatrix} u_2 \\ u_3 \\ u_4 \end{bmatrix}, \quad u_1 = F_T - mg$$

we derive

$$\dot{\xi} = A_\xi \xi + B \begin{pmatrix} u_2 \\ u_3 \end{pmatrix} \quad (3.19)$$

$$\ddot{\psi} = \frac{u_4}{I_{zz}} \quad (3.20)$$

$$\ddot{z} = \frac{u_1}{m} \quad (3.21)$$

where

$$A_\xi = \begin{pmatrix} 0 & E & 0 & 0 \\ 0 & 0 & gE & 0 \\ 0 & 0 & 0 & E \\ 0 & 0 & 0 & 0 \end{pmatrix}, \quad E = \begin{pmatrix} 1 & 0 \\ 0 & 1 \end{pmatrix}, \quad B = \begin{pmatrix} 0 \\ 0 \\ \frac{1}{I_{yy}} & 0 \\ 0 & \frac{1}{I_{xx}} \end{pmatrix}.$$

Denote $\Psi = \begin{bmatrix} \psi \\ \dot{\psi} \end{bmatrix}$, then the subsystem (3.20) becomes

$$\dot{\Psi} = A_\psi \Psi + B_\psi u_4 \quad (3.22)$$

where $A_\psi = \begin{bmatrix} 0 & 1 \\ 0 & 0 \end{bmatrix}$, $B_\psi = \begin{bmatrix} 0 \\ \frac{1}{I_{zz}} \end{bmatrix}$.

Denote $Z = \begin{bmatrix} z \\ \dot{z} \end{bmatrix}$, then system (3.21) becomes

$$\dot{Z} = A_z Z + B_z u_1 \quad (3.23)$$

where $A_z = \begin{bmatrix} 0 & 1 \\ 0 & 0 \end{bmatrix}$, $B_z = \begin{bmatrix} 0 \\ \frac{1}{m} \end{bmatrix}$.

The PID controller given by the manufacturer has the following form:

$$u_1 = K_z \begin{pmatrix} z \\ \dot{z} \end{pmatrix} + \int K_I Z dt, \quad \begin{pmatrix} u_2 \\ u_3 \end{pmatrix} = K_\xi \xi, \quad u_4 = K_\psi \begin{pmatrix} \psi \\ \dot{\psi} \end{pmatrix}$$

with the parameters

$$K_\psi = \begin{bmatrix} -0.59 & 0.11 \end{bmatrix}, \quad K_z = \begin{bmatrix} -35 & -14 \end{bmatrix}, \quad K_I = \begin{bmatrix} -4 & 0 \end{bmatrix}$$

$$K_\xi = \begin{pmatrix} -2.91 & 0 & -1.45 & 0 & -1.85 & 0 & -0.16 & 0 \\ 0 & -3.53 & 0 & -1.76 & 0 & -2.25 & 0 & -0.20 \end{pmatrix}$$

We use these gains of linear controller in order to design a homogeneous one.

3.3.2 Upgrade of linear controllers

The pairs $\{A_\xi, B_\xi\}$, $\{A_z, B_z\}$ and $\{A_\psi, B_\psi\}$ are controllable, the matrix A_ξ is \mathbf{d}_ξ -homogeneous of the degree -1 with

$$\mathbf{d}_\xi(s) = \text{diag}\{e^{4s}E, e^{3s}E, e^{2s}E, e^sE\}, \quad s \in \mathbb{R}$$

The matrix A_ϕ is \mathbf{d}_ϕ -homogeneous of the degree -1 with

$$\mathbf{d}_\phi(s) = \text{diag}\{e^{2s}, e^s\}, \quad s \in \mathbb{R}$$

and the matrix A_z is \mathbf{d}_z -homogeneous of the degree -0.5 with

$$\mathbf{d}_z(s) = \text{diag}\{e^{1s}, e^{0.5s}\}, \quad s \in \mathbb{R}$$

Moreover, the matrices A_ξ , A_ψ and A_z are nilpotent. For all subsystems we apply Corollary 3.2.2.1 and derive controllers of the form (3.2) with $K_0 = \mathbf{0}$ and the canonical homogeneous norms $\|\xi\|_{\mathbf{d}_\xi}$, $\|\psi\|_{\mathbf{d}_\psi}$ and $\|z\|_{\mathbf{d}_z}$ computed using the weighted Euclidean norms with the shape matrices

$$P_\xi = \begin{bmatrix} 226.71 & 0 & 81.56 & 0 & 78.43 & 0 & 2.40 & 0 \\ 0 & 234.31 & 0 & 84.21 & 0 & 79.33 & 0 & 2.28 \\ 81.56 & 0 & 31.32 & 0 & 38.19 & 0 & 12.26 & 0 \\ 0 & 84.20 & 0 & 37.47 & 0 & 38.84 & 0 & 1.20 \\ 78.43 & 0 & 38.19 & 0 & 59.92 & 0 & 2.53 & 0 \\ 0 & 79.33 & 0 & 38.84 & 0 & 62.06 & 0 & 2.40 \\ 2.40 & 0 & 1.26 & 0 & 2.53 & 0 & 0.24 & 0 \\ 0 & 2.28 & 0 & 1.20 & 0 & 2.40 & 0 & 0.23 \end{bmatrix}$$

$$P_\psi = \begin{bmatrix} 18.41 & 2.19 \\ 2.18 & 0.47 \end{bmatrix}, \quad P_z = \begin{bmatrix} 7.86 & 1.21 \\ 1.21 & 0.62 \end{bmatrix}$$

respectively. These matrices are obtained as solutions of the LMIs (3.13).

The original linear controller for z -subsystem contains the integrator. Taking into account Remark (3.2.2) and the form of the dilation \mathbf{d}_z we define its homogeneous counterpart as follows

$$u_z(Z) = \|Z\|_{\mathbf{d}_z}^{1/2} K_z \mathbf{d}_z(-\ln \|Z\|_{\mathbf{d}_z}) Z + K_I \int_0^t \mathbf{d}_z(-\ln \|Z\|_{\mathbf{d}_z}) Z(s) ds \quad (3.24)$$

3.3.3 Results of experiments

For practical implementation the term $\|\cdot\|_{\mathbf{d}_\alpha}$ in the homogeneous controller of each subsystems has to be replaced with $\text{sat}_{a_\alpha, b_\alpha}(\|\cdot\|_{\mathbf{d}_\alpha})$, where $\alpha \in \{\xi, \phi, z\}$

The parameters $0 < a_\alpha < b_\beta < +\infty$ (see Algorithm 1) has been selected for each

subsystem as follows. Each pair of a, b are tuned to guarantee that the proposed nonlinear controller is always better than linear one by comparing the system state precision and robustness property.

$$a_\xi = 0.6, \quad a_\psi = 0.65, \quad a_z = 0.3, \quad b_\xi = b_\psi = b_z = 1.$$

Quanser’s linear PID controller and the proposed homogeneous PID controller are compared on the experiment, which consists in the sequential set-points (unit: (m,m,m,rad)) tracking, which are defined as follows:

$$\begin{aligned} [x, y, z, \psi] &= [0, 0, 0, 0] \rightarrow [0, 0, 0.4, 0] \rightarrow [0.2, 0, 0.4, 0] \rightarrow [0.2, 0.2, 0.4, 0] \\ &\rightarrow [0, 0, 0.4, 0] \rightarrow [0, 0, 0.018, 0] \end{aligned}$$

Fig. 3.2 depicts the position tracking trajectory of x, y, z and ψ variables, respectively. The homogeneous PID controller has a faster response and a higher precision.

L_2 Error (m)	Linear	Homogeneous	Improvement
$\ error_x\ _{L_2}$	0.0226	0.0127	43.8%
$\ error_y\ _{L_2}$	0.0136	0.0067	50.7%
$\ error_z\ _{L_2}$	0.0203	0.0076	62.5%
$\ error_\psi\ _{L_2}$	0.0043	0.0017	60.4%

Table 3.1 – Mean values of stabilization error

The mean value stabilization errors are compared in Table 3.1. They are given by L_2 norms of the deference between the coordinate and the reference computed in steady states. We define that the steady state starts ≈ 2.5 sec after the set-point assignment and ends at the time instant when the new set-point is assigned. The obtained improvement is more than 40%.

The price of this improvement is a bit more energy consumption, which is estimated by using the L_2 norm of system inputs. In this test, L_2 norm of PID controller and homogeneous PID are about 54.14 and 54.75 respectively. The difference between these norms of Quanser PID controller and the homogeneous controller is about 1.1%, i.e., the proposed homogeneous controller consumes only 1.1% more than the Quanser PID controller, but it can improve about 40% precision. The input norm of linear PID and Homogeneous PID controller are plotted in Fig. 3.3.

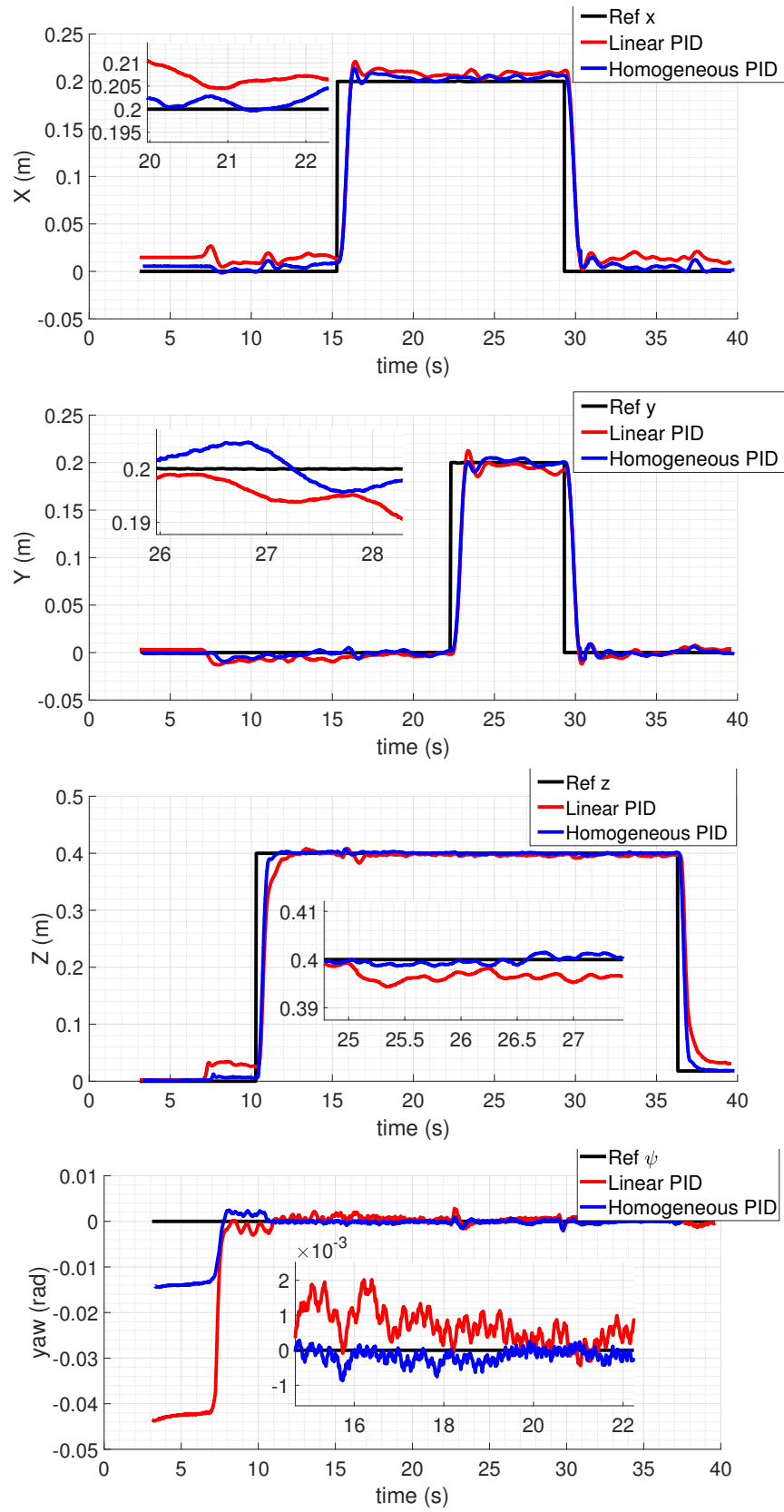
The robustness of the controllers is also compared by adding a mass (0.5 kg) for

a couple seconds on top of the quadrotor during the flight test. The results of the experiments are depicted in Fig. 3.4. The homogeneous controller again demonstrates a better control precision.

3.4 Conclusion

In this chapter, a scheme for an “upgrade” of a linear controller to a non-linear homogeneous one is developed and verified by experiment. The homogeneous controller uses the feedback gain of linear controller and scales it in a generalized homogeneous way which depends on the norm of the system states. The main advantages of this homogeneous controller include faster convergence, better robustness and no peaking effect. Its main drawbacks are the on-line computation of $\|x\|_d$ and sometimes a saturation function is required to avoid the infinite gain of homogeneous controller. In practice, this infinite

The experiments which are tested on the quadrotor platform QDrone of QuanserTM verify the good performance of this controller. The control precision has been improved more than 40% and the energy consuming increases only about 1.1%. Meanwhile the robustness of controller proposed with respect to the external disturbance is improved a lot as well. It is worth stressing that this method for “homogeneous upgrade” of linear controller can be applied to many other dynamical systems. The same idea of upgrading linear controller to homogeneous one can be extended to observer design, which will be introduced in the next chapter.

Figure 3.2 – Quadrotor position tracking comparison in x , y , z and ψ

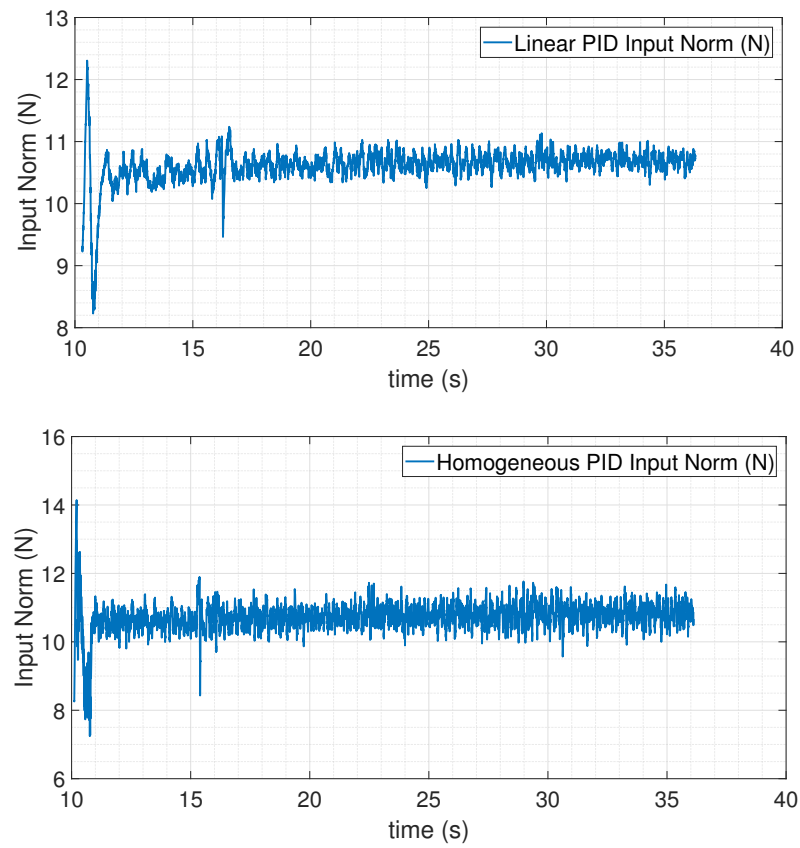


Figure 3.3 – Input L_2 norm of linear PID signal and Homogeneous PID signal

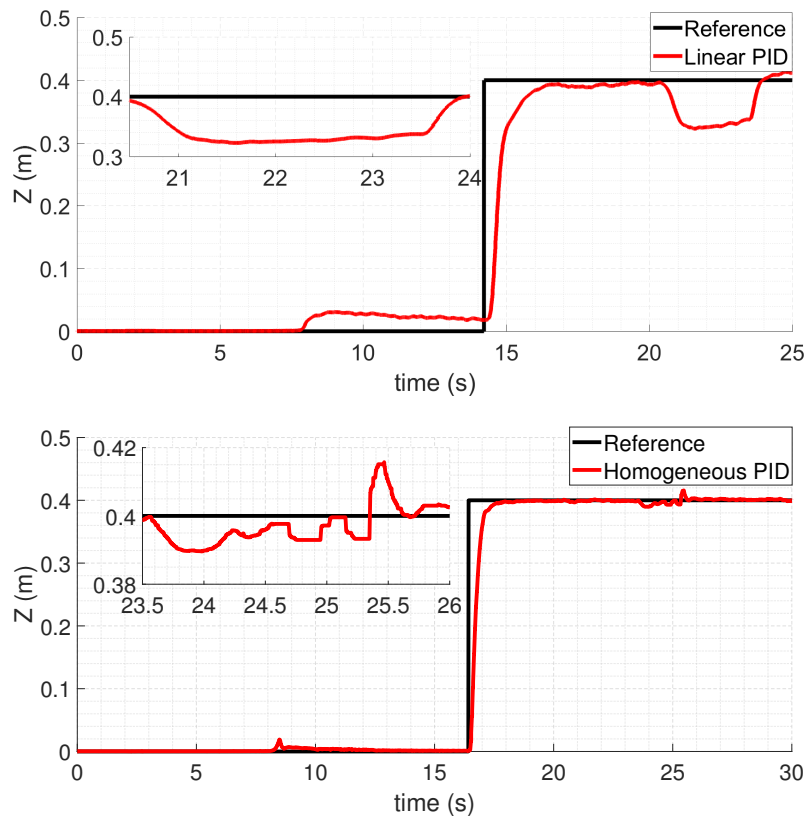


Figure 3.4 – The response of linear controller and homogeneous controller to the added load disturbance

Generalized homogenization of Linear Observer

The methodology of a "upgrade" of linear controllers to homogeneous ones is already developed in chapter 3, where the experiments show that the set-point tracking precision on the real experiment is improved about 40% and the homogeneous controller shows its better robustness than linear controller. This chapter extends the same ideas to observers design and shows the simultaneous "upgrade" of linear controller and linear observer implies more improvement of the control quality.

4.1 Homogeneous State-Estimation of Linear MIMO Systems

Let us consider the linear system

$$\dot{x} = Ax + Bu, \quad y = Cx, \quad t > 0, \quad (4.1)$$

where $A \in \mathbb{R}^{n \times n}$, $B \in \mathbb{R}^{n \times m}$, $C \in \mathbb{R}^{k \times n}$ are system matrices, $x(t) \in \mathbb{R}^n$ is the system state, $u(t) \in \mathbb{R}^m$ is a known as system input, $y(t) \in \mathbb{R}^k$ is the output measured.

Definition 4.1.1. *The system (4.1) is said to be \mathbf{d} -homogeneously observable of a degree $\mu \in \mathbb{R}$ if there exists an observer of the form*

$$\dot{z} = Az + Bu + g(Cz - y), \quad g : \mathbb{R}^k \rightarrow \mathbb{R}^n \quad (4.2)$$

such that the error equation

$$\dot{e} = Ae + g(Ce), \quad e = z - x \quad (4.3)$$

is globally uniformly asymptotically stable and \mathbf{d} -homogeneous of the degree $\mu \in \mathbb{R}$. For shortness, the corresponding observer (4.2) is called homogeneous.

In [78], it is shown that the system (4.1) can be homogeneously observable with a degree $\mu \neq 0$ if and only if the pair $\{A, C\}$ is observable (i.e. $\text{rank}(C, CA, \dots, CA^{n-1}) = n$). The following theorem refines Theorem 11.1 from [78] allowing a selection of the observer gains $L \in \mathbb{R}^{n \times k}$ by solving LMI which is very important for the development of a scheme for an upgrade of a linear Luenberger observer.

Theorem 4.1.1. *Let $C \in \mathbb{R}^k$ be a full row rank matrix and $G_0 \in \mathbb{R}^{n \times n}$ satisfy (4.4)*

$$AG_0 = (G_0 + I_n)A, \quad CG_0 = \mathbf{0} \quad (4.4)$$

Let $\mu \in \mathbb{R}$ be such that real parts of the eigenvalues of $I_n + \mu(I_n + G_0)$ are non-negative. Let $P \in \mathbb{R}^{n \times n}, L = P^{-1}C^\top \in \mathbb{R}^{n \times k}, \rho > 0, \gamma > 0$ and $\mu \in \mathbb{R}$ satisfy (4.5) and (4.6)

$$\begin{aligned} PA + A^\top P + C^\top L^\top P + PLC + 2\rho P &< 0, \\ (I_n + \mu G_0)^\top P + P(I_n + \mu G_0) &> 0, \\ P &> \gamma^2 C^\top C, \end{aligned} \quad (4.5)$$

$$\rho^2 P^{-1} > \Xi(\lambda) L L^\top \Xi^\top(\lambda), \quad \forall \lambda \in [0, \frac{1}{\gamma}], \quad (4.6)$$

where $\Xi(\lambda) = \lambda(\exp(\ln \lambda^\mu (G_0 + I_n)) - I_n)$. Then the dynamic observer (4.2) with the locally bounded function $g \in C(\mathbb{R}^k \setminus \{\mathbf{0}\}, \mathbb{R}^n)$

$$g(\sigma) = \exp(\ln \|\sigma\|_{\mathbb{R}^k} (G_0 + I_n) \mu) L \sigma, \quad \sigma \in \mathbb{R}^k \quad (4.7)$$

makes the error equation (4.3) to be globally uniformly asymptotically stable and \mathbf{d} -homogeneous of degree $\mu \in \mathbb{R}$ and $\exists c > 0 : \frac{d}{dt} \|e(t)\|_{\mathbf{d}} < -c \|e(t)\|_{\mathbf{d}}^{\mu+1}$ for all $t > 0 : \|e(t)\| \neq 0$, where the dilation \mathbf{d} is generated by $G_{\mathbf{d}} = I_n + \mu G_0$ and $\|\cdot\|_{\mathbb{R}^k}$ is the standard Euclidean norm in \mathbb{R}^k . Moreover, since the matrix $I_n + \mu(I_n + G_0)$ is anti-Hurwitz, g is continuous at zero.

Proof. Firstly we will analyze the continuous property of function g . According to the way of construction function g , the only one possible discontinuity point of g is at $\sigma = 0$. Since g can be rewritten as follows

$$g(\sigma) = \exp(\ln \|\sigma\|_{\mathbb{R}^k} ((G_0 + I_n) \mu + I_n)) L \frac{\sigma}{\|\sigma\|_{\mathbb{R}^k}}$$

then it is clear to see that $g(\sigma) \rightarrow \mathbf{0}$ as $\sigma \rightarrow \mathbf{0}$ and g is continuous at $\sigma = 0$ when the matrix

$I_n + \mu(G_0 + I_n)$ is anti-Hurwitz. If the real parts of eigenvalues of the matrix $I_n + \mu(I_n + G_0)$ are negatives, then g is possibly discontinuous at the point $\sigma = 0$, but it is bounded in any neighborhood of this point. In the latter case, the solution of observer equation can be analyzed by Filippov theorem.

Secondly, the matrix A is \mathbf{d} -homogeneous of a degree $\mu \in \mathbb{R}$ if and only if (4.8) is satisfied:

$$AG_{\mathbf{d}} = (\mu I_n + G_{\mathbf{d}})A \quad (4.8)$$

Since G_0 satisfies (4.4) then the matrix $G_{\mathbf{d}} = I_n + \mu G_0$ will satisfy the (4.8). Now the first term of right hand side of (4.3) is \mathbf{d} -homogeneous of degree μ . Then the function $e \rightarrow g(Ce)$ will be proved to be \mathbf{d} -homogeneous of degree μ . Indeed, given that $C\mathbf{d}(s) = C \exp(s)$ and $CG_{\mathbf{d}} = C$ implies that $CG_{\mathbf{d}}^i = C$ for $\forall s \in \mathbb{R}$. Hence, the following relation gives that function $g(Ce)$ is also \mathbf{d} -homogeneous of degree μ

$$\begin{aligned} g(C\mathbf{d}(s)e) &= \|\exp(s)Ce\|_{\mathbb{R}^k}^\mu \exp(\ln \|\exp(s)Ce\|_{\mathbb{R}^k}^\mu G_0)LC \exp(s)e \\ &= \exp((\mu + 1)s) \exp(\mu s G_0)g(Ce) = \exp(\mu s)\mathbf{d}(s)g(Ce) \end{aligned}$$

Finally from second inequality of (4.5) we conclude that the dilation \mathbf{d} is strictly monotone [85]. Meanwhile the canonical homogeneous norm $\|\cdot\|_{\mathbf{d}}$ induced by the weighted Euclidean norm $\|e\| = \sqrt{e^\top P e}$ is well defined and smooth on $\mathbb{R}^n \setminus \{0\}$. Since canonical norm $\|\cdot\|_{\mathbf{d}}$ is positive definite and continuously differentiable, it is expected to be a Lyapunov function for the error equation. Indeed, using the first matrix inequality of system (4.5) and the formula (2.28) then we drive the derivative of $\|e\|_{\mathbf{d}}$

$$\begin{aligned} \frac{d}{dt}\|e\|_{\mathbf{d}} &= \|e\|_{\mathbf{d}} \frac{e^\top \mathbf{d}^\top (-\ln \|e\|_{\mathbf{d}}) P \mathbf{d} (-\ln \|e\|_{\mathbf{d}}) (Ae + g(Ce))}{e^\top \mathbf{d}^\top (-\ln \|e\|_{\mathbf{d}}) P G_{\mathbf{d}} \mathbf{d} (-\ln \|e\|_{\mathbf{d}}) e} \\ &= \|e\|_{\mathbf{d}}^{1+\mu} \frac{e^\top \mathbf{d}^\top (-\ln \|e\|_{\mathbf{d}}) [P A \mathbf{d} (-\ln \|e\|_{\mathbf{d}}) e + P g(C\mathbf{d} (-\ln \|e\|_{\mathbf{d}}) e)]}{e^\top \mathbf{d}^\top (-\ln \|e\|_{\mathbf{d}}) P G_{\mathbf{d}} \mathbf{d} (-\ln \|e\|_{\mathbf{d}}) e} \\ &\leq \|e\|_{\mathbf{d}}^{1+\mu} \frac{-\rho - v^\top P L C v + \|Cv\|_{\mathbb{R}^k}^\mu v^\top P \exp(\ln \|Cv\|_{\mathbb{R}^k}^\mu G_0) L C v}{v^\top G_{\mathbf{d}} P v} \\ &= \|e\|_{\mathbf{d}}^{1+\mu} \frac{-\rho + v^\top P [\|Cv\|_{\mathbb{R}^k}^\mu \exp(\ln \|Cv\|_{\mathbb{R}^k}^\mu G_0) - I_n] L C v}{v^\top P G_{\mathbf{d}} v} \end{aligned}$$

where $v = \mathbf{d}(-\ln \|e\|_{\mathbf{d}})e$ belongs to the unit sphere, i.e. $v^\top P v = 1$. According to the second linear matrix inequality of the system (4.5), the following condition holds.

$$0 < v^\top P G_{\mathbf{d}} v = 0.5 v^\top (P G_{\mathbf{d}} + G_{\mathbf{d}}^\top P) v \leq 0.5 \lambda_{\max}(P^{-\frac{1}{2}} G_{\mathbf{d}}^\top P^{\frac{1}{2}} + P^{\frac{1}{2}} G_{\mathbf{d}} P^{-\frac{1}{2}})$$

Since for any $q \in \mathbb{R}^n$ we have

$$q^\top LCv \leq \|L^\top q\|_{\mathbb{R}^k} \|Cv\|_{\mathbb{R}^k}.$$

then denoting $\lambda := \|Cv\|_{\mathbb{R}^k}$ we derive

$$v^\top P[\lambda^\mu \exp(\ln \lambda^\mu G_0) - I_n]LCv \leq \|L^\top [\lambda^\mu \exp(\ln \lambda^\mu G_0^\top) - I_n]Pv\|_{\mathbb{R}^k} \lambda.$$

Therefore the inequality $\|L^\top [\lambda^\mu \exp(\ln \lambda^\mu G_0^\top) - I_n]Pv\|_{\mathbb{R}^k} \lambda < \rho$ can be represented as follows

$$P[\lambda^\mu \exp(\ln \lambda^\mu G_0) - I_n]LL^\top [\lambda^\mu \exp(\ln \lambda^\mu G_0^\top) - I_n]P < \frac{\rho^2 P}{\lambda^2}.$$

or, equivalently,

$$\Xi(\lambda)LL^\top \Xi(\lambda) < \rho^2 P^{-1}.$$

Finally, the matrix inequality $P > \gamma C^\top C$ implies $\lambda \in [0, 1/\gamma]$. Notice that the parameter μ is the homogeneous degree of system. ρ is used to tune the system's convergence rate, the bigger ρ leads to the faster convergence. γ is a parameter to relax the system conservatism.

Since $\sup_{\lambda \in [0, 1/\gamma]} \|\Xi(\lambda)\| \rightarrow 0$ as $\mu \rightarrow 0$ (see Proposition 11.1 in [78]) the system of matrix inequalities (4.5) and (4.6) is always feasible provided that μ is sufficiently small.

■

4.2 From a linear observer to a homogeneous one

Notice that for $\mu = 0$ the homogeneous observer (4.2) and (4.7) becomes the Luenberger one with

$$g(\sigma) = L\sigma, \quad \sigma = Ce \tag{4.9}$$

and the system of matrix inequalities (4.5) and (4.6) is reduced to

$$PA + A^\top P + 2\rho P + PLC + C^\top L^\top P < 0, \quad P > 0, \rho > 0 \tag{4.10}$$

It is well-know [12] that the feasibility of the latter inequality is the necessary and sufficient condition for the exponential stability of the error equation of the Luenberger observer (with the decay rate $\rho > 0$). For the similar reason with homogeneous controller design, when the homogeneous degree $\mu < 0$, the homogeneous observer may have a infinite gain as $\sigma \rightarrow 0$. In order to guarantee the homogeneous observer performance is

always better than linear observer, the following saturation function $\text{sat}_{a,b} : \mathbb{R}_+ \rightarrow \mathbb{R}_+$ is introduced.

$$\text{sat}_{a,b}(\rho) = \begin{cases} b & \text{if } \rho \geq b, \\ \rho & \text{if } a < \rho < b, \\ a & \text{if } \rho < a, \end{cases} \quad \rho \in \mathbb{R}_+. \quad (4.11)$$

Let us consider the following function

$$g_{a,b}(x) = \text{sat}_{a,b}(\|\sigma\|_{\mathbb{R}^k}^\mu) \exp(\ln \text{sat}_{a,b}(\|\sigma\|_{\mathbb{R}^k}^\mu) G_0) L \sigma, \quad (4.12)$$

where G_0 and L are defined in Theorem 4.1.1.

From (4.12) we conclude that

$$g_{1,1}(\sigma) = L\sigma, \quad g_{0,+\infty}(x) = \|\sigma\|_{\mathbb{R}^k}^\mu \exp(\ln \|\sigma\|_{\mathbb{R}^k}^\mu G_0) L\sigma.$$

In other words, the pair $a \in (0, 1]$ and $b \in [1, +\infty)$ parameterize a family of nonlinear observers which has the Luenberger and homogeneous filters as the limit cases. A smaller a provides a bigger gain of homogeneous observer in the case of $\mu < 0$. This motivates the following corollary for an "upgrade" of the Luenberger observer and indicates the relation between Luenberger observer and homogeneous observer.

Assume that the Luenberger observer

$$\dot{z} = Az + Bu + g(Cz - y) \quad (4.13)$$

such that the error equation

$$\dot{e} = Ae + g(\sigma), \quad g(\sigma) = L_{lin}\sigma, \quad \sigma = Ce \quad (4.14)$$

is already designed.

In order to apply the method proposed above, the following algorithm can be applied:

- 1) Take the gain $L_{lin} \in \mathbb{R}^{k \times n}$ of the existing Luenberger observer and select the parameters $G_0 \in \mathbb{R}^{n \times n}$ and $\mu \in \mathbb{R}$ such that the system of matrix inequalities (4.5) and (4.6) are feasible¹ with respect to $P > 0$, $\rho > 0$ and $\gamma > 0$.
- 2) Select $a = b = 1$ (i.e. we start from a linear controller).
- 3) Increase $b > 1$ and decrease $a < 1$ while this improves an estimation precision or the quality of the whole control system if the estimation precision cannot be

¹Computational procedures for solving the system of nonlinear matrix inequalities of the form (4.5) and (4.6) are developed in [55] for a linear dilations with diagonal matrix G_d .

evaluated from experiments.

Theoretically, an improvement of the control quality (e.g. faster transition) follows from Proposition 2.1.1 and Theorem 4.1.1. However, the proofs are based on the system model, and any model is just an approximation of the real system. The theoretical results may not happened due to the difference between the real system and its model. The saturation function introduced above guarantee that the nonlinear homogeneous observer always has a quality never worse than original linear one. In Section 4.3 we will illustrate the presented scheme on a real experiment with a quadrotor.

Notice that if the gains of the linear observer are already optimally adjusted, then improvements provided by homogeneous observer could not be huge and the parameters a and b could, possibly, be close to 1 in this case.

4.3 An “upgrade” of a linear filter for QDrone of QuanserTM

In this section, we will show how to apply the result presented in Section 4 to realize the control of quadrotor.

The system of QDrone was equipped with two types of sensors (External OptiTrack and on-board IMU) to measure different state variables in different frames, with different sampling frequency. Here is a short summary of output data from OptiTrack and IMU.

1. **External OptiTrack:** The OptiTrack system uses ultra-red camera to capture the movement of quadrotor in real-time, with a maximum sampling frequency equal to 100Hz (depending on the number of quadrotors need to be localized: in our case we localize only 1 quadrotor). This system can provide the following measurement in inertial frame: $^I[x, y, z, \phi, \theta, \psi]$ where (x, y, z) are the position and (ϕ, θ, ψ) represent the roll, pitch and yaw angle, all are in inertial frame.
2. **On-board IMU:** The on-board IMU sensor includes gyroscope, accelerometer, magnetometer and barometer, working with a high sampling frequency at 1000Hz. It can provide the following measurements:

$$^B[\dot{\phi}, \dot{\theta}, \dot{\psi}, a_x, a_y, a_z, T_x, T_y, T_z, P]$$

where $(\dot{\phi}, \dot{\theta}, \dot{\psi})$ are the angular velocities around (x, y, z) axis, (a_x, a_y, a_z) are the associated acceleration on each axis, (T_x, T_y, T_z) represent magnetism, and P is the air pressure, all are in body frame.

4.3.1 Controller implementation problems

For the QDrone platform, Quanser realized 4 independent PID controllers for the regulation of x, y, z and ϕ , respectively. Recently, we presented an efficient homogeneous PID controller see chapter 3, by upgrading the Quanser’s PID controller, which shows a substantial improvement of the control performance. However, two important problems need to be solved when applying those mentioned methods:

1. **Unavailable information:** All those mentioned controllers depend not only on $(x, y, z, \phi, \theta, \psi)$, but also on $(\dot{x}, \dot{y}, \dot{z}, \dot{\phi}, \dot{\theta}, \dot{\psi})$. However, neither the OptiTrack nor the IMU can provide the information of $(\dot{x}, \dot{y}, \dot{z})$ for the controller design;
2. **Asynchronous sampling frequency:** As we have presented that the frequency of IMU is much higher than that of the OptiTrack system, thus the provided measurements from the OptiTrack and the IMU are not synchronized.

Quanser proposed the following two filters to solve the above problems (Fig. 4.1):

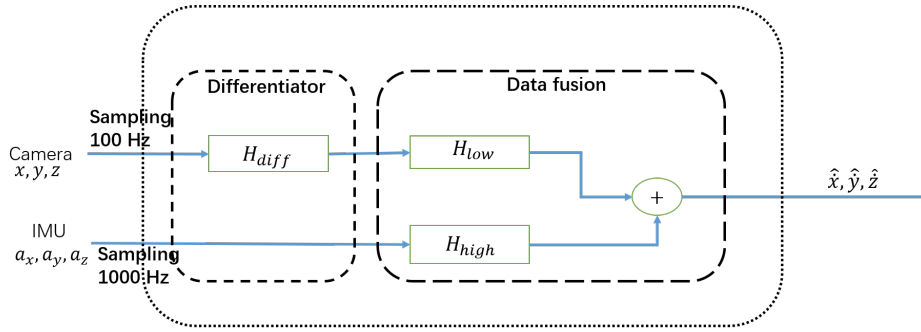


Figure 4.1 – Quanser’s filter

1. **Differentiation:** To solve the first problem, Quanser designed a filter to compute the derivative of a signal. Precisely, the following transfer function:

$$H_{diff}(s) = \frac{2500s}{s^2 + 100s + 2500} \quad (4.15)$$

was used to calculate the estimated derivative \dot{p} of the input signal $p(t)$, i.e..

$$s\hat{p}(s) = H_{diff}(s)p(s)$$

2. **Data fusion:** To overcome the second problem, Quanser designed another filter to fusion the reading from IMU (noted as a_{imu}) and the estimated derivative (via the

differentiation through the filter H_{diff} defined in (4.15)) of the reading from the OptiTrack (noted as p_{cam}). Given those two measurements with different sampling frequencies, the following two transfer functions:

$$H_{high}(s) = \frac{s}{s^2 + 4s + 0.1} \quad (4.16)$$

$$H_{low}(s) = \frac{4s + 0.1}{s^2 + 4s + 0.1} \quad (4.17)$$

are used to realize the data fusion functionality. Precisely, with the OptiTrack reading $p_{cam}(t)$, Quanser computes its derivative $\dot{p}_{cam}(t)$ by

$$s\hat{p}_{cam}(s) = H_{diff}(s)p_{cam}(s)$$

Due to the fact that $\dot{p}_{cam}(t)$ is with low frequency (100Hz) while the on-board frequency is 1000Hz (the same frequency as that of IMU), therefore a further improvement on the estimation of $\dot{p}_{cam}(t)$ by using the reading of IMU is realized via the transfer functions defined in (4.16-4.17) as follows:

$$s\hat{p}_{fus}(s) = H_{low}(s)s\hat{p}_{cam}(s) + H_{high}(s)a_{imu}(s) \quad (4.18)$$

In summary, with the reading of OptiTrack $p_{cam}(t)$ and IMU $a_{imu}(t)$, by taking into account the asynchronous frequency, Quanser uses the following transfer function to calculate the estimated derivative $\dot{p}_{fus}(t)$:

$$s\hat{p}_{fus}(s) = H_{Q_1}(s)p_{cam}(s) + H_{Q_2}(s)a_{imu}(s) \quad (4.19)$$

with

$$H_{Q_1}(s) = H_{low}(s)H_{diff}(s) = \frac{2500(4s+0.1)s}{(s^2+4s+0.1)(s^2+100s+2500)} \quad (4.20)$$

and

$$H_{Q_2}(s) = H_{high}(s) = \frac{s}{s^2 + 4s + 0.1} \quad (4.21)$$

With the position reading of OptiTrack (x, y, z) and the acceleration reading of IMU (a_x, a_y, a_z) (those two types of readings need to be transformed into the same frame), Quanser uses (4.19) to get the estimated linear velocity $(\dot{x}, \dot{y}, \dot{z})$, which is required to implement PID controller.

4.3.2 Upgrade of Quanser’s filters

In the above subsection, we detailed Quanser’s strategy by designing two filters to realize the derivative estimation from two asynchronous readings of OptiTrack and IMU. In this subsection, we will show how to apply the theoretic result presented in Section 4 to upgrade the Quanser’s filters. For this, two steps have been effectuated:

- **Step 1:** we seek a linear system (LTI) which enables us to estimate the linear velocity by using the position and acceleration measurements, the same objective as the two filters proposed by Quanser;
- **Step 2:** Based on the obtained LTI system, using the result presented in Section 4 to upgrade it to a homogeneous one.

The following gives the details how we realize those two steps to upgrade Quanser’s filters to a homogeneous observer.

Step 1: For the sake of simplicity, the following presents our method on how to estimate the linear velocity along x -axis with the OptiTrack x -axis position reading p_{cam_x} and IMU x -axis acceleration reading a_{imu_x} , and we use the same scheme to estimate the linear velocity along other axis.

Since the quadrotor is considered as a rigid body system, by applying the physical law, its dynamics can be written as follows:

$$\begin{aligned}\dot{p}_x &= v_x \\ \dot{v}_x &= a_x\end{aligned}\tag{4.22}$$

where p_x represents the x -position of the mass center of the quadrotor, $v_x = \dot{x}$ is the corresponding x -axis velocity and a_x represents the associated x -axis acceleration. Suppose now we have the two asynchronous readings p_{cam_x} and a_{imu_x} , we can write $p_x = p_{cam_x} - \omega(t)$ and $a_x = a_{imu_x} + d(t)$ where $\omega(t)$ represents the x -axis position measurement error between OptiTrack and the real position p_x , and $d(t)$ represents the x -axis acceleration measurement error between IMU and the real acceleration a_x . Generally $d(t)$ can be approximated as a high-order polynomial function of t , but in our study $d(t)$ is assumed to be constant, i.e. $\dot{d} = 0$. Hence, model (4.22) can be re-written into the following LTI model with noisy output:

$$\begin{aligned}\dot{X} &= AX + Bu = AX + Ba_{imu_x} \\ Y &= CX + \omega = p_{cam_x}\end{aligned}\tag{4.23}$$

where $X = [p_x, v_x, d]^\top$, $A = \begin{bmatrix} 0 & 1 & 0 \\ 0 & 0 & 1 \\ 0 & 0 & 0 \end{bmatrix}$, $B = [0, 1, 0]^\top$, $C = [1, 0, 0]$, and $u = a_{imu_x}$.

It is easy to verify that (4.23) is observable by checking the rank condition. Hence the following Luenberger observer is designed

$$\dot{\hat{X}} = A\hat{X} + Ba_{imu_x} + L(p_{cam_x} - C\hat{X}) \quad (4.24)$$

and it is clear that \hat{X} will converge to a neighborhood (depending on the bound of the noise ω) of X if the gain $L = [l_1, l_2, l_3]^\top$ is chosen such that $A - LC$ is Hurwitz.

Obviously, a more reasonable choice of L is to approximate the two transfer functions H_{Q_1} and H_{Q_2} defined in (4.20) and (4.21), since Quanser takes lots of time to find out those two optimal transfer functions. To this aim, by applying the Laplace transformation to (4.24), a straightforward calculation yields the following relation:

$$\hat{X}_2(s) = H_{L_1}(s)p_{cam_x} + H_{L_2}(s)a_{imu_x} \quad (4.25)$$

where

$$H_{L_1}(s) = \frac{s(l_2s + l_3)}{s^3 + l_1s^2 + l_2s + l_3}$$

and

$$H_{L_2}(s) = \frac{(s + l_1)s}{s^3 + l_1s^2 + l_2s + l_3}$$

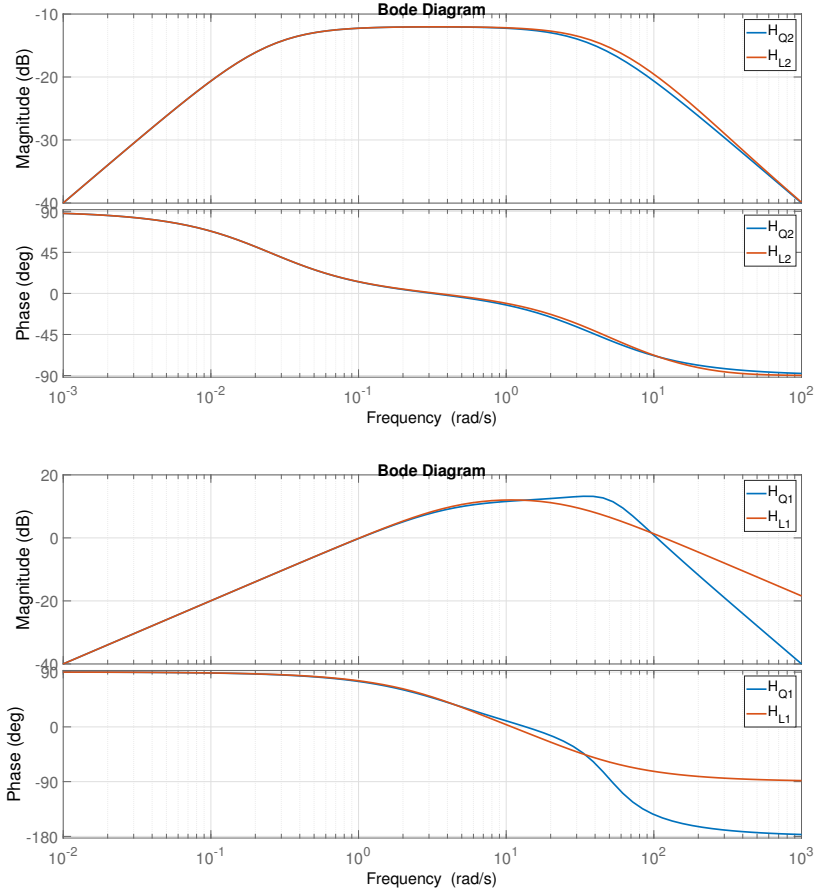
By comparing the above two transfer function with H_{Q_1} and H_{Q_2} defined in (4.20) and (4.21), the following values:

$$l_1 = 30, \quad l_2 = 4l_1 = 120, \quad l_3 = 0.1l_1 = 3 \quad (4.26)$$

are chosen for the purpose of well fitting the bode diagrams of H_{L_1} and H_{L_2} to those of H_{Q_1} and H_{Q_2} , such that the designed Luenberger observer processes the similar performance as Quanser's filters. The related bode diagrams are depicted in Fig.4.2, and we can see that, with the chosen parameters L , (4.24) performs, in the low frequency band 0 – 100Hz (which is the main operational frequency band for quadrotor), in a similar way as the two filters proposed by Quanser.

Step 2: Based on the Luenberger observer proposed in (4.24), we can then design the following homogeneous observer, proposed in Section 4, by using the same gains determined in (4.26):

$$\dot{z} = Az + Ba_{imu_x} + g(p_{cam_x} - C\hat{X}) \quad (4.27)$$

Figure 4.2 – Bode diagram of transfer functions H_{Q1}, H_{Q2} and H_{L1}, H_{L2}

where the function g , defined in (3.15), is of the following form:

$$g(p_{cam_x} - C\hat{X}) = \text{sat}_{a,b}(\|Ce\|_{\mathbb{R}^k}^\mu) \exp(\ln \text{sat}_{a,b}(\|Ce\|_{\mathbb{R}^k}^\mu) G_0) L C e \quad (4.28)$$

with $e = X - \hat{X}$, $G_0 = \begin{bmatrix} 0 & 0 & 0 \\ 0 & 1 & 0 \\ 0 & 0 & 1 \end{bmatrix}$, $L = [l_1, l_2, l_3]^\top$ is given in (4.26), and the parameters

a, b, μ , detailed in Section 4, are with the following values during our experiment test, $\mu = -0.25$, x and y direction: $a = 0.1, b = 2$, z direction: $a = 0.25, b = 1$. Each pair of a, b here are tuned to guarantee that the proposed nonlinear observer is always better than linear one by comparing the system state precision.

4.3.3 Experiment results

In this part, two experiments and their results will be presented. One is using Quanser's filters and homogeneous controller proposed in chapter 3. The other one is based on the homogeneous observer of the form (4.27) and the same homogeneous controller proposed in chapter 3. The experiment consists in the sequential set-points tracking which are defined in initial frame:

$$[x, y, z, \psi] = [0, 0, 0, 0] \rightarrow [0, 0, 0.2, 0] \rightarrow [0.5, 0, 0.2, \frac{\pi}{3}] \rightarrow [0.5, 0.5, 0.2, \frac{\pi}{3}] \\ \rightarrow [-0.5, -0.5, 0.8, 0] \rightarrow [0, 0, 0.8, 0] \rightarrow [0, 0, 0.018, 0]$$

Fig. 4.3-4.6 present the position stabilization trajectory of x, y, z and ψ respectively. It is obvious to see that the nonlinear homogeneous observer proposed in this paper has a faster response and a higher precision.

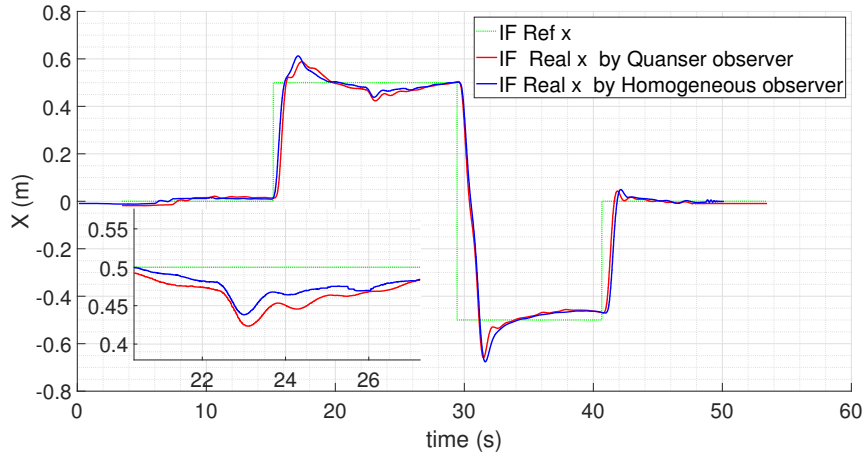
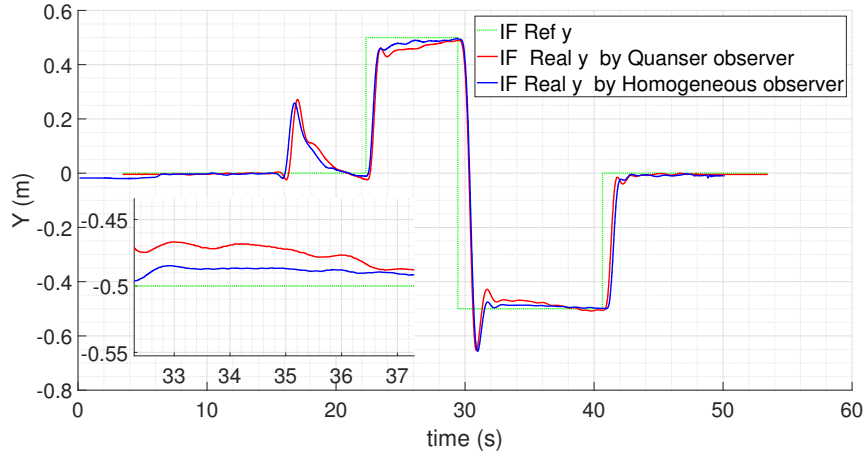
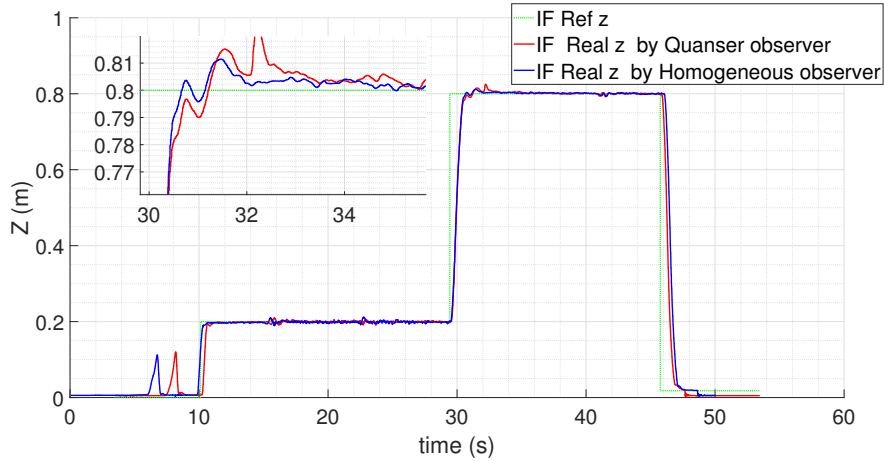


Figure 4.3 – Quadrotor position stabilization comparisons on x

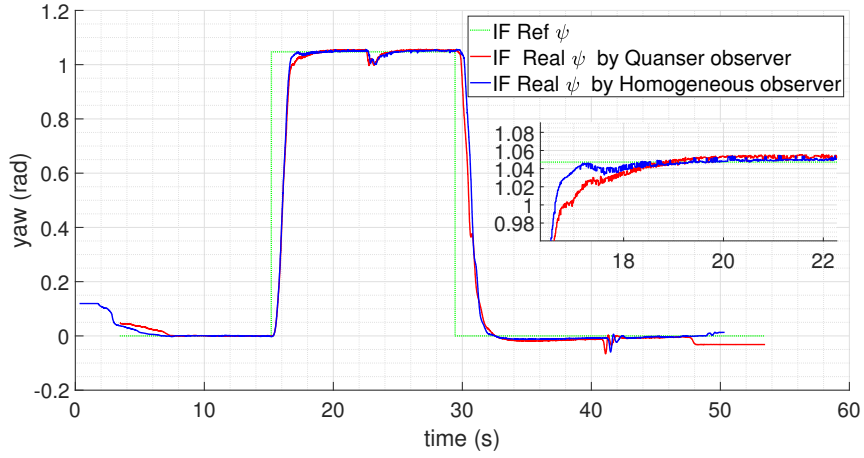
L_2 Error (m)	QF+HC	HF+HC	Improvement
$\ error_x\ _{L_2}$	0.0851	0.0760	10.69%
$\ error_y\ _{L_2}$	0.0491	0.0248	49.49%
$\ error_z\ _{L_2}$	0.0166	0.0089	46.39%
$\ error_\psi\ _{L_2}$	0.0426	0.0283	33.57%

Table 4.1 – Mean value of stabilization error

Table 4.1 compares the least square stabilization errors (L_2 -error) of Quanser's filter

Figure 4.4 – Quadrotor position stabilization comparisons on y Figure 4.5 – Quadrotor position stabilization comparisons on z

(QF) with homogeneous controller (HC) and homogeneous filter (HF) with homogeneous controller in the steady states. We define that the steady state of x, y, ψ and z starts ≈ 4 and ≈ 2 sec respectively after the z reference switches to $0.8m$ and ends at the time instant when the z reference switches to $0.018m$. The obtained improvement of the L_2 -error in y and z is more than 45%. The precision of ψ has been improved as well which coincides with the result in Table 4.1. Notice that Table 4.1 is the additional improvement by using the homogeneous filter with homogeneous controller comparing with chapter 3.

Figure 4.6 – Quadrotor position stabilization comparisons on ψ

4.4 Conclusion

In this chapter, a simple method of upgrading a linear observer to a nonlinear homogeneous one is developed. The nonlinear observer uses the gains of the linear one and scale them in a generalized homogeneous way depending on the norm of the available estimation error $Cz - y$. The generalized homogeneous systems has been proved to be faster and more robust than linear ones. Theoretical results have been supported with real experiments on the quadrotor QDrone of QuanserTM. The linear filter provided by the manufacturer has been “upgraded” using the proposed method, then control precision and robustness has been improved. However, in the practice, the system needs to work under certain constraints such as state constraints and time constraints, which is the problem to be studied in the next chapter.

Homogeneous stabilization under constraints

As well known, each kind of quadrotor has a limit payload capacity where the battery and processing unit is not as large as possible. This restricts the endurance time and the computation capacity of the quadrotor. Therefore one object of controller design is to make the quadrotor accomplish the task in limited period. Obviously, a simpler controller consumes less energy and responds faster than a complex one. Degradation of control precision could happen if the limits of computational power is exceeded. In [95] the authors show that a quadrotor controlled by linear PID consumes 5% less energy than the same quadrotor with a complex (backstepping) controller. Control of the quadrotor under state constraints is a difficult problem even in some particular cases (see e.g. [61]). In order to satisfy the input, output or state constraints, the control methods such as backstepping [15] and nested saturation [17], [104] has been applied. For linear algorithms an LMI-based schemes can be proposed in order to fulfill state constraints. Restrictions of transient times (i.e. time constraints) could be important, for example, for the trajectory tracking [105] or the formation control of quadrotors [23] and collision avoidance. Finite-time stabilization [50], is the simplest way to fulfill this time constraint. In this chapter we design the homogeneous control for quadrotor which fulfills some time and space constraints.

5.1 Problem statement

The quadrotor model has been built in (1.26)-(1.31), where

$$\sigma = (x, y, \dot{x}, \dot{y}, \phi, \theta, z, \psi, \dot{\phi}, \dot{\theta}, \dot{z}, \dot{\psi})^T$$

is the system state. The goal in this chapter is to design a controller that stabilizes the quadrotor system under the time constraint

$$\lim_{t \rightarrow \mathfrak{T}(\sigma_0)} \sigma(t) = 0, \quad \mathfrak{T}(x_0) \leq \mathfrak{T}_{max} \quad (5.1)$$

and the state constraints:

$$\begin{aligned} \sigma_1^2 + \sigma_2^2 &\leq \epsilon_{1,2}^2, \\ \sigma_3^2 + \sigma_4^2 &\leq \epsilon_{3,4}^2, \\ |\sigma_i| &\leq \epsilon_i, \quad i = 5, \dots, 12 \end{aligned} \quad (5.2)$$

where \mathfrak{T} is the settling time function, \mathfrak{T}_{max} is the time constraint, σ_0 is the initial state of system satisfying the space constraint and the positive constants

$$\begin{aligned} 0 &< \epsilon_{1,2}, \epsilon_{3,4}, \epsilon_7, \epsilon_8, \epsilon_9, \epsilon_{10}, \epsilon_{11}, \epsilon_{12} < +\infty \\ 0 &< \epsilon_5, \epsilon_6 < \frac{\pi}{2} \text{ such that } \cos(\epsilon_5)\cos(\epsilon_6) \geq \frac{1}{2} \end{aligned} \quad (5.3)$$

define the space constraints.

5.2 Controller Design with Time and state Constraint

For the considered state vector σ , the system model (1.26)-(1.31) can be represented in the form

$$\dot{\sigma} = \bar{A}\sigma + B(\bar{u} + d),$$

where $d \in \mathbb{R}^4$ is a constant exogenous perturbation and

$$\bar{A} = \bar{A}(\phi, \theta, \psi, F_T) = \begin{pmatrix} 0 & I & 0 & 0 & 0 & 0 \\ 0 & 0 & RE & 0 & 0 & 0 \\ 0 & 0 & 0 & 0 & I & 0 \\ 0 & 0 & 0 & 0 & 0 & I \\ 0 & 0 & 0 & 0 & 0 & 0 \\ 0 & 0 & 0 & 0 & 0 & 0 \end{pmatrix}, \quad B = \begin{pmatrix} 0 & 0 \\ 0 & 0 \\ 0 & 0 \\ 0 & 0 \\ \begin{pmatrix} \frac{1}{I_{xx}} & 0 \\ 0 & \frac{1}{I_{yy}} \end{pmatrix} & 0 \\ 0 & \begin{pmatrix} \frac{1}{m} & 0 \\ 0 & \frac{1}{I_{zz}} \end{pmatrix} \end{pmatrix}, \quad I = \begin{pmatrix} 1 & 0 \\ 0 & 1 \end{pmatrix}$$

$$E = E(\theta, \phi, F_T) := \begin{pmatrix} \frac{\sin \phi F_T}{\phi m} & 0 \\ 0 & \frac{\sin \theta \cos \phi F_T}{\theta m} \end{pmatrix}, \quad R = R(\psi) := \begin{pmatrix} \sin \psi & \cos \psi \\ -\cos \psi & \sin \psi \end{pmatrix}$$

Let us introduce the new variable $\zeta = T\sigma$ where T is the orthogonal matrix depending on ψ as follows

$$T = T(\psi) := \begin{pmatrix} R^{-1} & 0 & 0 & 0 & 0 & 0 \\ 0 & R^{-1} & 0 & 0 & 0 & 0 \\ 0 & 0 & I & 0 & 0 & 0 \\ 0 & 0 & 0 & I & 0 & 0 \\ 0 & 0 & 0 & 0 & I & 0 \\ 0 & 0 & 0 & 0 & 0 & I \end{pmatrix} \quad (5.4)$$

Thus the system can be rewritten in the form

$$\dot{\zeta} = (A + D)\zeta + B(\bar{u} + d), \quad \zeta(0) = \zeta_0 := T(\psi(0))\sigma_0 \quad (5.5)$$

where

$$A = \begin{pmatrix} 0 & I & 0 & 0 & 0 & 0 \\ 0 & 0 & E & 0 & 0 & 0 \\ 0 & 0 & 0 & 0 & I & 0 \\ 0 & 0 & 0 & 0 & 0 & I \\ 0 & 0 & 0 & 0 & 0 & 0 \\ 0 & 0 & 0 & 0 & 0 & 0 \end{pmatrix}, \quad D = D(\dot{\psi}) := \dot{T}T^{-1} \quad (5.6)$$

Let κ_i with $1 \leq i \leq 12$ be the identity vector from \mathbb{R}^{12} .

Lemma 5.2.1. *Let $\Delta \in [0, 1]$, the vector*

$$\epsilon = (\epsilon_{1,2}, \epsilon_{3,4}, \epsilon_5, \epsilon_6, \epsilon_7, \epsilon_8, \epsilon_9, \epsilon_{10}, \epsilon_{11}, \epsilon_{12}) \in \mathbb{R}_+^{10}$$

satisfies (5.3) and

$$A_i = \begin{pmatrix} G_i & I & 0 & 0 & 0 & 0 \\ 0 & G_i & E_i & 0 & 0 & 0 \\ 0 & 0 & 0 & 0 & I & 0 \\ 0 & 0 & 0 & 0 & 0 & I \\ 0 & 0 & 0 & 0 & 0 & 0 \\ 0 & 0 & 0 & 0 & 0 & 0 \end{pmatrix}, \quad 1 \leq i \leq 8 \quad (5.7)$$

where

$$G_1 = G_3 = G_5 = G_7 = \epsilon_{12} \begin{pmatrix} 0 & 1 \\ -1 & 0 \end{pmatrix}$$

$$G_2 = G_4 = G_6 = G_8 = -\epsilon_{12} \begin{pmatrix} 0 & 1 \\ -1 & 0 \end{pmatrix}$$

$$E_1 = E_2 = g(1 + \Delta) \begin{pmatrix} 1 & 0 \\ 0 & 1 \end{pmatrix}$$

$$E_3 = E_4 = g \begin{pmatrix} (1 + \Delta) & 0 \\ 0 & \frac{(1 - \Delta) \sin(\epsilon_6) \cos(\epsilon_5)}{\epsilon_6} \end{pmatrix}$$

$$E_5 = E_6 = g \begin{pmatrix} \frac{(1 - \Delta) \sin(\epsilon_5)}{\epsilon_5} & 0 \\ 0 & (1 + \Delta) \end{pmatrix}$$

$$E_7 = E_8 = g(1 - \Delta) \begin{pmatrix} \frac{\sin(\epsilon_5)}{\epsilon_5} & 0 \\ 0 & \frac{\sin(\epsilon_6) \cos(\epsilon_5)}{\epsilon_6} \end{pmatrix}$$

Then for any $\sigma \in \mathbb{R}^{12}$ satisfying (5.2), for any $\lambda \in [0, 1]$ and for any $F_T \in mg[1 - \Delta, 1 + \Delta]$ there exist $\alpha_i \geq 0$:

$$\sum_{i=1}^8 \alpha_i = 1 \quad \text{and} \quad \sum_{i=1}^8 \alpha_i A_i = A + \lambda D$$

Proof. If σ satisfies (5.2) and $F_T \in mg[1 - \Delta, 1 + \Delta]$ then, obviously, there exist $\mu_j \geq 0$ such that

$$E = \mu_1 E_1 + \mu_2 E_3 + \mu_3 E_5 + \mu_4 E_7, \quad \sum_{j=1}^4 \mu_j = 1.$$

On the other hand, since

$$-R^2 \dot{R} R = \dot{\psi} \begin{pmatrix} 0 & 1 \\ -1 & 0 \end{pmatrix}$$

then for any $\lambda \in [0, 1]$ there exist $\delta_1, \delta_2 \geq 0$ such that

$$-\lambda R^2 \dot{R}R = \delta_1 G_1 + \delta_2 G_2, \quad \delta_1 + \delta_2 = 1.$$

Hence the simple calculations shows that

$$A + \lambda D = A + \lambda \dot{T}T^{-1} = \sum_{i=1}^8 \alpha_i A_i$$

with $\alpha_1 = \mu_1 \delta_1$, $\alpha_2 = \mu_1 \delta_2$, $\alpha_3 = \mu_2 \delta_1$, $\alpha_4 = \mu_2 \delta_2$, $\alpha_5 = \mu_3 \delta_1$, $\alpha_6 = \mu_3 \delta_2$, $\alpha_7 = \mu_4 \delta_1$, $\alpha_8 = \mu_4 \delta_2$. Obviously, $\alpha_i \geq 0$ and $\sum_{i=1}^8 \alpha_i = 1$. ■

The latter lemma proves possibility of application of the so-called convex embedding approach(see e.g. [88]) for control design. Introduce the following implicit Lyapunov function candidate

$$Q(V, \zeta) := \zeta^T D_r(V^{-1}) P D_r(V^{-1}) \zeta - 1 \quad (5.8)$$

where $V \in \mathbb{R}_+$, $\zeta \in \mathbb{R}^{12}$, $P \in \mathbb{R}^{12 \times 12}$ is a symmetric positive definite matrix $P > 0$ and $D_r(\lambda) \in \mathbb{R}^{12 \times 12}$ is a dilation matrix of the form

$$D_r(\lambda) = \begin{pmatrix} \lambda^4 I & 0 & 0 & 0 \\ 0 & \lambda^3 I & \dots & 0 \\ 0 & 0 & \lambda^2 \begin{pmatrix} I & 0 \\ 0 & I \end{pmatrix} & 0 \\ 0 & 0 & 0 & \lambda \begin{pmatrix} I & 0 \\ 0 & I \end{pmatrix} \end{pmatrix}, \quad \lambda \in \mathbb{R}_+ \quad (5.9)$$

Denote

$$H := \begin{pmatrix} 4I & 0 & 0 & 0 & 0 & 0 \\ 0 & 3I & 0 & 0 & 0 & 0 \\ 0 & 0 & 2I & 0 & 0 & 0 \\ 0 & 0 & 0 & 2I & 0 & 0 \\ 0 & 0 & 0 & 0 & I & 0 \\ 0 & 0 & 0 & 0 & 0 & I \end{pmatrix}$$

Theorem 5.2.2. *Let for some*

$$\Delta \in \left[\frac{1}{\cos(\epsilon_5) \cos(\epsilon_6)} - 1, 1 \right]$$

the tuple

$$(X, Y, \gamma) \in \mathbb{R}^{12 \times 12} \times \mathbb{R}^{4 \times 12} \times \mathbb{R}_+$$

satisfy the system of LMIs

$$\left\{ \begin{array}{l} A_i X + X A_i^T + B Y + Y^T B^T + \gamma (X H + H X) \leq 0 \\ X H + H X > 0, \begin{pmatrix} X & X \kappa_j \\ e_j^T X & \epsilon_j^2 \end{pmatrix} \geq 0, \quad X > 0, \\ \begin{pmatrix} X & X \begin{pmatrix} I \\ 0 \\ 0 \\ 0 \\ 0 \end{pmatrix} \\ \begin{pmatrix} I \\ 0 \\ 0 \\ 0 \\ 0 \end{pmatrix}^T X & \epsilon_{1,2}^2 I \end{pmatrix} \geq 0, \quad \begin{array}{l} 1 \leq i \leq 8 \\ 5 \leq j \leq 12 \end{array} \\ \begin{pmatrix} X & X \begin{pmatrix} 0 \\ I \\ 0 \\ 0 \\ 0 \end{pmatrix} \\ \begin{pmatrix} 0 \\ I \\ 0 \\ 0 \\ 0 \end{pmatrix}^T X & \epsilon_{3,4}^2 I \end{pmatrix} \geq 0, \begin{pmatrix} X & Y^T \begin{pmatrix} 0 \\ 0 \\ 1 \\ 0 \end{pmatrix} \\ \begin{pmatrix} 0 \\ 0 \\ 1 \\ 0 \end{pmatrix}^T Y & \frac{\tau^2 - \frac{1}{\sqrt{q}} - \frac{1}{q}}{1 + \frac{1}{\sqrt{q}}} \end{pmatrix} \geq 0 \\ \tau = mg \left(\cos(\epsilon_5) \cos(\epsilon_6) (1 + \Delta) - 1 \right) \end{array} \right. \quad (5.10)$$

and the controller have the following form

$$\bar{u} = K D_r (V^{-1}) \zeta + \int_0^t K_I D_r (V^{-1}) \zeta(s) ds, \quad (5.11)$$

where

$$K = Y X^{-1} \quad (5.12)$$

$$K_I = - \frac{P_I^{-1} B^T P}{\zeta^T D_r (V^{-1}) (P H + H P) D_r (V^{-1}) \zeta} \quad (5.13)$$

$$V \in \mathbb{R}_+ : \zeta^T D_r (V^{-1}) P D_r (V^{-1}) \zeta = 1, \quad (5.14)$$

then for any initial condition $\zeta(0) = \zeta_0$

$$\zeta_0^T D_r ((1 - d^T P_I d)^{-1}) P D_r ((1 - d^T P_I d)^{-1}) \zeta_0 \leq 1 \quad (5.15)$$

$$P = X^{-1}$$

where $0 < P_I = qI, P_I \in \mathbb{R}^{4 \times 4}$ such that $d^T P_I d < 1$, the system (5.5) converges to zero in a finite

time

$$\mathfrak{T}(\zeta_0) \leq \frac{V(\sigma_0)}{\gamma} \leq \frac{1}{\gamma}.$$

Moreover the control \bar{u} is bounded by

$$\|\bar{u}\|_{\mathbb{R}^4}^2 \leq (1 + \frac{1}{\sqrt{q}}) \lambda_{\max}(P^{-\frac{1}{2}} K^T K P^{-\frac{1}{2}}) + \frac{1}{\sqrt{q}} + \frac{1}{q} \quad (5.16)$$

and the state constraints (5.2) are fulfilled for all $t \geq 0$.

Proof. The system (5.5) with controller (5.11) and disturbance d could be rewritten in the following form

$$\dot{\bar{\zeta}} = \begin{bmatrix} A+D & B \\ 0 & 0 \end{bmatrix} \bar{\zeta} + \begin{bmatrix} B & 0 \\ 0 & I \end{bmatrix} \bar{K} \bar{\zeta} \quad (5.17)$$

where $\bar{\zeta} = [\zeta, \zeta_{n+1}]^T$, and suppose $\zeta_{n+1} = \int_0^t K_I D_r(V^{-1}) \zeta(s) ds + d$, $\bar{K} = \begin{pmatrix} KD(V^{-1}) & 0 \\ K_I D(V^{-1}) & 0 \end{pmatrix}$.

Introduce the extended Lyapunov function

$$\bar{V} = V + \zeta_{n+1}^T P_I \zeta_{n+1} \quad (5.18)$$

Since V is the solution of (5.14), it is easy to develop following result under the initial condition(5.15):

$$\zeta_0^T D_r((1 - d^T P_I d)^{-1}) P D_r((1 - d^T P_I d)^{-1}) \zeta_0 \leq \zeta_0^T D_r(V(0)^{-1}) P D_r(V(0)^{-1}) \zeta_0$$

which is equivalent to

$$\begin{aligned} V(0) &\leq 1 - d^T P_I d, \quad d = \zeta_{n+1}(0) \\ \bar{V}(0) &= V(0) + d^T P_I d \leq 1 \end{aligned} \quad (5.19)$$

In [83] it was shown that the implicit Lyapunov function of the form (5.8) satisfies the conditions C1)-C3) of Theorem 2.2.7. Since

$$\frac{\partial Q(V, \zeta)}{\partial V} = -V^{-1} \zeta^T D_r(V^{-1}) (PH + HP) D_r(V^{-1}) \zeta$$

$P = X^{-1}$ and $XH + HX > 0$, then $\frac{\partial Q}{\partial V} < 0$ for $\forall V \in \mathbb{R}_+$ and $\zeta \in \mathbb{R}^{12} \setminus \{0\}$. So the condition C4) of Theorem 2.2.7 also holds.

Since $D_r(V^{-1}) A D_r^{-1}(V^{-1}) = V^{-1} A$ and $D_r(V^{-1}) B K D_r(V^{-1}) \zeta = V^{-1} B K D_r(V^{-1}) \zeta$ then

we have

$$\begin{aligned} & \frac{\partial Q(V, \zeta)}{\partial \zeta} (A\zeta + B\bar{u} + D\zeta) \\ &= 2 \frac{\zeta^T D_r(V^{-1})(PA + PBK + VPD)D_r(V^{-1})\zeta}{V} \\ &= 2 \sum_{i=1}^8 \alpha_i \frac{\zeta^T D_r(V^{-1})(PA_i + PBK)D_r(V^{-1})\zeta + \zeta^T D_r(V^{-1})PB\zeta_{n+1}}{V} \end{aligned}$$

with

$$\alpha_i \geq 0, \quad \sum_{i=1}^8 \alpha_i = 1$$

where Lemma 5.2.1 is utilized on the last step under. Therefore, the inequality

$$\begin{aligned} \dot{V} &= - \left(\frac{\partial Q(V, \zeta)}{\partial V} \right)^{-1} \frac{\partial Q(V, \zeta)}{\partial \zeta} \left((A + D)\zeta + B\bar{u} \right) \\ &\leq 2 \sum_{i=1}^8 \alpha_i \frac{\zeta^T D_r(V^{-1})(PA_i + PBK)D_r(V^{-1})\zeta + \zeta^T D_r(V^{-1})PB\zeta_{n+1}}{\zeta^T D_r(V^{-1})(PH + HP)D_r(V^{-1})\zeta} \\ &\leq -\gamma + 2 \frac{\zeta^T D_r(V^{-1})PB\zeta_{n+1}}{\zeta^T D_r(V^{-1})(PH + HP)D_r(V^{-1})\zeta} \\ \dot{\bar{V}} &= \dot{V} + 2\dot{\zeta}_{n+1}^T P_I \zeta_{n+1} \\ &\leq -\gamma + 2 \frac{\zeta^T D_r(V^{-1})PB\zeta_{n+1}}{\zeta^T D_r(V^{-1})(PH + HP)D_r(V^{-1})\zeta} + 2\zeta^T D_r(V^{-1})K_i^T P_I \zeta_{n+1} \\ &\leq -\gamma \leq 0 \end{aligned} \tag{5.20}$$

According to (5.19) and (5.20), we have

$$\bar{V}(t) \leq 1 \Rightarrow V(t) \leq 1 \tag{5.21}$$

and the system (5.17) converges to 0 in finite time

$$\mathfrak{T}(\zeta_0) \leq \frac{1}{\gamma} \tag{5.22}$$

provided that the phase constraints are fulfilled, $V \leq 1$ and $F_T \in mg[1 - \Delta, 1 + \Delta]$.

To complete the proofs let us show that the phase constraints and the inclusion $F_T \in mg[1 - \Delta, 1 + \Delta]$ hold if $V \leq 1$ (or, equivalently, $\zeta^\top P \zeta \leq 1$). Indeed, the required

phase constraints for $j = 5, \dots, 12$ comes from

$$\begin{aligned} \begin{bmatrix} \epsilon_j^2 X & X \kappa_j \\ \kappa_j^T X & 1 \end{bmatrix} \geq 0 &\Leftrightarrow X \kappa_j e_j^T X \leq \epsilon_j^2 X \\ &\Leftrightarrow \kappa_j e_j^T \leq \epsilon_j^2 P \\ &\Leftrightarrow \zeta_j^2 = \zeta^T \kappa_j e_j^T \zeta \leq \epsilon_j^2 \zeta^T P \zeta \leq \epsilon_j^2 \end{aligned}$$

The constraints for σ_1, σ_2 and σ_3, σ_4 can be checked similarly taking into account that

$$\begin{bmatrix} \sigma_1 \\ \sigma_2 \end{bmatrix}^T \begin{bmatrix} \sigma_1 \\ \sigma_2 \end{bmatrix} = \begin{bmatrix} \sigma_1 \\ \sigma_2 \end{bmatrix}^T R^T R \begin{bmatrix} \sigma_1 \\ \sigma_2 \end{bmatrix} = \begin{bmatrix} \zeta_1 \\ \zeta_2 \end{bmatrix}^T \begin{bmatrix} \zeta_1 \\ \zeta_2 \end{bmatrix}$$

Since $\zeta^T D_r(V^{-1}) P D_r(V^{-1}) \zeta = 1$, by using Young's inequality, then the norm square of controller (5.17) can be estimated as follows

$$\begin{aligned} \|\bar{u}\|_{\mathbb{R}^4}^2 &\leq (1 + \sqrt{q}^{-1}) \zeta^T D_r(V^{-1}) K^T K D_r(V^{-1}) \zeta + (1 + \sqrt{q}^{-1}) \zeta_{n+1}^T \zeta_{n+1} \\ &= (1 + \sqrt{q}^{-1}) \zeta^T D_r(V^{-1}) K^T K D_r(V^{-1}) \zeta + \frac{(1 + \sqrt{q}^{-1}) \zeta_{n+1}^T \zeta_{n+1} q}{q} \end{aligned}$$

Since $\bar{V} < 1$, we have $\zeta_{n+1}^T \zeta_{n+1} q < 1$, then

$$\|\bar{u}\|_{\mathbb{R}^4}^2 \leq (1 + \frac{1}{\sqrt{q}}) \lambda_{\max}(P^{-\frac{1}{2}} K^T K P^{-\frac{1}{2}}) + \frac{1}{\sqrt{q}} + \frac{1}{q}$$

Similarly we derive

$$\|\bar{u}_1\|_{\mathbb{R}^4}^2 \leq (1 + \frac{1}{\sqrt{q}}) \lambda_{\max}(P^{-\frac{1}{2}} K^T \begin{pmatrix} 0 \\ 0 \\ 1 \\ 0 \end{pmatrix} \begin{pmatrix} 0 \\ 0 \\ 1 \\ 0 \end{pmatrix}^T K P^{-\frac{1}{2}}) + \frac{1}{\sqrt{q}} + \frac{1}{q} \leq \tau^2$$

which is equivalent to the last inequality of (5.10).

■

It is worth stating that if some states are not constraint, the corresponding LMIs simply disappear for (5.10). If we need to minimize the input bound, the right part of inequality (5.16) need to be minimized under constraints of (5.10).

The main issue that may lead to infeasibility of (5.10) is its last LMI. To guarantee the LMIs (5.10) are always feasible, we need to select q and τ such that $\tau^2 > \frac{1}{q} + \frac{1}{\sqrt{q}}$. Indeed, the first and the second LMI (considered as independence of other LMIs) are feasible together. If \tilde{X}, \tilde{Y} is their solution then $X = r\tilde{X}, Y = r\tilde{Y}$ is a solution as well (for

any $r > 0$). Using Schur complement we derive that all the other LMIs are feasible as well for a sufficiently small r .

The parameter γ introduced in (5.10) is for tuning of the settling time. This time can be minimized by means of solving the semi-definite programming problem

$$\gamma \rightarrow \gamma_{\max}$$

subject to (5.10).

Remark: When the disturbance d is zero, then we can select $K_I = 0$ and the controller becomes the PD controller [101].

5.3 Simulation results

3. The parameters applied in the simulation is provided by Quanser and listed in Table 1.5.

Suppose that the state constraints are given as

$$|\dot{\psi}| \leq 1, \quad |\phi| \leq \frac{\pi}{5}, \quad |\theta| \leq \frac{\pi}{5}$$

Solving LMIs (5.10) gives the following gain matrix

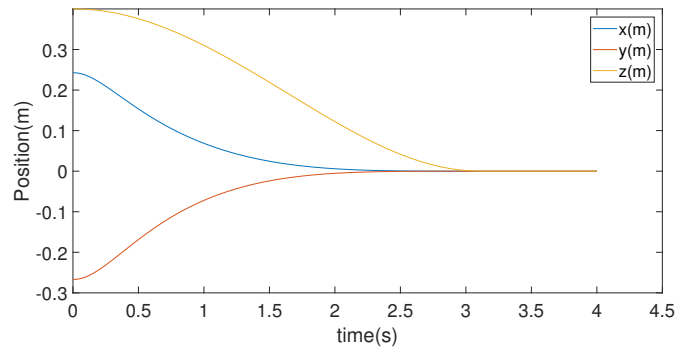
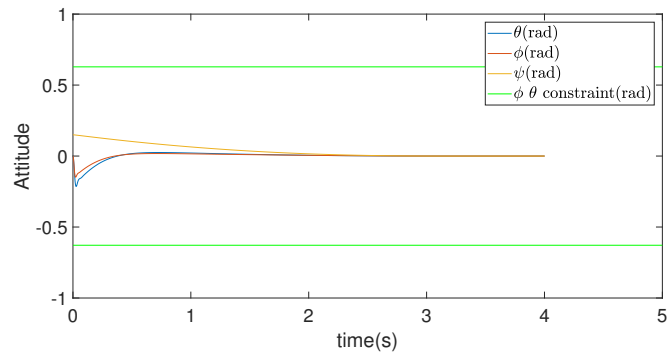
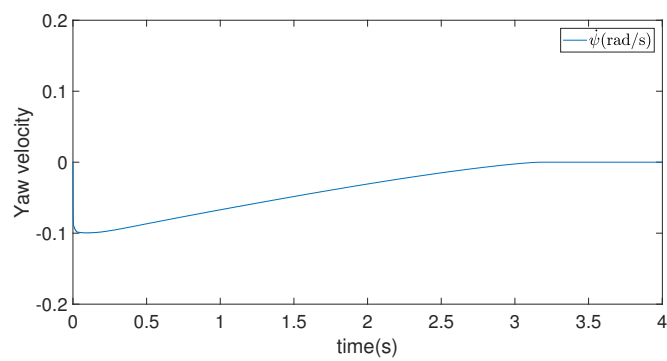
$$K = \begin{pmatrix} -64.52 & 0 & -71.89 & 0 & -110.33 & 0 & 0 & 0 & -0.76 & 0 & 0 & 0 \\ 0 & -72.98 & 0 & -83.07 & 0 & -107.53 & 0 & 0 & 0 & -0.75 & 0 & 0 \\ 0 & 0 & 0 & 0 & 0 & 0 & -0.31 & 0 & 0 & 0 & -0.84 & 0 \\ 0 & 0 & 0 & 0 & 0 & 0 & 0 & -15.69 & 0 & 0 & 0 & -27.43 \end{pmatrix}$$

The initial condition here is $\sigma_0 = [0.24; -0.27; 0; 0; 0; 0; 0.4; 0.15; 0; 0; 0; 0]$ which makes $\sigma_0^T P \sigma_0 = 0.958 < 1$, $d = (3 \ 3 \ 0.4 \ 1)^T$ and $\gamma = 0.21$.

Fig. 5.1 and Fig. 5.2 depict that position and attitude converge to zero in finite time by implicit PID controller which means that full states will converge to zero less than $\frac{1}{\gamma} = 4.77s$. Since the full state of the system is considered together in the controller design, the position and attitude state will converge together in the simulation. The constraint of $\dot{\psi}, \theta, \phi$ are satisfied and confirmed by Fig. 5.2 and Fig. 5.3. In the Fig. 5.4, it is clear to see the property of finite-time stability.

The simulation results show that the controller is robust and able to stabilize the quadrotor to the original position under the state and time constraints even if there are some the initial constant errors.

Fig. 5.5 and Fig. 5.6 depict that position and attitude cannot converge to the desired position without integrator term (Part of results in this chapter is published in [101]).

Figure 5.1 – Quadrotor position x, y, z by implicit PID controllerFigure 5.2 – Quadrotor attitude ϕ, θ, ψ by implicit PID controllerFigure 5.3 – Angle velocity $\dot{\psi}$ by implicit PID controller

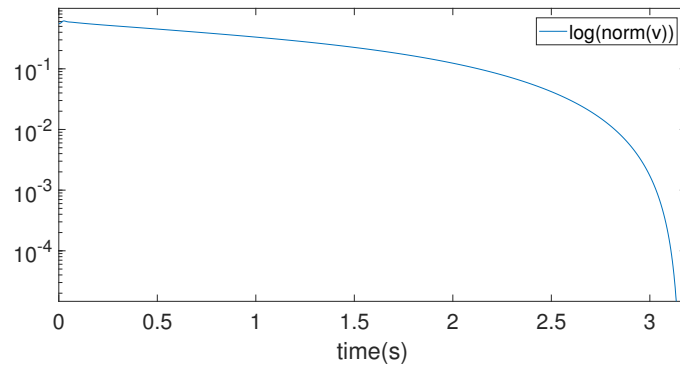


Figure 5.4 – Log of the norm of vector $v = [x, y, \phi, \theta, z, \psi]$ by implicit PID controller

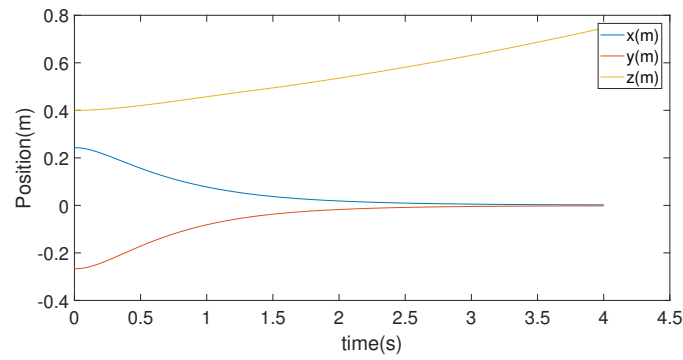


Figure 5.5 – Quadrotor position x, y, z by implicit PD controller

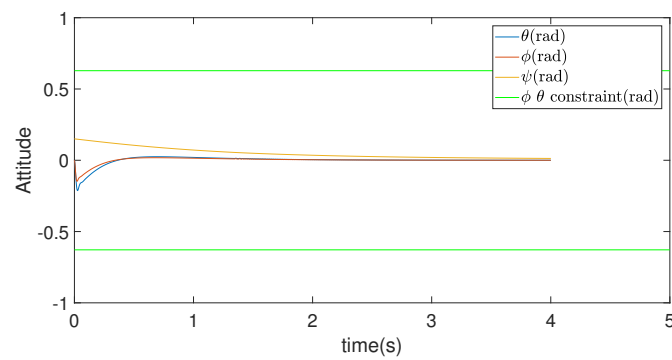


Figure 5.6 – Quadrotor attitude ϕ, θ, ψ by implicit PD controller

5.4 Conclusion

In this chapter the problem of homogeneous stabilization of quadrotor under state constraints is studied. Convex embedding technique is utilized to construct LMIs required for tuning feedback gains. A non-linear implicit PID controller proposed provide a good performance to compensate the matched disturbance with initial constant error. For this moment, only simulation results are presented in this thesis. The future work is to implement the proposed method on the quadrotor platform.

Conclusion and perspective

Conclusion

In this thesis, the problem of upgrading linear control and estimation algorithms to nonlinear ones with an improvement of control quality is studied. It shows that such an upgrade is possible based on the concept of generalized (linear geometric) homogeneity

The whole research is conducted around quadrotor control problem. It starts with investigating the quadrotor background including its applications, advantages, challenges, dynamic model and existing control solutions. Due to the irreplaceable advantage, Quadrotor is becoming more and more popular in our daily life by offering transportation, videography, monitoring and support in the air. However, quadrotor still have many challenges due to the nonlinearity, multi-variable and hardware limitations. Although many kinds of controllers have been applied on quadrotor, a controller having a better performance such as better precision, more robustness and faster reaction is still an actual problem.

Homogeneous controller is a possible solution to improve the the precision, robustness and reaction time at same time. The homogeneity is a certain symmetry with respect to dilation. In this thesis we use a special kind of dilation called linear geometric dilation. The homogeneous controller can be designed by combining the homogeneity theory and implicit Lyapunov function method. Besides, the LMI is applied for stability analysis and controller design.

The main method of upgrading a linear controller to homogeneous one is presented in chapter 3. This method provides a new idea to design the nonlinear homogeneous controller, and propose an easier way to improve the performance of existing systems that governed by linear controller. Using the system state value, the homogeneous controller scales the linear feedback gain (or part of the gain) dynamically. By introducing an appropriate saturation function, we can guarantee that the homogeneous controller will never be worse than linear one. The experimental results show that the precision

can be improved a lot. Besides the robustness of quadrotor is significantly improved by homogeneous controller. On line calculation asks for a bit more computation power than linear controller, and the experimental results prove that the homogeneous controller consumes only 1 – 1.5% more energy than linear one.

The same idea of homogeneous controller design is extended to the observer design which is presented in chapter 4. The homogeneous observer design is based on the Luenberger observer. The experimental results show that this upgrade may additionally improve the precision around 10% – 49%.

Homogeneous stabilization of quadrotor under constraints is to design the homogeneous controller such that it satisfies certain restrictions of quadrotor operating condition. Convex embedding technique is utilized in chapter 5 to construct LMIs that is required for tuning feedback gains. The simulation results support the theoretical design. The experimental results may be provided in the future work.

List of Publications

Published

1. [112] Generalized Homogenization of Linear Controllers: Theory and Experiments. In: *International Journal of Robust and Nonlinear Control*.
Video about upgrade of Quanser's controller : <https://youtu.be/wnSi6jj1TwE>
2. [111] Generalized Homogenization of Linear Quadrotor Controller. In: *IEEE International Conference on Robotics and Automation 2020*.
3. [114] Finite Time LMI based Quadrotor control design under time State Constraints. In: *European Control Conference 2019*.

Submitted papers

1. [113] Generalized Homogenization of Linear Observer: Theory and Experiments. In *International Journal of Robust and Nonlinear Control*.
Video about upgrade of Quanser's observer : <https://youtu.be/4cwXG1k7Ojo>
2. [115] Quadrotor stabilization under time and space constraints using implicit PID controller. In *Journal of Franklin Institute*.

Patent

- **Title:** "Utilisation de l'homogénéité généralisée pour améliorer une commande PID"
- **Deposit number:** FR2004684
- **Date of submission:** 12 May 2020

Perspective

Following the encouraging results of homogeneous controller, several important research directions can be proposed for the future.

- **Robustness analysis:** In general, the stability and robustness analysis answers the following four questions: 1. (Norminal stability) Is the closed-loop system stable when the plant is known exactly? 2. (Robust stability) Is the closed-loop system stable when there is uncertainty in our knowledge of the plant? 3. (Nominal performance) Does the closed-loop system meet the performance specification when the plant is known exactly? 4. (Robust performance) Does the closed-loop system meet the performance specification when there is uncertainty in our knowledge of the plant? This thesis answers the first and third question with details. There are still two questions concerning model uncertainty to be studied deeply. Uncertainty is always a challenge for the control engineer. Therefore, the question, how the model uncertainty effects the closed-loop system stability and performance, is very important for successful application of the proposed control design methodology. Combining with homogeneous controller, many methods such as input state stability and attractive (invariant) ellipsoid method may provide a possible solution to solve this problem. One more issue, if one of the quadrotor's motor broken in the air, how the quadrotor behaves in this case ?
- **Applications:** The homogeneous controller can be applied to many other systems such as electric drives, robots, etc. Since homogeneous controller seems to be more robust than linear controller, it may be very useful for control of systems operating under disturbances and uncertainty conditions.

Many research topics around homogeneous control systems are still open so far.

Bibliography

- [1] J. Adamy and A. Flemming. “Soft variable-structure controls: a survey”. In: *Automatica* 40.11 (2004), pp. 1821–1844 (cit. on p. 51).
- [2] T. S. Alderete. “Simulator aero model implementation”. In: *NASA Ames Research Center, Moffett Field, California* (1995), p. 21 (cit. on pp. 5, 6).
- [3] K. Alexis, G. Nikolakopoulos, and A. Tzes. “Model predictive quadrotor control: attitude, altitude and position experimental studies”. In: *IET Control Theory & Applications* 6.12 (2012), pp. 1812–1827 (cit. on p. 19).
- [4] V. Andrieu, L. Praly, and A. Astolfi. “Homogeneous Approximation, Recursive Observer Design, and Output Feedback”. In: *SIAM Journal of Control and Optimization* 47.4 (2008), pp. 1814–1850 (cit. on pp. 29–31, 41).
- [5] A. Bacciotti and L. Rosier. *Lyapunov Functions and Stability in Control Theory*. Springer, 2001 (cit. on pp. 41, 42).
- [6] E. Bernuau, D. Efimov, W. Perruquetti, and A. Polyakov. “On homogeneity and its application in sliding mode control”. In: *Journal of The Franklin Institute* 351.4 (2014), pp. 1866–1901 (cit. on pp. 26, 30).
- [7] S. P. Bhat and D. S. Bernstein. “Geometric homogeneity with applications to finite-time stability”. In: *Mathematics of Control, Signals and Systems* 17 (2005), pp. 101–127 (cit. on pp. 30, 31).
- [8] S. P. Bhat and D. S. Bernstein. “Finite-time stability of continuous autonomous systems”. In: *SIAM Journal on Control and Optimization* 38.3 (2000), pp. 751–766 (cit. on pp. 45, 47, 50).
- [9] I. Boiko. *Non-parametric Tuning of PID Controllers*. Springer-Verlag London, 2013 (cit. on p. 30).
- [10] S. Bouabdallah, A. Noth, and R. Siegwart. “PID vs LQ control techniques applied to an indoor micro quadrotor”. In: *Intelligent Robots and Systems, 2004.(IROS 2004). Proceedings. 2004 IEEE/RSJ International Conference on*. Vol. 3. IEEE. 2004, pp. 2451–2456 (cit. on p. 15).
- [11] S. Bouabdallah and R. Siegwart. “Backstepping and sliding-mode techniques applied to an indoor micro quadrotor”. In: *Proceedings of the 2005 IEEE international conference on robotics and automation*. IEEE. 2005, pp. 2247–2252 (cit. on pp. 3, 17).

- [12] S. Boyd, E. Ghaoui, E. Feron, and V. Balakrishnan. *Linear Matrix Inequalities in System and Control Theory*. Philadelphia: SIAM, 1994 (cit. on p. 90).
- [13] S. Boyd, L. El Ghaoui, E. Feron, and V. Balakrishnan. *Linear matrix inequalities in system and control theory*. Vol. 15. Siam, 1994 (cit. on p. 53).
- [14] V. Brégeault, F. Plestan, Y. Shtessel, and A. Poznyak. “Adaptive sliding mode control for an electropneumatic actuator”. In: *2010 11th International Workshop on Variable Structure Systems (VSS)*. IEEE. 2010, pp. 260–265 (cit. on p. 18).
- [15] M. Bürger and M. Guay. “A backstepping approach to multivariable robust constraint satisfaction with application to a VTOL helicopter”. In: *Proceedings of the 48th IEEE Conference on Decision and Control (CDC) held jointly with 2009 28th Chinese Control Conference*. IEEE. 2009, pp. 5239–5244 (cit. on p. 101).
- [16] F. Caccavale, G. Giglio, G. Muscio, and F. Pierri. “Cooperative impedance control for multiple UAVs with a robotic arm”. In: *2015 IEEE/RSJ International Conference on Intelligent Robots and Systems (IROS)*. IEEE. 2015, pp. 2366–2371 (cit. on p. 2).
- [17] N. Cao and A. F. Lynch. “Inner-outer loop control for quadrotor UAVs with input and state constraints”. In: *IEEE Transactions on Control Systems Technology* 24.5 (2016), pp. 1797–1804 (cit. on p. 101).
- [18] N. Chen, Y. Chen, Y. You, H. Ling, P. Liang, and R. Zimmermann. “Dynamic urban surveillance video stream processing using fog computing”. In: *2016 IEEE second international conference on multimedia big data (BigMM)*. IEEE. 2016, pp. 105–112 (cit. on p. 2).
- [19] F. Chernous’ko, I. Ananievski, and S. Reshmin. *Control of nonlinear dynamical systems: methods and applications*. Springer Science & Business Media, 2008 (cit. on p. 30).
- [20] J.-M. Coron and L. Praly. “Adding an integrator for the stabilization problem”. In: *Systems & Control Letters* 17.2 (1991), pp. 89–104 (cit. on p. 30).
- [21] I. D. Cowling, O. A. Yakimenko, J. F. Whidborne, and A. K. Cooke. “A prototype of an autonomous controller for a quadrotor UAV”. In: *Control Conference (ECC), 2007 European*. IEEE. 2007, pp. 4001–4008 (cit. on p. 15).
- [22] C. Diao, B. Xian, Q. Yin, W. Zeng, H. Li, and Y. Yang. “A nonlinear adaptive control approach for quadrotor UAVs”. In: *Control Conference (ASCC), 2011 8th Asian*. IEEE. 2011, pp. 223–228 (cit. on p. 18).
- [23] H. Du, W. Zhu, G. Wen, and D. Wu. “Finite-time formation control for a group of quadrotor aircraft”. In: *Aerospace Science and Technology* 69 (2017), pp. 609–616 (cit. on p. 101).
- [24] D. Efimov and W. Perruquetti. “Homogeneity for time-delay systems”. In: *IFAC Proceedings Volumes* 44.1 (2011), pp. 3861–3866 (cit. on p. 41).
- [25] M. Faessler, D. Falanga, and D. Scaramuzza. “Thrust mixing, saturation, and body-rate control for accurate aggressive quadrotor flight”. In: *IEEE Robotics and Automation Letters* 2.2 (2016), pp. 476–482 (cit. on p. 3).

- [26] A. Filippov. *Differential equations with discontinuous righthand sides*. Springer Science & Business Media, 1988 (cit. on pp. 67, 68).
- [27] F. Fraundorfer, L. Heng, D. Honegger, G. H. Lee, L. Meier, P. Tanskanen, and M. Pollefeys. "Vision-based autonomous mapping and exploration using a quadrotor MAV". In: *2012 IEEE/RSJ International Conference on Intelligent Robots and Systems*. IEEE. 2012, pp. 4557–4564 (cit. on p. 2).
- [28] G. Gioioso, A. Franchi, G. Salvietti, S. Scheggi, and D. Prattichizzo. "The flying hand: A formation of UAVs for cooperative aerial tele-manipulation". In: *2014 IEEE International conference on robotics and automation (ICRA)*. IEEE. 2014, pp. 4335–4341 (cit. on p. 2).
- [29] S. Grzonka, G. Grisetti, and W. Burgard. "A fully autonomous indoor quadrotor". In: *IEEE Transactions on Robotics* 28.1 (2011), pp. 90–100 (cit. on p. 2).
- [30] H. Hermes. "Nilpotent approximations of control systems and distributions". In: *SIAM journal on control and optimization* 24.4 (1986), pp. 731–736 (cit. on p. 36).
- [31] G. M. Hoffmann, H. Huang, S. L. Waslander, and C. J. Tomlin. "Quadrotor helicopter flight dynamics and control: Theory and experiment". In: *Proc. of the AIAA Guidance, Navigation, and Control Conference*. Vol. 2. 2007, p. 4 (cit. on pp. 2, 15).
- [32] Y. Hong. " H_∞ control, stabilization, and input–output stability of nonlinear systems with homogeneous properties". In: *Automatica* 37.6 (2001), pp. 819–829 (cit. on p. 30).
- [33] X. Huo, M. Huo, and H. R. Karimi. "Attitude stabilization control of a quadrotor UAV by using backstepping approach". In: *Mathematical Problems in Engineering* 2014 (2014) (cit. on p. 17).
- [34] L. Husch. "Topological characterization of the dilation and the translation in frechet spaces". In: *Mathematische Annalen* 190.1 (1970), pp. 1–5 (cit. on p. 37).
- [35] J. Hwangbo, I. Sa, R. Siegwart, and M. Hutter. "Control of a quadrotor with reinforcement learning". In: *IEEE Robotics and Automation Letters* 2.4 (2017), pp. 2096–2103 (cit. on p. 19).
- [36] A. Ilka. "Gain-Scheduled Controller Design". PhD thesis. Slovak University of Technology In Bratislava, 2015 (cit. on p. 16).
- [37] A. Isidori. *Nonlinear control systems*. Springer Science & Business Media, 2013 (cit. on p. 17).
- [38] R. Izmailov. "THE PEAK EFFECT IN STATIONARY LINEAR-SYSTEMS WITH MULTIVARIATE INPUTS AND OUTPUTS". In: *Automation and Remote Control* 49.1 (1988), pp. 40–47 (cit. on pp. 62, 64).

- [39] Q. Jiang, D. Mellinger, C. Kappeyne, and V. Kumar. "Analysis and synthesis of multi-rotor aerial vehicles". In: *ASME 2011 International Design Engineering Technical Conferences and Computers and Information in Engineering Conference*. American Society of Mechanical Engineers Digital Collection. 2011, pp. 711–720 (cit. on p. 3).
- [40] A. E. Jimenez-Cano, J. Martin, G. Heredia, A. Ollero, and R. Cano. "Control of an aerial robot with multi-link arm for assembly tasks". In: *2013 IEEE International Conference on Robotics and Automation*. IEEE. 2013, pp. 4916–4921 (cit. on p. 2).
- [41] M. Kowski. "Geometric homogeneity and stabilization". In: *IFAC Proceedings Volumes* 28.14 (1995), pp. 147–152 (cit. on pp. 26, 37).
- [42] H. K. Khalil and J. W. Grizzle. *Nonlinear systems*. Vol. 3. Prentice hall Upper Saddle River, NJ, 2002 (cit. on p. 51).
- [43] P. V. Kokotovic. "The joy of feedback: nonlinear and adaptive". In: *IEEE Control Systems Magazine* 12.3 (1992), pp. 7–17 (cit. on p. 17).
- [44] J. La Salle and S. Lefschetz. *Stability by Liapunov's Direct Method with Applications*. Elsevier Science, 1961 (cit. on p. 69).
- [45] S. Laghrouche, F. Plestan, and A. Glumineau. "Higher order sliding mode control based on integral sliding mode". In: *Automatica* 43.3 (2007), pp. 531–537 (cit. on p. 17).
- [46] I. D. Landau, R. Lozano, M. M'Saad, and A. Karimi. *Adaptive control: algorithms, analysis and applications*. Springer Science & Business Media, 2011 (cit. on p. 18).
- [47] D. Lee, H. J. Kim, and S. Sastry. "Feedback linearization vs. adaptive sliding mode control for a quadrotor helicopter". In: *International Journal of control, Automation and systems* 7.3 (2009), pp. 419–428 (cit. on p. 17).
- [48] K. U. Lee, H. S. Kim, J. B. Park, and Y. H. Choi. "Hovering control of a quadrotor". In: *Control, Automation and Systems (ICCAS), 2012 12th International Conference on*. IEEE. 2012, pp. 162–167 (cit. on p. 15).
- [49] M.-H. Lee and S. Yeom. "Multiple target detection and tracking on urban roads with a drone". In: *Journal of Intelligent & Fuzzy Systems* 35.6 (2018), pp. 6071–6078 (cit. on p. 2).
- [50] A. Levant. "Homogeneity approach to high-order sliding mode design". In: *Automatica* 41.5 (2005), pp. 823–830 (cit. on pp. 30, 101).
- [51] A. Levant. "Quasi-continuous high-order sliding-mode controllers". In: *42nd IEEE International Conference on Decision and Control (IEEE Cat. No. 03CH37475)*. Vol. 5. IEEE. 2003, pp. 4605–4610 (cit. on p. 47).
- [52] A. Levant. "Sliding order and sliding accuracy in sliding mode control". In: *International Journal of Control* 58.6 (1993), pp. 1247–1263 (cit. on p. 68).
- [53] J. Li and Y. Li. "Dynamic analysis and PID control for a quadrotor". In: *Mechatronics and Automation (ICMA), 2011 International Conference on*. IEEE. 2011, pp. 573–578 (cit. on p. 15).

- [54] D. Liberzon. *Switching in systems and control*. Springer Science & Business Media, 2003 (cit. on p. 77).
- [55] F. Lopez-Ramirez, A. Polyakov, D. Efimov, and W. Perruquetti. “Finite-time and fixed-time observer design: Implicit Lyapunov function approach”. In: *Automatica* 87.1 (2018), pp. 52–60 (cit. on pp. 31, 91).
- [56] R. Lozano and B. Brogliato. “Adaptive control of robot manipulators with flexible joints”. In: *IEEE Transactions on Automatic Control* 37.2 (1992), pp. 174–181 (cit. on p. 18).
- [57] L. Luque-Vega, B. Castillo-Toledo, and A. G. Loukianov. “Robust block second order sliding mode control for a quadrotor”. In: *Journal of the Franklin Institute* 349.2 (2012), pp. 719–739 (cit. on p. 17).
- [58] A. M. Lyapunov. “The general problem of motion stability”. In: *Annals of Mathematics Studies* 17 (1892) (cit. on p. 48).
- [59] T. Madani and A. Benallegue. “Backstepping control for a quadrotor helicopter”. In: *2006 IEEE/RSJ International Conference on Intelligent Robots and Systems*. IEEE. 2006, pp. 3255–3260 (cit. on p. 17).
- [60] A. Mercado-Uribe, J. A. Moreno, A. Polyakov, and D. Efimov. “Integral Control Design using the Implicit Lyapunov Function Approach”. In: *2019 IEEE 58th Conference on Decision and Control (CDC)*. IEEE. 2019, pp. 3316–3321 (cit. on pp. 64, 68, 70).
- [61] N. Metni and T. Hamel. “A UAV for bridge inspection: Visual servoing control law with orientation limits”. In: *Automation in construction* 17.1 (2007), pp. 3–10 (cit. on p. 101).
- [62] N. Michael, S. Shen, K. Mohta, V. Kumar, K. Nagatani, Y. Okada, S. Kiribayashi, K. Otake, K. Yoshida, K. Ohno, et al. “Collaborative mapping of an earthquake damaged building via ground and aerial robots”. In: *Field and service robotics*. Springer. 2014, pp. 33–47 (cit. on p. 2).
- [63] L. D. Minh and C. Ha. “Modeling and control of quadrotor MAV using vision-based measurement”. In: *Strategic Technology (IFOST), 2010 International Forum on*. IEEE. 2010, pp. 70–75 (cit. on p. 16).
- [64] A. Mokhtari, A. Benallegue, and B. Daachi. “Robust feedback linearization and GH/sub/spl infin//controller for a quadrotor unmanned aerial vehicle”. In: *Intelligent Robots and Systems, 2005.(IROS 2005). 2005 IEEE/RSJ International Conference on*. IEEE. 2005, pp. 1198–1203 (cit. on p. 16).
- [65] H. Nakamura, Y. Yamashita, and H. Nishitani. “Smooth Lyapunov functions for homogeneous differential inclusions”. In: *Proceedings of the 41st SICE Annual Conference*. 2002, pp. 1974–1979 (cit. on p. 44).

- [66] T. Ng, F. Leung, and P. Tam. “A simple gain scheduled PID controller with stability consideration based on a grid-point concept”. In: *Industrial Electronics, 1997. ISIE'97., Proceedings of the IEEE International Symposium on*. IEEE. 1997, pp. 1090–1094 (cit. on p. 16).
- [67] C Nicol, C. Macnab, and A Ramirez-Serrano. “Robust neural network control of a quadrotor helicopter”. In: *Electrical and Computer Engineering, 2008. CCECE 2008. Canadian Conference on*. IEEE. 2008, pp. 001233–001238 (cit. on p. 19).
- [68] C. Olalla, R. Leyva, A. El Aroudi, and I. Queinnec. “Robust LQR control for PWM converters: An LMI approach”. In: *IEEE Transactions on industrial electronics* 56.7 (2009), pp. 2548–2558 (cit. on p. 15).
- [69] Y. Orlov. *Discontinuous systems: Lyapunov analysis and robust synthesis under uncertainty conditions*. Springer, 2008 (cit. on p. 69).
- [70] Y. Orlov. “Finite Time Stability and Robust Control Synthesis of Uncertain Switched Systems”. In: *SIAM Journal of Control and Optimization* 43.4 (2005), pp. 1253–1271 (cit. on pp. 29, 47).
- [71] I. Palunko and R. Fierro. “Adaptive control of a quadrotor with dynamic changes in the center of gravity”. In: *IFAC Proceedings Volumes* 44.1 (2011), pp. 2626–2631 (cit. on pp. 17, 18).
- [72] A. Pazy. *Semigroups of linear operators and applications to partial differential equations*. Vol. 44. Springer Science & Business Media, 1983 (cit. on p. 38).
- [73] D. Perez, I. Maza, F. Caballero, D. Scarlatti, E. Casado, and A. Ollero. “A ground control station for a multi-UAV surveillance system”. In: *Journal of Intelligent & Robotic Systems* 69.1-4 (2013), pp. 119–130 (cit. on p. 2).
- [74] W. Perruquetti, T. Floquet, and E. Moulay. “Finite-time observers: application to secure communication”. In: *IEEE Transactions on Automatic Control* 53.1 (2008), pp. 356–360 (cit. on p. 30).
- [75] F. Plestan, Y. Shtessel, V. Brégeault, and A. Poznyak. “Sliding mode control with gain adaptation—Application to an electropneumatic actuator”. In: *Control Engineering Practice* 21.5 (2013), pp. 679–688 (cit. on p. 17).
- [76] B. T. Polyak and G. Smirnov. “Large deviations for non-zero initial conditions in linear systems”. In: *Automatica* 74 (2016), pp. 297–307 (cit. on p. 62).
- [77] A. Polyakov. “Fixed-time stabilization of linear systems via sliding mode control”. In: *2012 12th International Workshop on Variable Structure Systems*. IEEE. 2012, pp. 1–6 (cit. on p. 32).
- [78] A. Polyakov. *Generalized Homogeneity in Systems and Control*. Springer, 2020 (cit. on pp. 26, 30, 61, 68, 88, 90).
- [79] A. Polyakov. “Nonlinear feedback design for fixed-time stabilization of linear control systems”. In: *IEEE Transactions on Automatic Control* 57.8 (2012), pp. 2106–2110 (cit. on pp. 30, 31, 48).

- [80] A. Polyakov, J.-M. Coron, and L. Rosier. “On Homogeneous Finite-Time Control for Linear Evolution Equation in Hilbert Space”. In: *IEEE Transactions on Automatic Control* 63.9 (2018), pp. 3143–3150 (cit. on pp. 41, 65, 130).
- [81] A. Polyakov, D. Efimov, and B. Brogliato. “Consistent discretization of finite-time and fixed-time stable systems”. In: *SIAM Journal on Control and Optimization* 57.1 (2019), pp. 78–103 (cit. on p. 77).
- [82] A. Polyakov, D. Efimov, E. Fridman, and W. Perruquetti. “On homogeneous distributed parameters equations”. In: *IEEE Transactions on Automatic Control* 61.11 (2016), pp. 3657–3662 (cit. on p. 29).
- [83] A. Polyakov, D. Efimov, and W. Perruquetti. “Robust stabilization of MIMO systems in finite/fixed time”. In: *International Journal of Robust and Nonlinear Control* 26.1 (2016), pp. 69–90 (cit. on pp. 66, 67, 107).
- [84] A. Polyakov. “Quadratic stabilizability of homogeneous systems”. In: *56th IEEE Conference on Decision and Control*. 2017 (cit. on p. 39).
- [85] A. Polyakov. “Sliding Mode Control Design Using Canonical Homogeneous Norm”. In: *International Journal of Robust and Nonlinear Control* 29.3 (2018), pp. 682–701 (cit. on pp. 39, 40, 42, 43, 70, 73, 89).
- [86] A. Polyakov, D. Efimov, and W. Perruquetti. “Finite-time and fixed-time stabilization: Implicit Lyapunov function approach”. In: *Automatica* 51 (2015), pp. 332–340 (cit. on pp. 52, 76).
- [87] A. Polyakov and L. Fridman. “Stability notions and Lyapunov functions for sliding mode control systems”. In: *Journal of the Franklin Institute* 351.4 (2014), pp. 1831–1865 (cit. on pp. 44, 50).
- [88] A. Polyakov, L. Hetel, and C. Fiter. “Relay control design using attractive ellipsoids method”. In: *2017 IEEE 56th Annual Conference on Decision and Control (CDC)*. IEEE. 2017, pp. 6646–6651 (cit. on p. 105).
- [89] P. Pounds, R. Mahony, and P. Corke. “Modelling and control of a large quadrotor robot”. In: *Control Engineering Practice* 18.7 (2010), pp. 691–699 (cit. on p. 2).
- [90] A. Poznyak, A. Polyakov, and V. Azhmyakov. *Attractive ellipsoids in robust control*. Springer, 2014 (cit. on p. 54).
- [91] A. S. Poznyak. *Advanced mathematical tools for automatic control engineers: Stochastic techniques*. Elsevier, 2009 (cit. on pp. 49, 57).
- [92] Y. Qi, J. Wang, and J. Shan. “Collision-Free Formation Control for Multiple Quadrotor-Manipulator Systems”. In: *IFAC-PapersOnLine* 50.1 (2017), pp. 7923–7928 (cit. on p. 2).
- [93] G. V. Raffo, M. G. Ortega, and F. R. Rubio. “MPC with Nonlinear H_∞ Control for Path Tracking of a Quad-Rotor Helicopter”. In: *IFAC Proceedings Volumes* 41.2 (2008), pp. 8564–8569 (cit. on p. 19).

- [94] E. Reyes-Valeria, R. Enriquez-Caldera, S. Camacho-Lara, and J. Guichard. “LQR control for a quadrotor using unit quaternions: Modeling and simulation”. In: *CONIELECOMP 2013, 23rd International Conference on Electronics, Communications and Computing*. IEEE. 2013, pp. 172–178 (cit. on p. 16).
- [95] A. Rodić, G. Mester, and I. Stojković. “Qualitative Evaluation of Flight Controller Performances for Autonomous Quadrotors”. In: *Intelligent Systems: Models and Applications*. Springer, 2013, pp. 115–134 (cit. on p. 101).
- [96] E. Roxin. “On finite stability in control systems”. In: *Rendiconti del Circolo Matematico di Palermo* 15.3 (1966), pp. 273–282 (cit. on p. 47).
- [97] A. L. Salih, M. Moghavvemi, H. A. Mohamed, and K. S. Gaeid. “Flight PID controller design for a UAV quadrotor”. In: *Scientific research and essays* 5.23 (2010), pp. 3660–3667 (cit. on p. 15).
- [98] M. Santos, V. Lopez, and F. Morata. “Intelligent fuzzy controller of a quadrotor”. In: *Intelligent Systems and Knowledge Engineering (ISKE), 2010 International Conference on*. IEEE. 2010, pp. 141–146 (cit. on p. 19).
- [99] Q. Shen, B. Jiang, and V. Cocquempot. “Adaptive fault-tolerant backstepping control against actuator gain faults and its applications to an aircraft longitudinal motion dynamics”. In: *International Journal of Robust and Nonlinear Control* 23.15 (2013), pp. 1753–1779 (cit. on p. 17).
- [100] Y. Shtessel, M. Taleb, and F. Plestan. “A novel adaptive-gain supertwisting sliding mode controller: Methodology and application”. In: *Automatica* 48.5 (2012), pp. 759–769 (cit. on p. 17).
- [101] W. Siyuan, A. Polyakov, and G. Zheng. “Finite-Time LMI based Quadrotor control design under time and State Constraints”. In: *2019 IEEE Annual European Control Conference (ECC)*. IEEE. 2019 (cit. on pp. 30, 110).
- [102] E. Sontag. “Nonlinear and Optimal Control Theory”. In: Springer-Verlag, Berlin, 2007. Chap. Input to state stability: Basic concepts and results, pp. 163–220 (cit. on p. 30).
- [103] S. Tarbouriech, G. Garcia, J. M. G. da Silva Jr, and I. Queinnec. *Stability and stabilization of linear systems with saturating actuators*. Springer Science & Business Media, 2011 (cit. on p. 3).
- [104] A. R. Teel. “Global stabilization and restricted tracking for multiple integrators with bounded controls”. In: *Systems & control letters* 18.3 (1992), pp. 165–171 (cit. on p. 101).
- [105] B. Tian, H. Lu, Z. Zuo, Q. Zong, and Y. Zhang. “Multivariable finite-time output feedback trajectory tracking control of quadrotor helicopters”. In: *International Journal of Robust and Nonlinear Control* 28.1 (2018), pp. 281–295 (cit. on p. 101).

- [106] M. Tognon, A. Testa, E. Rossi, and A. Franchi. “Takeoff and landing on slopes via inclined hovering with a tethered aerial robot”. In: *2016 IEEE/RSJ International Conference on Intelligent Robots and Systems (IROS)*. IEEE. 2016, pp. 1702–1707 (cit. on p. 3).
- [107] V. I. Utkin. *Sliding Modes in Control Optimization*. Berlin: Springer-Verlag, 1992 (cit. on p. 30).
- [108] V. I. Utkin. *Sliding modes in control and optimization*. Springer Science & Business Media, 2013 (cit. on p. 17).
- [109] R. È. Vinograd. “Inapplicability of the method of characteristic exponents to the study of non-linear differential equations”. In: *Matematicheskii Sbornik* 83.4 (1957), pp. 431–438 (cit. on p. 45).
- [110] Q.-G. Wang, T.-H. Lee, H.-W. Fung, Q. Bi, and Y. Zhang. “PID tuning for improved performance”. In: *IEEE Transactions on control systems technology* 7.4 (1999), pp. 457–465 (cit. on p. 30).
- [111] S. Wang, A. Polyakov, and G. Zheng. “On Generalized Homogenization of Linear Quadrotor Controller”. In: *International Conference on Robotics and Automation (ICRA)*. 2020 (cit. on pp. 64, 116).
- [112] S. Wang, A. Polyakov, and G. Zheng. “Generalized Homogenization of Linear Controllers: Theory and Experiment”. In: *International Journal of Robust and Nonlinear Control* (2020) (cit. on pp. 64, 116).
- [113] S. Wang, A. Polyakov, and G. Zheng. “Generalized Homogenization of Linear observer: Theory and experiments”. In: *IEEE Transactions on Systems, Man, and Cybernetics Systems (submitted)* (2020) (cit. on p. 116).
- [114] S. Wang, A. Polyakov, and G. Zheng. “Quadrotor Control Design under Time and State Constraints: Implicit Lyapunov Function Approach”. In: *2019 18th European Control Conference (ECC)*. IEEE. 2019, pp. 650–655 (cit. on p. 116).
- [115] S. Wang, A. Polyakov, and G. Zheng. “Quadrotor stabilization under time and space constraints using implicit PID controller”. In: *Journal of Franklin Institute (submitted)* (2020) (cit. on p. 116).
- [116] R. Xu and U. Ozguner. “Sliding mode control of a quadrotor helicopter”. In: *Proceedings of the 45th IEEE Conference on Decision and Control*. IEEE. 2006, pp. 4957–4962 (cit. on pp. 9, 17).
- [117] V. Yakubovich. “S-procedure in nonlinear control theory”. In: *Vestnick Leningrad Univ. Math.* 4 (1997), pp. 73–93 (cit. on p. 56).
- [118] K. Zimenko, A. Polyakov, D. Efimov, and W. Perruquetti. “Robust Feedback Stabilization of Linear MIMO Systems Using Generalized Homogenization”. In: *IEEE Transactions on Automatic Control* (2020) (cit. on pp. 65, 66).
- [119] V. I. Zubov. “Systems of ordinary differential equations with generalized-homogeneous right-hand sides”. In: *Izvestiya Vysshikh Uchebnykh Zavedenii. Matematika* 1 (1958), pp. 80–88 (cit. on pp. 26, 29, 35, 36, 38).

-
- [120] A. Zulu and S. John. “A review of control algorithms for autonomous quadrotors”. In: (2016) (cit. on pp. 17, 19).

Résumé substantiel

Au cours des dernières décennies, les problèmes liés au contrôle des quadrotors attirent plus d'attention des chercheurs par rapport aux autres véhicules volants. Cependant, la plupart des produits commerciaux utilisent encore le contrôleur PID linéaire, qui offre une performance suffisamment bonne. Le développement d'un contrôleur, qui pourrait convaincre l'industrie de l'utiliser à la place du contrôleur PID linéaire, reste toujours un défi. L'objectif de cette thèse est de montrer que le contrôleur homogène est une alternative au contrôleur PID linéaire. Pour ce faire, une nouvelle méthode est proposée : mettre à niveau de l'algorithme linéaire vers un algorithme homogène. Elle utilise les avantages du contrôleur (observateur) linéaire fournis par le constructeur pour le réglage de l'algorithme homogène. Les résultats expérimentaux soutiennent les développements théoriques et confirment une amélioration significative de la qualité du contrôle du quadrotor: meilleure précision, plus de robustesse et réponse plus rapide.

Chapitre 1 présente le contexte et la motivation de la recherche. Ensuite, il examine le l'état de l'art de la commande quadrotor, qui comprend linéaire, non linéaire et intelligent contrôleurs. La plate-forme expérimentale est également considérée. La contribution et la les grandes lignes de la thèse sont présentées dans la dernière section.

C'est l'un des éléments importants de ce chapitre, nous avons introduit les équations dynamiques suivantes du système quadrotor.

$$\ddot{x} = \frac{F_T}{m}(\cos \phi \sin \theta \cos \psi + \sin \phi \sin \psi) \quad (23)$$

$$\ddot{y} = \frac{F_T}{m}(\cos \phi \sin \theta \sin \psi - \sin \phi \cos \psi) \quad (24)$$

$$\ddot{z} = \frac{F_T}{m} \cos \phi \cos \theta - g \quad (25)$$

$$\ddot{\phi} = \bar{\tau}_\phi \quad (26)$$

$$\ddot{\theta} = \bar{\tau}_\theta \quad (27)$$

$$\ddot{\psi} = \bar{\tau}_\psi \quad (28)$$

Notez que dans la plupart des cas d'expérimentation, le ϕ et le θ sont censés être petits, telle que $\cos \theta \approx 1$, $\cos \phi \approx 1$ et $\sin \theta \approx \theta$, $\sin \phi \approx \phi$.

Le modèle de quadrotor construit dans la partie précédente est non linéaire, ce qui n'est parfois pas pratique pour la conception de contrôleurs. Un modèle simplifié de

quadrotor sera utilisé par la suite. D'après (23)-(28), supposons que

$$\sigma = (x, y, \dot{x}, \dot{y}, \phi, \theta, z, \psi, \dot{\phi}, \dot{\theta}, \dot{z}, \dot{\psi})^\top$$

$$\bar{u} = \left(\frac{F_T \cos \phi \cos \theta}{m} - g, \bar{\tau}_\phi, \bar{\tau}_\theta, \bar{\tau}_\psi \right)^\top$$

et ensuite introduire la nouvelle variable $\zeta = T\sigma$ où T est la matrice orthogonale dépendant de ψ comme suit

$$T = T(\psi) := \begin{pmatrix} R^{-1} & 0 & 0 & 0 & 0 & 0 \\ 0 & R^{-1} & 0 & 0 & 0 & 0 \\ 0 & 0 & I & 0 & 0 & 0 \\ 0 & 0 & 0 & I & 0 & 0 \\ 0 & 0 & 0 & 0 & I & 0 \\ 0 & 0 & 0 & 0 & 0 & I \end{pmatrix} \quad (29)$$

$$E = E(\theta, \phi, F_T) := \begin{pmatrix} \frac{\sin \phi F_T}{\phi m} & 0 \\ 0 & \frac{\sin \theta \cos \phi F_T}{\theta m} \end{pmatrix}, \quad R = R(\psi) := \begin{pmatrix} \sin \psi & \cos \psi \\ -\cos \psi & \sin \psi \end{pmatrix} \quad (30)$$

Enfin, le modèle du quadrotor peut être réécrit sous la forme

$$\dot{\zeta} = (A + D)\zeta + B\bar{u}, \quad \zeta(0) = \zeta_0 := T(\psi(0))\sigma_0 \quad (31)$$

où

$$A = \begin{pmatrix} 0 & I & 0 & 0 & 0 & 0 \\ 0 & 0 & E & 0 & 0 & 0 \\ 0 & 0 & 0 & 0 & I & 0 \\ 0 & 0 & 0 & 0 & 0 & I \\ 0 & 0 & 0 & 0 & 0 & 0 \\ 0 & 0 & 0 & 0 & 0 & 0 \end{pmatrix}, \quad D = D(\dot{\psi}) := \dot{T}T^{-1} \quad (32)$$

Dans la suite de cette thèse, la conception du contrôleur sera principalement basée sur ce modèle reformulé (31).

Chapitre 2 présente les outils mathématiques utilisés dans cette thèse. Les concepts d'homogénéité standard et généralisée sont introduites. En particulier, l'homogénéité géométriques linéaires est prise en compte. En tant que l'outil principal pour l'analyse de la stabilité du système, le Lyapunov méthode est brièvement abordée dans la deuxième section. Enfin, la théorie des inégalités matricielles linéaires (IMT) est présentée dans la dernière section.

Un outil mathématique important que nous avons introduit est appelé norme homogène canonique([80]). The function $\|\cdot\|_{\mathbf{d}} : \mathbb{R}^n \setminus \{0\} \rightarrow (0, +\infty)$ defined as

$$\|x\|_{\mathbf{d}} = e^{s_x}, \text{ where } s_x \in \mathbb{R} : \|\mathbf{d}(-s_x)x\| = 1, \quad (33)$$

is called the canonical homogeneous norm, where \mathbf{d} is a strictly monotone dilation.

Cette norme canonique homogène est considérée comme un candidat à la fonction de Lyapunov dans la conception du contrôleur de thèse.

Dans chapitre 3, nous commençons par donner un exemple motivant pour montrer une autre possibilité avantage d'un contrôleur homogène par rapport à un contrôleur linéaire. Ensuite, le deuxième présente les principaux résultats de la mise à niveau d'un contrôleur linéaire vers un contrôleur homogène un. Les résultats théoriques sont étayés par des expériences de quadrotor dans la dernière section.

Dans ce chapitre, le contrôleur homogène que nous avons présenté est le suivant

$$u(x) = K_0 x + u_{hom}(x) + \int_0^t u_{int}(x(s)) ds, \quad (34)$$

$$u_{hom}(x) = \|x\|_{\mathbf{d}}^{1+\mu} K \mathbf{d} (-\ln \|x\|_{\mathbf{d}}) x,$$

$$u_{int}(x) = -\|x\|_{\mathbf{d}}^{1+2\mu} \frac{QB^T P \mathbf{d} (-\ln \|x\|_{\mathbf{d}}) x}{x^T \mathbf{d}^T (-\ln \|x\|_{\mathbf{d}}) P G \mathbf{d} (-\ln \|x\|_{\mathbf{d}}) x}$$

qui peut stabiliser l'origine du système

$$\dot{x} = Ax + B(u + p),$$

where p is a constant. Le contrôleur homogène (34) peut être conçu sur la base des paramètres du contrôleur PID existant et il a été testé sur la plate-forme quadrotor, ce qui le rend très potentiel pour de nombreuses applications.

La méthodologie d'une "mise à niveau" des contrôleurs linéaires vers des contrôleurs homogènes est déjà développé au chapitre 3, où les expériences montrent que la précision de suivi des points de consigne sur l'expérience réelle est amélioré d'environ 40% et le contrôleur homogène montre sa meilleure robustesse que le contrôleur linéaire. Ce chapitre 4 étend les mêmes idées à les observateurs conçoivent et montrent la "mise à niveau" simultanée du contrôleur linéaire et de l'observateur implique une plus grande amélioration de la qualité du contrôle.

Dans ce chapitre, nous présentons un observateur homogène :

The system (4.1) is said to be \mathbf{d} -homogeneously observable with a degree $\mu \in \mathbb{R}$ if there exists an observer of the form

$$\dot{z} = Az + Bu + g(Cz - y), \quad g: \mathbb{R}^k \rightarrow \mathbb{R}^n \quad (35)$$

telle que l'équation d'erreur

$$\dot{e} = Ae + g(Ce), \quad e = z - x \quad (36)$$

est globalement asymptotiquement stable et \mathbf{d} -homogène avec degré $\mu \in \mathbb{R}$.

Ensuite, la fonction délimitée g est définie sous la forme suivante

$$g(\sigma) = \exp(\ln \|\sigma\|_{\mathbb{R}^k} (G_0 + I_n) \mu) L \sigma, \quad \sigma \in \mathbb{R}^k \quad (37)$$

Enfin, l'équation d'erreur (36) est garantie d'être globalement asymptotiquement stable et \mathbf{d} -homogène avec le degré $\mu \in \mathbb{R}$.

De la même manière du contrôleur homogène, observateur homogène peut être conçu sur la base des paramètres du Luenberger observateur existant et il a été testé sur la plate-forme quadrotor, ce qui le rend très potentiel pour de nombreuses applications.

Le problème de la conception d'une rétroaction d'état pour le contrôle d'un système quadrotor sous des contraintes d'état et de temps est étudié dans chapitre 5. Le modèle est décomposé en trois sous-systèmes. Le premier et le second système sont utilisés pour le contrôle de l'altitude et de l'ambardée, respectivement. Le dernier sous-système est sous-actionné pour contrôler simultanément la position horizontale (x, y) , le roulis ϕ et les angles de tangage θ . La fonction implicite de Lyapunov (ILF) est utilisée pour la conception du contrôle. La stabilité robuste du système en boucle fermée est prouvée et confirmée par des simulations.

Dans cette thèse, le problème de la mise à niveau des algorithmes de contrôle linéaire et d'estimation vers des algorithmes homogènes avec une amélioration de la qualité du contrôle est étudié. Elle montre qu'une telle mise à niveau est possible pour améliorer de manière significative les performances du système. Le contrôleur PID homogène offre une alternative potentielle au contrôleur PID.

Résumé

Au cours des dernières décennies, les problèmes liés au contrôle des quadrotors attirent plus d'attention des chercheurs par rapport aux autres véhicules volants. Cependant, la plupart des produits commerciaux utilisent encore le contrôleur PID linéaire, qui offre une performance suffisamment bonne. Le développement d'un contrôleur, qui pourrait convaincre l'industrie de l'utiliser à la place du contrôleur PID linéaire, reste toujours un défi. L'objectif de cette thèse est de montrer que le contrôleur homogène est une alternative au contrôleur PID linéaire. Pour ce faire, une nouvelle méthode est proposée : mettre à niveau de l'algorithme linéaire vers un algorithme homogène. Elle utilise les avantages du contrôleur / observateur linéaire fournis par le constructeur pour le réglage de l'algorithme homogène. Les résultats expérimentaux soutiennent les développements théoriques et confirment une amélioration significative de la qualité du contrôle du quadrotor: meilleure précision, plus de robustesse et réponse plus rapide.

Keywords: système homogène, contrôle de quadrotor, contrôle nonlinéaire

Abstract

In the past several decades, quadrotor control problems attract more attentions of the researcher comparing with other flying vehicles. However, most of the commercial products still use linear PID controller, which provides sufficiently good performance. Development of a controller, which would convince the industry to use it instead of linear PID, is still a challenge. The aim of this thesis is to show that homogeneous controller is a possible alternative to linear one. For this purpose, a new method of upgrading linear algorithm to homogeneous one is proposed. It uses the gains of linear controller/observer provided by the manufacturer for tuning of homogeneous algorithm. The experimental results support the theoretical developments and confirm a significant improvement of quadrotor's control quality : better precision, more robustness and faster response.

Mots clés : homogeneous system, quadrotor control, nonlinear control